

РОССИЙСКИЙ КАРДИОЛОГИЧЕСКИЙ ЖУРНАЛ

Russian Journal of Cardiology

SCIENTIFIC, PEER-REVIEWED MEDICAL JOURNAL

RUSSIAN SOCIETY OF CARDIOLOGY

IN ISSUE:

Left ventricular myocardial cellular perfusion against the background of cardiac contractility modulation in patients with heart failure and atrial fibrillation

Post-COVID-19 syndrome: morpho-functional abnormalities of the heart and arrhythmias

Algorithm for selecting predictors and prognosis of atrial fibrillation in patients with coronary artery disease after coronary artery bypass grafting

Evaluation of the long-term effectiveness of cardiac resynchronization therapy

Electroanatomic substrate of atrial fibrillation in patients after COVID-19

Molecular mechanisms of left atrial fibrosis development in patients with atrial fibrillation and metabolic syndrome: what biomarkers should be used in clinical practice?

IN FOCUS:

Arrhythmology



РОССИЙСКОЕ
КАРДИОЛОГИЧЕСКОЕ
ОБЩЕСТВО

Russian Society of Cardiology

Scientific peer-reviewed medical journal

Mass media registration certificate № 017388
dated 06.04.1998

Periodicity — 12 issues per year
Circulation — 7 000 copies

The Journal is in the List of the leading
scientific journals and publications
of the Supreme Examination Board (VAK)

The Journal is included in Scopus, EBSCO, DOAJ

Russian Citation Index:
SCIENCE INDEX (2019) 2,710
Impact-factor (2019) 1,668

Complete versions of all issues are published:
www.elibrary.ru

Instructions for authors:
[https://russjcardiol.elpub.ru/jour/about/
submissions#authorGuidelines](https://russjcardiol.elpub.ru/jour/about/submissions#authorGuidelines)

Submit a manuscript:
www.russjcardiol.elpub.ru

Subscription: www.roscardio.ru/ru/subscription.html

Open Access

For information on how to request permissions
to reproduce articles/information from
this journal, please contact with publisher

The mention of trade names, commercial
products or organizations, and the inclusion
of advertisements in the journal do not imply
endorsement by editors, editorial board
or publisher

Printed: OneBook, Sam Poligraphist, Ltd.
129090, Moscow, Protopopovskiy per., 6.
www.onebook.ru

© Russian Journal of Cardiology

Font's license № 180397 or 21.03.2018

RUSSIAN JOURNAL OF CARDIOLOGY

№ 26 (7) 2021

founded in 1996

EDITOR-IN-CHIEF

Evgeny V. Shlyakhto (St. Petersburg) Professor, Academician RAS

ASSOCIATE EDITORS

Bagrat G. Alekryan (Moscow) Professor, Academician RAS

Yury N. Belenkov (Moscow) Professor, Academician RAS

Sergey A. Boytsov (Moscow) Professor, Academician RAS

Yury A. Vasyuk (Moscow) Professor

Mikhail I. Voevoda (Novosibirsk) Professor, Academician RAS

Albert S. Galyavich (Kazan) Professor

Rostislav S. Karpov (Tomsk) Professor, Academician RAS

Yury A. Karpov (Moscow) Professor

Vasily V. Kashtalap (Kemerovo) MScD

Natalya A. Koziolova (Perm) Professor

Aleksandra O. Konradi (St. Petersburg) Professor, Corresponding
member of RAS

Yury M. Lopatin (Volgograd) Professor

Viacheslav Yu. Mareev (Moscow) Professor

Evgeny N. Mikhaylov (St. Petersburg) MScD

Alexandr O. Nedoshivin (St. Petersburg) Professor

Svetlana Yu. Nikulina (Krasnoyarsk) Professor

Dmitry A. Ovchinnikov (St. Petersburg)

Amiran Sh. Revishvili (Moscow) Professor, Academician RAS

Vitalii V. Skibitskiy (Krasnodar) Professor

Evgeny O. Taratukhin (Moscow) Associate Professor

Irina E. Chazova (Moscow) Professor, Academician RAS

Anna A. Chernova (Krasnoyarsk) MScD

Galina A. Chumakova (Barnaul) Professor

Svetlana A. Shalnova (Moscow) Professor

Sergey S. Yakushin (Ryazan) Professor

EXECUTIVE SECRETARY

Evgeny O. Taratukhin (Moscow)

EXECUTIVE EDITORS OF THE ISSUE

Dmitry S. Lebedev (St-Petersburg)

Sergey V. Popov (Tomsk)

Editorial office:

119049, Moscow,

ul. Shabolovka, 23-254

e-mail: cardiojournal@yandex.ru

Tel. +7 (985) 768 43 18

Publisher:

Silicea-Poligraf

e-mail: cardio.nauka@yandex.ru

ADVISORY BOARD

Aligadzhi A. Abdullaev (Makhachkala)

Oleg Yu. Atkov (Moscow)

Grigory P. Arutyunov (Moscow)

Yan L. Gabinsky (Ekaterinburg)

Valery V. Gafarov (Novosibirsk)

Anatoly V. Govorin (Chita)

Sergei L. Dzemeshkevich (Moscow)

Dmitry V. Duplyakov (Samara)

Alexandr M. Karaskov (Novosibirsk)

Anna V. Kontsevaya (Moscow)

Dmitry S. Lebedev (St. Petersburg)

Roman A. Libis (Orenburg)

Andrei M. Nedbaikin (Bryansk)

Sergey V. Nedogoda (Volgograd)

Valentin E. Oleynikov (Penza)

Philip N. Paleev (Moscow)

Sergey N. Pokrovskiy (Moscow)

Igor V. Pershukov (Voronezh)

Konstantin V. Protasov (Irkutsk)

Tatiana V. Tyurina (Leningradskaya oblast)

Elena A. Khludeeva (Vladivostok)

Vladimir A. Shulman (Krasnoyarsk)

INTERNATIONAL ADVISORY BOARD

Karlen Adamyan (Armenia)

Stefan Anker (Germany)

Salim Berkinbayev (Kazakhstan)

Richard Ceska (Czech Republic)

Francesco Cosentino (Italy)

Roberto Ferrari (Italy)

Jean Charles Fruchart (France)

Vladimir Gabinsky (USA)

Vladimir Kovalenko (Ukraine)

Michel Komajda (France)

Ravshanbek Kurbanov (Uzbekistan)

Steven Lentz (USA)

Gilbert Massard (France)

Markku Nieminen (Finland)

Peter Nilsson (Sweden)

Gianfranco Parati (Italy)

Mihail Popovici (Moldova)

Fausto J. Pinto (Portugal)

Adam Torbicki (Poland)

Jarle Vaage (Norway)

Panagiotis Vardas (Greece)

Margus Viigimaa (Estonia)

Jose-Luis Zamorano (Spain)

EDITORIAL OFFICE

Managing Editor *Yulia V. Rodionova*

Secretary *Petr A. Kulakov*

e-mail: cardiodrug@yandex.ru

Assistant Managing Editor *Elena V. Ryzhova*

Science Editor *Elena Yu. Morosova*

Senior translator *Anton S. Kleschenogov*

Design, desktop publishing *Vladislava Yu. Andreeva, Elena Yu. Morosova*

Distribution department *Anna Guseva*

e-mail: guseva.silicea@yandex.ru

Advertising department *Alina Abrosimova*

Tel.: 8 (812) 702-37-49 ext. 005543

e-mail: partners@scardio.ru

CONTENTS

Address to the readers 4

ORIGINAL ARTICLES

- Amanatova V. A., Safiullina A. A., Uskach T. M., Ansheles A. A., Tereshchenko S. N., Sergienko V. B.* 5
Left ventricular myocardial cellular perfusion against the background of cardiac contractility modulation in patients with heart failure and atrial fibrillation
- Chistyakova M. V., Zaitsev D. N., Govorin A. V., Medvedeva N. A., Kurokhtina A. A.* 12
Post-COVID-19 syndrome: morpho-functional abnormalities of the heart and arrhythmias
- Geltser B. I., Shahgeldyan K. I., Rublev V. Yu., Shcheglov B. O., Kokarev E. A.* 19
Algorithm for selecting predictors and prognosis of atrial fibrillation in patients with coronary artery disease after coronary artery bypass grafting
- Chumarnaya T. V., Lyubimtseva T. A., Solodushkin S. I., Lebedeva V. K., Lebedev D. S., Solovieva O. E.* 27
Evaluation of the long-term effectiveness of cardiac resynchronization therapy
- Osadchy An. M., Semenyuta V. V., Kamenev A. V., Shcherbak S. G., Lebedev D. S.* 39
Electroanatomic substrate of atrial fibrillation in patients after COVID-19
- Ionin V. A., Zaslavskaya E. L., Barashkova E. I., Pavlova V. A., Borisov G. I., Averchenko K. A., Morozov A. N., Baranova E. I., Shlyakhto E. V.* 47
Molecular mechanisms of left atrial fibrosis development in patients with atrial fibrillation and metabolic syndrome: what biomarkers should be used in clinical practice?

Dear readers, colleagues and friends!

We would like to present you another issue of the Russian Journal of Cardiology on arrhythmology. Arrhythmology is a modern, rapidly developing area of medicine that combines clinical traditions and novel technologies. The problems of diagnosis, treatment and prevention do not lose their relevance since arrhythmias are a serious and sometimes fatal complication of cardiovascular diseases. More than 90% of sudden deaths are caused by ventricular arrhythmias. It should be noted that in Russia up to 300 thousand people die due to arrhythmia every year, and several million people suffer from cardiac arrhythmias, including atrial fibrillation, which cause about 70 thousand ischemic strokes per year. The number of inherited electrical heart diseases is on the rise. Prevalence of arrhythmias is continuously increasing in patients after COVID-19.

This issue was developed taking into account the relevant topics of modern science: clinical and interventional arrhythmology, pediatric, sports and geriatric arrhythmology, molecular and structural bases of arrhythmias, imaging and functional tests in arrhythmology, prevention and treatment of arrhythmogenic diseases.

A special role assigned to modern clinical research, fundamental and experimental arrhythmology and electrophysiology modeling, novel technologies, including in non-invasive diagnostics and treatment using radiofrequency catheter ablation.

Topics on translational and fundamental arrhythmology became an important section of the issue. The authors consider the most modern issues worldwide — mechanisms of arrhythmia development, artificial intelligence and mathematical modeling, cell biology, optical mapping and much more.

A separate area of issue was publications devoted to clinical guidelines and healthcare standards, remote monitoring, sudden death and ventricular arrhythmias, interventional, surgical and medication treatment of arrhythmias, arrhythmias in children, COVID-19 and arrhythmias, and stroke prevention.

It is worth noting that a characteristic feature of this issue is the works of authors presented at the IX All-Russian Congress of Arrhythmology held in May 2021 — Arrhythmology Without Frontiers: from a Research Lab to Clinical Guidelines. This is the main research and practical forum for specialists in many scientific fields, united by a common task — development, implementation and evaluation of diagnostic methods, treatment and prevention of cardiac arrhythmias. This year the congress was held in St. Petersburg, which gave the country doctors and scientists who laid the foundations of modern arrhythmology, as well as contemporaries, known for their intelligence and innovative approach, providing high-tech care to patients with arrhythmias not only in the north west, but also throughout the Russian Federation. For the first time, the Congress of Arrhythmology was held in 2005, while this event became the ninth and brought together more than a thousand participants from Russia and other countries.

The current number corresponds to motto of the last congress. We tried to show the versatility of the possibilities and achievements of modern arrhythmology, taking into account the relevance of published content for practical healthcare and scientific community. We hope this issue will be interesting and useful to you.

Best regards,

Sergey V. Popov, Vice President of the Russian Society of Arrhythmology, Academician of the Russian Academy of Sciences

Dmitriy S. Lebedev, Vice President of the Russian Society of Arrhythmology, Chief arrhythmologist of the Northwestern Federal District, Academician of the Russian Academy of Sciences



Sergey V. Popov



Dmitriy S. Lebedev



Left ventricular myocardial cellular perfusion against the background of cardiac contractility modulation in patients with heart failure and atrial fibrillation

Amanatova V. A.¹, Safiullina A. A.¹, Uskach T. M.^{1,2}, Ansheles A. A.¹, Tereshchenko S. N.^{1,2}, Sergienko V. B.¹

Aim. To assess the effect of cardiac contractility modulation (CCM) in patients with heart failure (HF) and atrial fibrillation (AF) on left ventricular (LV) myocardial cellular perfusion using perfusion single photon emission computed tomography (SPECT).

Material and methods. ^{99m}Tc-MIBI SPECT gated myocardial perfusion imaging was performed in 60 patients with HF and AF before implantation of CCM device and after 6-months follow-up. All patients received long-term optimal medication therapy for HF.

Results. The results obtained indicate a significant positive effect of CCM use in patients with HF and AF on LV ejection fraction (increase from 22 [18;30] to 25,5 [19;38] ($p=0,002$)), LV volume (decrease in LV end-systolic volume from 187 [114;238] to 154 [100;201] ($p=0,001$), end-diastolic volume from 229 [174;290] to 209 [159;259] ($p=0,007$)), as well as myocardial perfusion values. There is a favorable myocardial perfusion dynamic, which was more pronounced in non-ischemic HF: increase in SRS from 6 [5;9] to 8,0 [6;11] after 6 months ($p=0,01$)). The extent of impaired perfusion significantly decreases from 12 [9;17] to 9 [6;16] ($p=0,04$). An indicator reflecting the total impairment of LV myocardial perfusion significantly decreases: total perfusion deficit decreased from 10 [8;14] to 7 [6;14] after 6 months ($p=0,02$), compared with ischemia-related HF.

Conclusion. Perfusion SPECT makes it possible to assess the myocardial cellular perfusion during CCM therapy in patients with HF of various origin and AF. CCM therapy improves myocardial contractility and perfusion in patients with HF and AF.

Keywords: perfusion single photon emission computed tomography, heart failure, cardiac contractility modulation.

Relationships and Activities: none.

¹National Medical Research Center of Cardiology, Moscow;

²Russian Medical Academy of Continuous Professional Education, Moscow, Russia.

Amanatova V. A.* ORCID: 0000-0002-0678-9538, Safiullina A. A. ORCID: 0000-0002-2675-3276, Uskach T. M. ORCID: 0000-0003-4318-0315, Ansheles A. A. ORCID: 0000-0002-2675-3276, Tereshchenko S. N. ORCID: 0000-0001-9234-6129, Sergienko V. B. ORCID 0000-0002-0487-6902.

*Corresponding author: Amanatova.v@yandex.ru

Received: 13.12.2020

Revision Received: 17.02.2021

Accepted: 28.02.2021



For citation: Amanatova V. A., Safiullina A. A., Uskach T. M., Ansheles A. A., Tereshchenko S. N., Sergienko V. B. Left ventricular myocardial cellular perfusion against the background of cardiac contractility modulation in patients with heart failure and atrial fibrillation. *Russian Journal of Cardiology*. 2021;26(7):4238. (In Russ.) doi:10.15829/1560-4071-2021-4238

In developed countries, ~1-2% of the adult population have heart failure (HF), the risk of which increases with population aging; among patients over 70 years of age, it increases by 10% [1]. According to epidemiological studies, the proportion of HF in Russian population is 7%, including severe — 4,5% [2]. Atrial fibrillation (AF) is the most common arrhythmia in clinical practice. In the world, >33 million patients have AF, while every year it develops in more than 5 million people [3].

HF and AF are often combined with each other, having a negative effect on the patient's prognosis [4-7].

Currently, there is growing interest in a novel device-based therapy for HF — cardiac contractility modulation (CCM), indicated primarily to patients with HF and a QRS complex <130 ms [8-12]. The mechanism of CCM therapy is mediated through the cellular electrophysiology by applying a two-phase high voltage pulse to interventricular septum during the absolute refractory period of cardiomyocyte depolarization. MCC therapy is performed using implantable Optimizer system (Impulse Dynamics, Germany) [12].

With the advent of a novel device generation (Optimizer Smart®), which does not require implantation of an atrial lead, it became possible to use CCM in AF [13]. It seems important and relevant to study the effect of this method on left ventricular (LV) myocardial changes in patients with HF and AF.

For a comprehensive assessment of myocardium, a promising method is single-photon emission computed tomography (SPECT) [14]. The advantage of radioisotope diagnostic methods is that they can be used in patients with various implanted devices, as well as with impaired renal function. Perfusion radiopharmaceuticals (RP) based on ^{99m}technetium-methoxy-isobutyl-isonitrile (^{99m}Tc-MIBI) and tetrofosmin (^{99m}Tc-TF) penetrate the sarcolemmal and mitochondrial membranes of cardiomyocytes by passive diffusion with transmembrane electrochemical gradient and are retained in the mitochondria. In this case, it is possible to perform ECG-gated SPECT with estimation of all the necessary parameters of systolic and diastolic myocardial function [15, 16].

Regarding HF of ischemic origin, it is important to highlight such a concept as a hibernating myocardium, which is a viable areas with chronic reduced perfusion, reduced or absent contractility, but preserved metabolism and potential restoration of function with adequate therapy. According to myocardial perfusion SPECT, it is possible to assess the presence and area of hibernating myocardium by comparing perfusion and contractility maps [17]. It

can be assumed that CCM will have a favorable effect on areas of such myocardium, thereby improving both perfusion and myocardial contractility.

Considering the above, the aim was to assess the effect of CCM therapy in patients with HF and AF on LV myocardial cell perfusion using perfusion SPECT.

Material and methods

The study included 60 patients. Inclusion criteria were NYHA class II-III HF with reduced ejection fraction (EF) (not <20%) for at least 3 months, paroxysmal or permanent AF, optimal medication therapy for at least 3 months, stable condition >1 month, no left bundle branch block. There were following exclusion criteria: patient's refusal to participate in the study; inclusion in heart transplant waiting list, or after heart transplantation, NYHA class IV HF; acute diseases that, in the researcher's opinion, could adversely affect the safety and/or effectiveness of treatment; reversible HF causes; recent major surgery or trauma; recent cardiac events, including myocardial infarction, percutaneous coronary intervention, or heart surgery within previous 3 months; decompensated HF; acute myocarditis; hypertrophic obstructive cardiomyopathy; class IV angina; mechanical tricuspid valve replacement; impaired vascular access; medical conditions limiting life expectancy to 1 year. The follow-up period lasted 6 months.

All patients signed informed consent to undergo perfusion ^{99m}Tc-MIBI SPECT. The study was limited by contraindications to nuclear diagnostics (pregnancy, lactation, acute fever, acute mental disorders).

Perfusion SPECT was performed using a Phillips BrightView XCT system, which is a combined system equipped with a gamma camera and an X-ray computed tomograph. We used ^{99m}Tc-MIBI (10 mCi). The investigation was carried 30-45 minutes after its intravenous injection. Reconstruction and projection processing was carried out in the Cedar-Sinai AutoSPECT and QPS/QGS software package with iterative Astonish algorithm. Myocardial RP distribution at rest was analyzed by tomoscintigraphy and polar maps. Perfusion defects were assessed using standard 17-segment model with Summed Rest Score (SRS), Extent, and total perfusion deficit (TPD) parameters. SRS reflects the sum of relative perfusion disorder values — from 0 (normal) to 4 (transmural perfusion defect). The Extent reflects the area (in %) of significant perfusion disorders, and TPD is an integral parameter that takes into account both the area and depth of defects. These parameters are cumulative and do not take into account defect localization. Their high value can correspond to both

Table 1
Clinical and demographic characteristics of patients

Parameter	Value
Age, years	59 [56,0;66,0]
Men/women, %	51 (85%)/9 (15%)
HF etiology	
Old myocardial infarction	31 (51,6%)
DCM	29 (48,4%)
NYHA HF class	II ФК — 24 (40%)/ III ФК — 36 (60%)
LVEF, %	35,0 [28,0;34,5]
HF duration, months	24 [18,0;48,0]
AF duration, months	24 [12,0;48,0]
Paroxysmal AF	30 (50%)
Permanent AF	30 (50%)
Diabetes mellitus type 2, %	11 (27,5%)
BMI, kg/m ²	30 [27,0;34,5]

Abbreviations: DCM — dilated cardiomyopathy, CAD — coronary artery disease, BMI — body mass index, LVEF — left ventricular ejection fraction, AF — atrial fibrillation, HF — heart failure.

focal scarring and multiple diffuse defects caused by other causes [14]. In addition, the intensity of PR accumulation in each pixel receives its own shade and value as a percentage, which provides a visual assessment of perfusion distribution. This makes it possible to assess the relative perfusion for each segment of blood supply. Apical perfusion defects were considered on a case-by-case basis, since they are considered as a norm [15]. During ECG-gated SPECT, data were collected in 8 frames within the R-R interval and standard parameters of LV contractile function were analyzed: EF, end diastolic volume (EDV), end systolic volume (ESV) of LV [16].

Statistical analysis was carried out using the Excel 2010 and STATISTICA 10 software (StatSoft Inc., USA). Qualitative variables are presented as absolute values and percentages. The following statistical methods were used: two-sided Fisher's exact test, Mann-Whitney U-test. Correlation analysis was carried out using Spearman's rank correlation coefficient. The sample parameters shown in the table are presented as M (sd) and Me [Lq;Uq], where M is the mean, sd — standard deviation, Me — median, Lq;Uq — interquartile range. Differences were considered significant at $p < 0,05$.

Results and discussion

The clinical characteristics of patients are presented in Table 1.

Table 2
Changes of standard contractility parameters according to myocardial SPECT at rest

Parameter	Baseline	After 6 months	p
Contractility parameters			
LVEF	22 [18;30]	25,5 [19;38]	0,002
LV EDV	229 [174;290]	209 [159;259]	0,007
LV ESV	187 [114;238]	154 [100;201]	0,001
CO	3,5 [3,02;4,2]	3,9 [2,9;4,9]	0,5

Abbreviations: LV EDV — left ventricular end diastolic volume, LV ESV — left ventricular end systolic volume, CO — cardiac output, LVEF — left ventricular ejection fraction.

Of 60 patients included in the study, 85% were men and 15% were women (age, 59 [56;66] years). There were 40% of all patients with class II HF, 60% — class III HF. The study included patients with paroxysmal (n=30) and permanent (n=30) AF. The median LVEF at inclusion in the study according to echocardiography was 35 [28,0;34,5] %.

Repeated myocardial SPECT was performed in patients 6 months after implantation of CCM.

Changes in standard parameters of contractility and perfusion according to myocardial SPECT is presented in Table 2.

It should be noted that ejection fraction is estimated with echocardiography using a special equation after measuring the LV linear parameters (end diastolic and systolic dimensions), while its correctness depends on accuracy of determining these indicators [17]. With SPECT, LV volumetric parameters are initially obtained (EDV and ESV), and the LVEF is estimated automatically. In addition, when calculating EDV and ESV, the average cardiac cycle is used, which is the sum of all cardiac beats (except for premature contractions) recorded (10 min) under ECG guidance [18-21]. Due to the different methods of estimating LVEF with these two research methods, its values may differ, and according to SPECT, LVEF is usually on average 7-10% lower than with echocardiography.

After 6 months, all patients (n=60) with HF and AF had a significant increase in LVEF according to SPECT from 22 [18;30] to 25,5 [19;38] ($p=0,002$). There is a significant decrease in both LV ESV from 187 [114;238] to 154 [100;201] ($p=0,001$) and EDV from 229 [174;290] to 209 [159;259] ($p=0,007$). A decrease in perfusion disorder indicators such as SRS, Extent, TPD was obtained.

According to generally accepted technique, CCM leads are implanted into the interventricular septum in right ventricle. CCM stimuli directly act on myocardium with an area of 4×7 cm due to spread along the peripheral conduction system.

Table 3

Changes of LV contractility parameters depending on HF origin according to C-SPECT

Parameters	Ischemic HF (n=31)		p	Non-ischemic HF (n=29)		p
	Baseline	After 6 months		Baseline	After 6 months	
LVEF	21 [17,5;26,0]	25 [18;25]	0,01	23 [18;30]	37,5 [20;41]	0,009
LV EDV	255 [221;290]	221 [209;262]	0,09	226 [165;290]	162 [135;250]	0,03
LV ESV	192 [171;226]	166 [155;220]	0,08	170 [107;240]	102 [86;164]	0,005
CO	3,4 [2,9;3,8]	3,7 [3,0;4,5]	0,2	3,8 [3,1;4,3]	4,2 [2,7;4,9]	0,5

Abbreviations: LV EDV — left ventricular end diastolic volume, LV ESV — left ventricular end systolic volume, CO — cardiac output, LVEF — left ventricular ejection fraction, HF — heart failure.

Table 4

LV myocardial perfusion parameters depending on HF origin according to myocardial C-SPECT

Parameters	Ischemic HF (n=31)		p	Non-ischemic HF (n=29)		p
	Baseline	After 6 months		Baseline	After 6 months	
SRS	24 [17;34]	23,5 [17;30,5]	0,2	8,0 [6;11]	6 [5;9]	0,01
Extent	44 [29,5;52]	42 [31;51]	0,9	12 [9;17]	9 [6;16]	0,04
TPD	36,5 [23;52]	39 [23;46]	0,8	10 [8;14]	7 [6;14]	0,02

Abbreviations: SRS — summed rest score, TPD — total perfusion deficit.

The effect on activity of key regulatory proteins (phospholamban) is immediately obtained [22]. This quick response helps to restore cell function and increase the contraction strength. Further, local changes lead to a decrease in stress in distant myocardial areas and, over time, to normalization of gene expression. The electrical communication between cells is improved and direct effect of stimuli is increased. Over the months, a significant stress reduction can be observed, which disrupts the remodeling cascade, which promotes reverse remodeling. Studies containing a biopsy examination confirm the development of effect after 3 months [23].

In addition to myocardial perfusion, cardiac SPECT allows to assess its contractility. In this study, it was possible to determine HF nature, since perfusion in ischemic and non-ischemic genesis have precise quantitative parameters. To assess the parameters of perfusion and contractility depending on HF etiology, patients were divided into 2 groups: ischemic (n=31) and non-ischemic (n=29) HF origin.

Standard contractility parameters according to SPECT are presented in Table 3. In the group of patients with ischemic HF origin, there is a significant increase in LVEF from 21 [17,5;26,0] to 25 [18;25] ($p=0,01$). There is a decrease in LV volumes, however, it does not reach significance at the moment. An insignificant increase in cardiac output is also recorded. In the group of patients

with non-ischemic HF origin, LVEF significantly increases from 23 [18;30] to 37,5 [20;41] ($p=0,009$). LV volumes decreased: EDV — from 226 [165;290] to 162 [135;250] ($p=0,03$), ESV — from 170 [107;240] to 102 [86;164] ($p=0,005$). Cardiac output increased, but not significant.

Table 4 shows the standard myocardial perfusion parameters in groups of patients with different HF origin.

SRS is the summed index of deep perfusion defects in all segments of perfusion map at rest. This indicator allows to draw a clear boundary between patients with heart failure of ischemic and non-ischemic origin. So, for patients with significant myocardial scarring, $SRS \geq 15$ is characteristic. At the same time, in patients with non-ischemic HF origin, SRS, as a rule, vary in the range from 0 to 15.

In the group of patients with ischemic HF origin, no significant perfusion changes were revealed with CCM therapy, which is due to irreversible perfusion defects, and also partly due to chronic impairment of myocardial blood supply (for example, due to chronic coronary total occlusions). Figures 1 and 2 show an example of myocardial SPECT of the patient with ischemic HF origin.

The patient had prior myocardial infarction, as a result of which a large anterior-apical-lateral perfusion defect developed. The SRS amounted to 36, Extent — 51%, TPD — 46%. Initially, there was a sharply reduced systolic wall thickening, decreased LVEF, and significant dilatation of cardiac cavities.

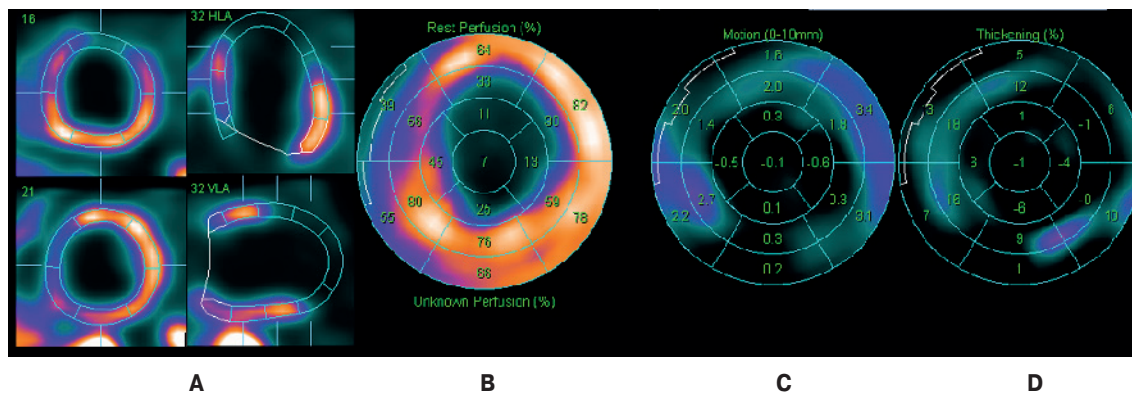


Figure 1. Initial myocardial perfusion SPECT in the patient with ischemic HF. **A.** Perfusion scintigrams. **B.** Polar map of LV perfusion. Uneven RP distribution. A large-focal perfusion defect (transmural old myocardial infarction) of the apex, apical and middle segments of the anterior, anterolateral walls with spread to the apical and partially middle segments of the anterior septal wall and apical segments of LV inferior wall with a total area of about 40% of LV is visualized. **C.** Polar map of systolic LV wall motion. LV dilatation, diffuse hypo(a) kinesis, dyskinesia of the apex, apical segments of the lateral, septal walls of LV (signs of fibromuscular aneurysm, EDV of 411 ml, ESV of 378 ml, stroke volume of 33 ml, LVEF of 8% ($N>50\%$) with heart rate of 84 bpm, cardiac output of 2,7 l/min). **D.** Polar map of LV systolic wall thickening. Systolic thickening of all LV walls is sharply reduced.

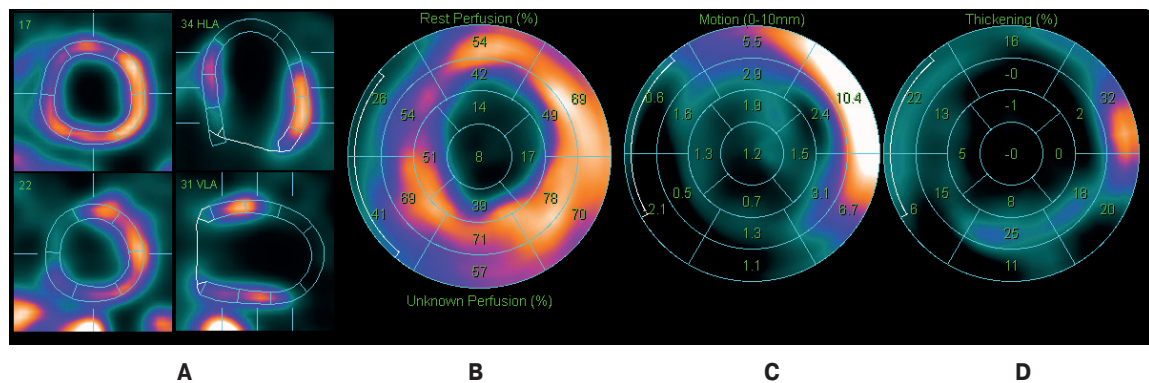


Figure 2. Myocardial perfusion SPECT of the patient with ischemic HF after CCM device implantation. **A.** Perfusion scintigrams. **B.** Polar map of LV perfusion. No worsening. Anterior-apical-lateral perfusion defect persists with the development of an aneurysm with an area of 35%. **C.** Polar map of systolic LV wall motion. LV dilatation, diffuse hypo(a)kinesis, dyskinesia of the apex, apical segments of the lateral, septal walls of LV (signs of fibromuscular aneurysm), EDV of 361 ml, ESV of 299 ml, LVEF of 17% ($N>50\%$). **D.** Polar map of LV systolic wall thickening. Systolic thickening is moderately restored in the inferolateral and anterolateral LV segments.

With repeated SPECT 6 months after CCM device implantation, there is an increase in LVEF and a decrease in LV volumes. Perfusion defect parameters also show a favorable trend: SRS decreases to 32, Extent — 49%, TPD — 44%. However, in patients with ischemic HF origin, a significant perfusion improvement did not occur due to stable perfusion defect after myocardial infarction.

In the group of patients with non-ischemic HF etiology, there was a significant decrease in deep perfusion defects — SRS after 6 months of 6 [5;9] compared with the initial SRS of 8 [6;11] ($p=0,01$). The Extent significantly decreases from 12 [9;17] to 9 [6;16] ($p=0,04$), while TPD decreases from 10 [8;14] to 7 [6;14] ($p=0,02$).

Non-ischemic HF is characterized by dilatation of cardiac cavities and, as a consequence, relative coronary insufficiency with unchanged or slightly altered coronary arteries. Pathological examination in such patients reveals microvasculature impairment, in particular, disorganization and atrophy of basement membranes of supplying vessels and a ruffled endothelial lining with pinocytotic activity. In addition, there is a high detection rate of microthrombi, prestasis and stasis of blood corpuscles [24]. In this case, CCM stimuli lead to an increase in intracellular calcium content and, as a consequence, to an increase in cardiomyocyte contractile force due to the phosphorylation of phospholamban, which is responsible for the activity of

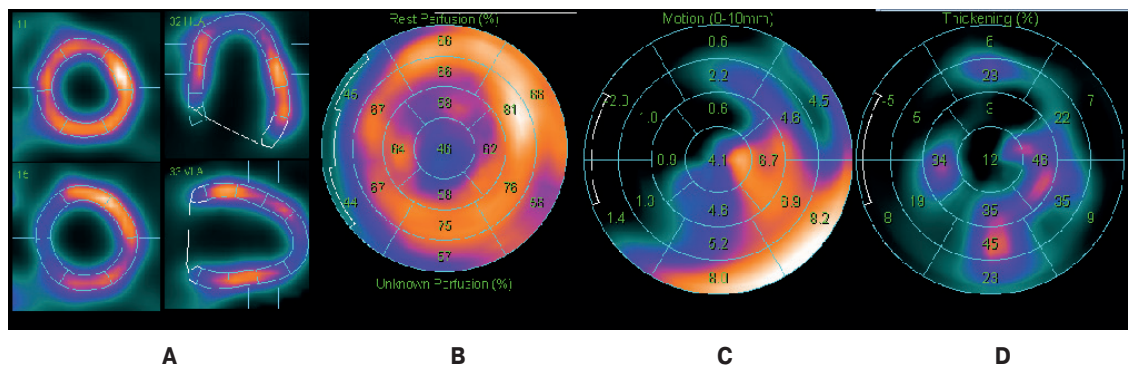


Figure 3. Initial myocardial perfusion SPECT in the patient with non-ischemic HF.

A. Perfusion scintigrams. **B.** Polar map of LV perfusion. There is a diffuse uneven RP distribution, no reliable focal defects. Signs of small focal perfusion defects in the septal and inferolateral LV segments. **C.** Polar map of systolic LV wall motion. LV dilatation, diffuse hypo(a) kinesis of all LV walls, except for the inferolateral, up to dyskinesia of the anterior and septal LV segments. EDV of 139 ml, ESV of 97 ml, stroke volume of 42 ml, LVEF of 30% (N>50%) with heart rate of 117 bpm, cardiac output of 4,7 l/min. **D.** Polar map of LV systolic wall thickening. Systolic thickening of all LV walls is sharply reduced.

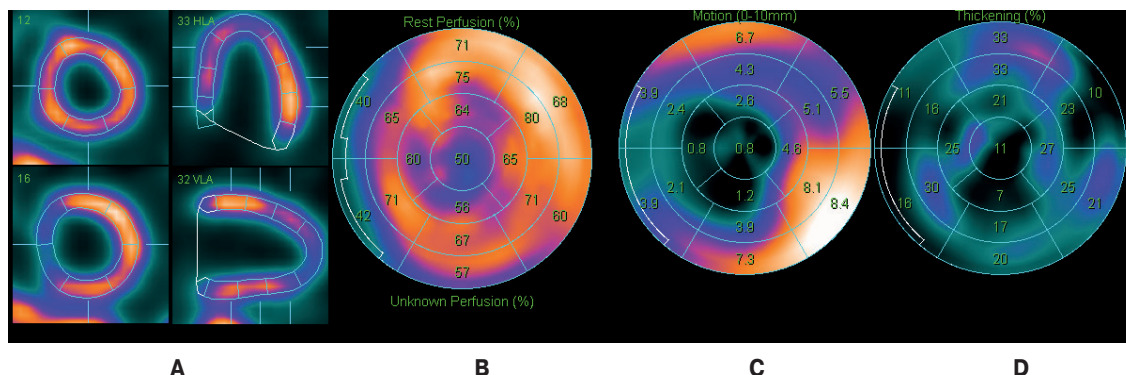


Figure 4. Myocardial perfusion SPECT of the patient with non-ischemic HF after CCM device implantation.

A. Perfusion scintigrams. **B.** Polar map of LV perfusion. No worsening. **C.** Polar map of systolic LV wall motion. Reduction of LV cavity, restoration of systolic motion almost to normokinesis along all LV walls, except for the septal one. EDV of 125 ml, ESV of 79 ml, stroke volume of 46 ml, LVEF of 37% (N>50%) with heart rate of 86 bpm, cardiac output of 3,9 l/min. **D.** Polar map of LV systolic wall thickening. Reduction of LV systolic wall thickening persists.

sarco/endoplasmic reticulum Ca²⁺ adenosine triphosphatase-2a (SERCA2a). In the early CCM therapy stages, there is a local effect, then a change in SERCA2a expression in other parts of ventricular myocardium occurs. Thus, CCM therapy has a positive inotropic effect without increasing myocardial oxygen demand [25]. The positive inotropic effect of CCM therapy is probably a stimulus to reverse myocardial remodeling activation, including improving the state of capillary endothelium, and, consequently, improving microcirculation and cell perfusion in patients with non-ischemic HF.

As an illustration of changes of contractility and perfusion parameters according to myocardial SPECT at rest, a patient with non-ischemic HF is shown as an example in Figures 3 and 4.

At baseline, this patient had SRS of 7, Extent score of 11%, and TPD score of 8%. There is a sharply reduced systolic wall thickening, decreased

LVEF, and significant dilatation of cardiac cavities.

Six months after implantation of CCM device, there is an increase in LVEF up to 37% and a decrease in LV volumes. Perfusion defect parameters also show favorable dynamics: SRS decreases to 6 points, Extent — 8%, TPD — 7%

Conclusion

It should be noted that in none of the previous studies in patients with CCM therapy, the assessment of myocardial cell perfusion using SPECT was carried out. Thus, the results of our work for the first time show the effect of CCM therapy on myocardial contractility and cellular perfusion in patients with HF with reduced EF and AF. Taking into account the data obtained, CCM therapy is able to improve perfusion and myocardial contractility according to SPECT in patients with HF of non-ischemic

origin. In patients with ischemic HF, there was no significant improvement in perfusion, which is most likely due to irreversible myocardial scarring. In such patients, it is necessary to study other ways for improving contractile function, one of which is a decrease in hibernating myocardium extent.

Summarizing the above, it should be noted that SPECT is a promising and relevant method for assessing myocardial cell perfusion in patients with implanted devices, including CCM.

Relationships and Activities: none.

References

- Ponikowski P, Voors AA, Anker SD, et al. 2016 ESC Guidelines for the diagnosis and treatment of acute and chronic heart failure. The Task Force for the diagnosis and treatment of acute and chronic heart failure of the European Society of Cardiology (ESC) Developed with the special contribution of the Heart Failure Association (HFA) of the ESC. *Rev Esp Cardiol (Engl Ed)*. 2016;69(12):1167. doi:10.1016/j.rec.2016.11.005.
- Ageev FT, Belenkov UN, Fomin IV, et al. Prevalence of chronic heart failure in the European part of the Russian Federation data from EPOCH-CHF. *Chronic Heart Failure*. 2006;7(1):112-5. (In Russ.)
- Chugh S, Havmoeller R, Narayanan K. Worldwide epidemiology of atrial fibrillation: a global burden of disease 2010 study. *Circulation*. 2014;129:837-47.
- Wang T, Larson M, Levy D. Temporal relations of atrial fibrillation and congestive heart failure and their joint influence on mortality: the Framingham Heart Study. *Circulation*. 2003;107:2920-5.
- Maisel W, Stevenson L. Atrial fibrillation in heart failure: epidemiology, pathophysiology and rationale for therapy. *Am J Cardiol*. 2003;91(6A):2D-8D.
- The SOLVD Investigators. Effect of enalapril on mortality and the development of heart failure in asymptomatic patients with reduced left ventricular ejection fractions. *N Engl J Med*. 1992;327:685-91.
- Zhirov IV, Romanova NV, Tereshchenko SN, Osmolovskaya YuF. Epidemiology and management of heart failure patients with atrial fibrillation. *Kardiologiya*. 2015;55(3):91-6. (In Russ.) doi:10.18565/cardio.2015.3.91-96.
- McMurray JJV, Adamopoulos S, Anker SD, et al. Erratum: ESC Guidelines for the diagnosis and treatment of acute and chronic heart failure 2012. *Eur. J. Heart Fail*. 2013;15(3):361-2.
- Russian Society of Cardiology (RSC). 2020 Clinical practice guidelines for Chronic heart failure. *Russian Journal of Cardiology*. 2020;25(11):4083. (In Russ.) doi:10.15829/1560-4071-2020-4083.
- Packer DL, Prutkin JM, Hellkamp AS, et al. Impact of implantable cardioverter-defibrillator, amiodarone, and placebo on the mode of death in stable patients with heart failure: Analysis from the sudden cardiac death in heart failure trial. *Circulation*. 2009;120(22):2170-6. doi:10.1161/CIRCULATIONAHA.109.853689.
- Cleland JGF, Daubert J-C, Erdmann E, et al. Longer-term effects of cardiac resynchronization therapy on mortality in heart failure [the CARDiac RESynchronizationHeart Failure (CARE-HF) trial extension phase]. *Eur. Heart J*. 2006;27(16):1928-32. doi:10.1093/eurheartj/ehl099.
- Pappone C, Vicedomini G, Salvati A, et al. Electrical modulation of cardiac contractility: clinical aspects in congestive heart failure. *Heart Failure Reviews*. 2001;6(1):55-60.
- Kloppe A, Boesche L, Aweimer A, et al. Acute and short-term safety and feasibility of the new OPTIMIZER SMART-system: Is it reasonable to avoid an atrial lead? *EP Europace*. 2018;20(suppl_1):i48. doi:10.1093/europace/euy015.128.
- Verberne HJ, Acampa W, Anagnostopoulos C, et al. EANM procedural guidelines for radionuclide myocardial perfusion imaging with SPECT and SPECT/CT: 2015 revision. *Eur J Nucl Med Mol Imaging*. 2015;42(12):1929-40. doi:10.1007/s00259-015-3139-x.
- Ansheles AA, Sergienko VB. Interpretation of myocardial perfusion SPECT with attenuation correction. Part 2. *Bulletin of Radiology and Radiology*. 2020;101(1):6-18. (In Russ.) doi:10.20862/0042-4676-2020-101-1-6-18.
- Braunwald's heart disease: a textbook of cardiovascular medicine, Peter Libby, et al., 8th ed. Volume 1: Moscow: Logosphere, 2015. 624 p. (In Russ.) ISBN 978-5-98657-048-8.
- Trufanov GE. Myocardial perfusion scintigraphy. ELBI-SPb Russia. 2012. 80 p. (In Russ.)
- Rahimtoola SH. The hibernating myocardium. *Am Heart J*. 1989;117(1):211-21. doi:10.1016/0002-8703(89)90685-6-14.
- Practical echocardiography: A guide to echocardiographic diagnostics. Eds. Flakskampf FA, Sandrikova VA. 2 Ed. M.: MEDpress-inform, 2019. 872 p. (In Russ.)
- Ansheles AA. Specific features of interpretation of myocardial perfusion single-photon emission computed tomography with computed tomographic absorption correction. *Journal of radiology and nuclear medicine*. 2014;(2):5-20. (In Russ.) doi:10.20862/0042-4676-2014-0-2-5-20.
- Bugri ME, Satlykova DF, Mareev VYu, Sergienko VB. D-tomoventriculography — a novel method in diagnostics of contractile function of the heart. *Cardiology*. 2009;49(6):54-60. (In Russ.)
- Butter C, Rastogi S, Minden H-H, et al. Cardiac Contractility Modulation Electrical Signals Improve Myocardial Gene Expression in Patients With Heart Failure. *JACC*. 2008;51(18):1784-9. doi:10.1016/j.jacc.2008.01.036.
- Imai M, Sabbah HN. Therapy with Cardiac Contractility Modulation Electrical Signals Improves Left Ventricular Function and Remodeling in Dogs with Chronic Heart Failure. *JACC*. 2007;49(21):2120-8.
- Amosova EN. *Cardiomyopathy*. Kiev. Book plus. 1999. 182 p. (In Russ.)
- Mareev YuV. Modulation of cardiac contractility in the treatment of patients with chronic heart failure. *Circulatory pathology and cardiac surgery*. 2014;18(4):158-63. (In Russ.)



Post-COVID-19 syndrome: morpho-functional abnormalities of the heart and arrhythmias

Chistyakova M. V., Zaitsev D. N., Govorin A. V., Medvedeva N. A., Kurokhtina A. A.

Aim. To study the myocardial morpho-functional abnormalities, the incidence and nature of cardiac arrhythmias in patients 3 months after the coronavirus disease 2019 (COVID-19).

Material and methods. The study included 77 patients (mean age, 35,9 years) treated for coronavirus infection, which underwent echocardiography and 24-hour Holter monitoring 3 months after COVID-19. The patients were divided into 3 groups: group 1 — 31 patients with upper respiratory tract involvement; group 2 — 27 patients with bilateral pneumonia (CT grade 1, 2), 3 — 19 patients with severe pneumonia (CT grade 3, 4). Statistical processing was carried out using Statistica 10.0.

Results. According to echocardiography, the peak tricuspid late diastolic velocity and isovolumetric contraction time in all groups increased ($P<0,001$). The tricuspid and mitral Em/Am ratio decreased depending on the disease severity. In group 3, the right ventricular and atrial size increased ($P<0,001$). The pulmonary artery systolic pressure, left atrial volume in patients of the 2nd and 3rd groups was higher than in the control one ($P<0,001$). In group 1 and 2 patients, the regional strain in basal and basal/middle segments decreased, respectively, while, in group 3, not only regional but also global left ventricular (LV) strain decreased ($P<0,001$). In all groups, cardiac arrhythmias and pericardial effusion were found. The relationship was established between coronavirus activity and the structural and functional myocardial parameters ($P<0,001$).

Conclusion. Cardiovascular injury 3 months after COVID-19 was found in 71%, 93%, and 95% of patients with mild,

moderate and severe course. In mild course patients, a decrease in regional myocardial strain in LV basal segments, signs of past pericarditis, and various cardiac arrhythmias were noted. In patients of moderate severity, these changes were more pronounced and were accompanied by an additional decrease in regional strain in LV middle segments, impaired right ventricular diastole and increased pulmonary artery pressure. In severe patients, in addition to the above changes, dilatation of the right heart and inferior vena cava was recorded, as well as LV diastolic and global systolic function decreased.

Keywords: heart, COVID-19, arrhythmia.

Relationships and Activities: none.

Chita State Medical Academy, Chita, Russia.

Chistyakova M.V.* ORCID: 0000-0001-6280-0757, Zaitsev D.N. ORCID: 0000-0002-2741-3783, Govorin A.V. ORCID: 0000-0003-1340-9190, Medvedeva N.A. ORCID: 0000-0002-3602-4034, Kurokhtina A.A. ORCID: 0000-0002-7086-773X.

*Corresponding author:
marina_vladi@internet.ru

Received: 25.04.2021

Revision Received: 08.06.2021

Accepted: 03.07.2021



For citation: Chistyakova M. V., Zaitsev D. N., Govorin A. V., Medvedeva N. A., Kurokhtina A. A. Post-COVID-19 syndrome: morpho-functional abnormalities of the heart and arrhythmias. *Russian Journal of Cardiology*. 2021;26(7):4485. (In Russ.) doi:10.15829/1560-4071-2021-4485

A dangerous infectious disease, coronavirus disease 2019 (COVID-19), is still characterized by high morbidity and mortality. It is known that mild to moderate course is most common, but majority of COVID-19 survivors note a slow recovery rate. A year after the pandemic start, it was established that the virus is dangerous with long-term complications (post-COVID-19 syndrome). Thus, numerous studies confirm long-term involvement of some organs and systems, including the lungs, brain, kidneys, as well as the cardiovascular system with developing severe heart injury [1-13]. There is evidence that there is a direct effect of virus on cardiomyocytes with destruction, as well as vascular endothelial damage with impaired microcirculation and formation of multiple thrombosis [1-2]. In some patients, as a result of immune response, a cytokine storm develops causing fulminant myocarditis, heart failure, and cardiogenic shock [2, 4, 11]. Myocardial damage can also result from aggressive treatment methods for COVID-19 [7].

When studying the cardiovascular system of professional athletes in the United States, the detection rate of myocarditis after COVID-19 (mild or asymptomatic) ranged from 15% to 30% [13]. At autopsy of 39 patients after COVID-19, SARS-CoV-2 virus were found in the heart in more than 60%, while 16 people had clinically significant levels of tissue viral load at the time of death [14]. In addition, a cardiovascular involvement was revealed in patients on average 71 days after COVID-19 diagnosis [15]. According to magnetic resonance imaging, in 78% of subjects, an increase in the volume and mass of myocardium and a decrease in left ventricular (LV) ejection fraction (LVEF) were found; myocardial biopsy revealed active lymphocytic inflammation in 60% of patients [15].

In this regard, the aim of our study was to investigate myocardial morpho-functional abnormalities, the incidence and nature of cardiac arrhythmias in patients 3 months after COVID-19.

Material and methods

Seventy-seven patients treated for COVID-19 3 months (median, 98 days) after the diagnosis, the heart was examined: echocardiography using Vivid E95 ultrasound system, Holter electrocardiography (ECG) monitoring (HM). The virus was identified with polymerase chain reaction test for SARS-CoV-2. All COVID-19 survivors before the disease were practically healthy and did not note chronic diseases, including cardiovascular ones. The patients were divided into 3 groups: 1 (n=31) — patients without complications (with upper respiratory tract involvement), who were treated on an outpatient basis (according to computed tomography (CT),

lungs were not involved); 2 (n=27) — patients with bilateral, multisegmental, viral/bacterial pneumonia, CT 1, <25% (n=16) and CT 2, 25-50% (n=11); 3 (n=19) — patients with severe course, CT 3-4 (n=11), CT 4 (n=8). The mean age of patients in group 1 was 35,5 [23; 46] years, 2 — 36 [27; 43,5] years, 3 — 36,9 [35,2; 48] years. According to CT, all patients of group 2 had bilateral lung involvement, moderate fibrous and interstitial changes, pleuropulmonary adhesions, and irregular-shaped ground-glass opacities. In patients of group 3 with moderate fibrous and interstitial changes, dense areas of parenchymal infiltration are observed due to interstitial interlobular and consolidation. Patients in both groups had single moderately enlarged mediastinal lymph nodes. Group 1 patients took antiviral drugs, vitamin C, diazolin. Patients of groups 2 and 3 received antibiotics of the macrolide group, third-generation cephalosporins, anti-coagulants, expectorant and antiviral drugs. Patients of group 3 were also prescribed detoxification agents. In addition, 17 (58%) patients in group 2 and all patients in group 3 were prescribed conventional hydroxychloroquine therapy. It should be noted that according to current guidelines of the Russian Ministry of Health for prevention, diagnosis and treatment of COVID-19 (version 11, revision of 07.05.2021), hydroxychloroquine is excluded from the list of recommended therapy at all disease stages, while this study was conducted at the time of earlier guidelines version, which included chloroquine drugs in combination therapy for COVID-19.

The control group consisted of 22 healthy volunteers of comparable age without COVID-19, who had negative test for anti-SARS-CoV-2 IgM and IgG antibodies.

Doppler echocardiography was performed according to standard technique using VIVID E95 ultrasound system. Doppler echocardiography was performed using apical 2- and 4- chamber view. Spectral Doppler signal was recorded from annulus of mitral, tricuspid valves and ventricular segments. The following parameters were estimated: peak myocardial systolic (Sm), early diastolic (Em), and late diastolic (Am) velocities, Em/Am ratio, myocardial isovolumetric contraction (IVC) period, isovolumetric relaxation (IVR) period.

Regional longitudinal strain and LV strain rate were investigated using two-dimensional non-Doppler strain imaging. The investigation was performed using the apical long axis view with a frame rate of 50 to 80 frames per sec with ECG monitoring. Endocardium was manually traced, while epicardial surface was traced automatically. The program estimated from frame to frame the displacement of spots area-of-interest throughout

Table 1

Doppler echocardiography and Holter ECG monitoring data in patients after COVID-19

Parameters	Control, n=22	Group 1, n=31	Group 2, n=27	Group 3, n=19
Tricuspid A, cm/s	0,29 [0,27;0,31]	0,33 [0,32;0,41]*	0,41 [0,38;0,48]*,†	0,49 [0,3;0,6]*,†,§
Tricuspid annular Am, cm/s	0,13 [0,11;0,14]	0,15 [0,11;0,18]*	0,16 [0,12;0,18]*,†	0,41 [0,38;0,88]*,†,§
Tricuspid annular Em/Am	1,21 [1,09;1,31]	0,91 [0,90;1,36]*	0,8 [0,65;1,06]*,†	0,73 [0,38;0,92]*,†,§
IVC, ms (RV)	67,3 [62,5;72,4]	81,5 [73;82]	82 [72,7;98,5]	92 [71;99,1]*
Inferior vena cava diameter, mm	17,3 [15,2;20,1]	20,5 [12,4;21,3]	21,9 [15,3;22,4]	26,3 [24,8;27,4]*
RV, mm	27 [22,1;32,3]	29,4 [22,9;33,1]	32,8 [25,3;35,8]	34,2 [28,1;35,1]*,†,§
RAVI, ml/m ²	21,3 [18,4;22,8]	21,8 [20,7;24,5]	22,5 [18,9;23,3]	25 [24,1;25,4]*,†,§
LA pressure, mm Hg	27,3 [22,1;32,3]	29,4 [22,9;33,1]	35,8 [25,9;36,8]*	39,7 [28,1;45,2]*,§
Mitral annular Em/Am	1,3 [1,2;1,77]	1,36 [1,04;1,7]	1,1 [0,8;1,36]*	0,9 [0,3;1,42]*,†,§
Mitral annular Em, cm/s	13,3 [9,1;15,4]	12 [10,1;15,18]*	10 [8,12;13,18]*	9,3 [6,42;12,1]*,†,§
LAVI, ml/m ²	20,3 [18,5;23,4]	22,5 [20,75;23,5]	22,8 [20,4;24,1]*	24,2 [24,8;26,4]*,§
E/Em	6,13 [5,11;7,14]	6,15 [5,11;7,18]	7,16 [7,12;9,18]*	8,1 [8,42;12,88]*,§
SDNN	136 [122;177]	121 [107;173]*	104 [97;197]*	117 [96;210]*
Lf/Hf	2,57 [2,49;3,6]	3,39 [2,5;4,9]*	5,5 [2,9;6,8]*	4,9 [2,5;6,1]*

Note: * — significance of differences compared with control group ($P < 0,001$), † — significance of differences compared with group 1 ($P < 0,001$), § — significance of differences compared with group 2 ($P < 0,001$).

Abbreviations: Tricuspid A, cm/s — peak late diastolic tricuspid velocity; Tricuspid annular Am, cm/s — late diastolic tricuspid annular velocity; IVC, ms (RV) — tricuspid annular isovolumetric contraction period; RV, mm — right ventricle diastolic dimension; RAVI, ml/m² — right atrial volume index; Mitral annular Em/Am — diastolic mitral annular velocity ratio; LAVI, ml/m² — left atrial volume index; E/Em — left ventricular filling pressure; SDNN — standard deviation of all normal sinus R-R intervals; Lf/Hf — ratio of power in the high frequency band of HRV spectrum (0,15-0,40 Hz) to power in the low frequency band of HRV spectrum (0,04-0,15 Hz).

the entire cardiac cycle. After optimization of area-of-interest, the software generated strain curves for each segment.

Holter ECG monitoring was performed using the Astrocad system. The analysis of heart rate variability (HRV) was carried out in accordance with guidelines of the European Society of Cardiology and the North American Society of Pacing and Electrophysiology. HRV was studied by statistical analysis obtained with 24-hour ECG monitoring, with the estimation of following parameters: 1) temporal: average heart rate in 1 min, standard deviation of all normal sinus R-R intervals (SDNN), standard deviation of the 5-minute mean R-R intervals (SDANN), SDNN index, root mean square of consecutive R-R intervals (RMSSD), and percentage of successive R-R intervals differing by more than 50 ms (pNN50); 2) spectral, obtained using the fast Fourier transform: power in the high frequency band of HRV spectrum (0,15-0,40 Hz) — HF, power in the low frequency band of HRV spectrum (0,04-0,15 Hz) — LF, LF/HF ratio. The study was carried out in accordance with Good Clinical Practice and Declaration of Helsinki. The study protocol was approved by the ethics committees of all participating clinical centers. Written informed consent was obtained

from all participants. There were no potential study limitations. Statistical processing was carried out using the statistical software package Statistica 10.0. Distribution of almost all variation series was non-normal; therefore, the analysis used nonparametric statistics methods. Differences between groups were assessed using the nonparametric Mann-Whitney test. Correlation analysis was performed using Spearman's rank correlation coefficient.

Results

Ninety eight [92; 103] days after the diagnosis of COVID-19, almost all patients with mild (n=26; 83,8%), moderate (n=24; 89%) and severe course (n=18; 94,7%) had complaints for asthenia, fatigue, performance impairment, sleep loss. Chest pain was noted by 4 (13%) patients of group 1, 9 (33,3%) patients of group 2 and 11 (57%) of group 3, while mixed dyspnea was found in 7 (22,5%), 14 (51,8%) and 12 (63%) patients, respectively. Palpitations was revealed in 3 (9,6%) patients with mild COVID-19, 10 (37%) patients with moderate and 15 (78%) patients with severe disease. Hypertension was detected in 4 (12,9%), 4 (14,8%) and 9 (47%) patients of group 1, 2 and 3, respectively.

According to echocardiography, the peak late diastolic tricuspid velocity (A), as well as late

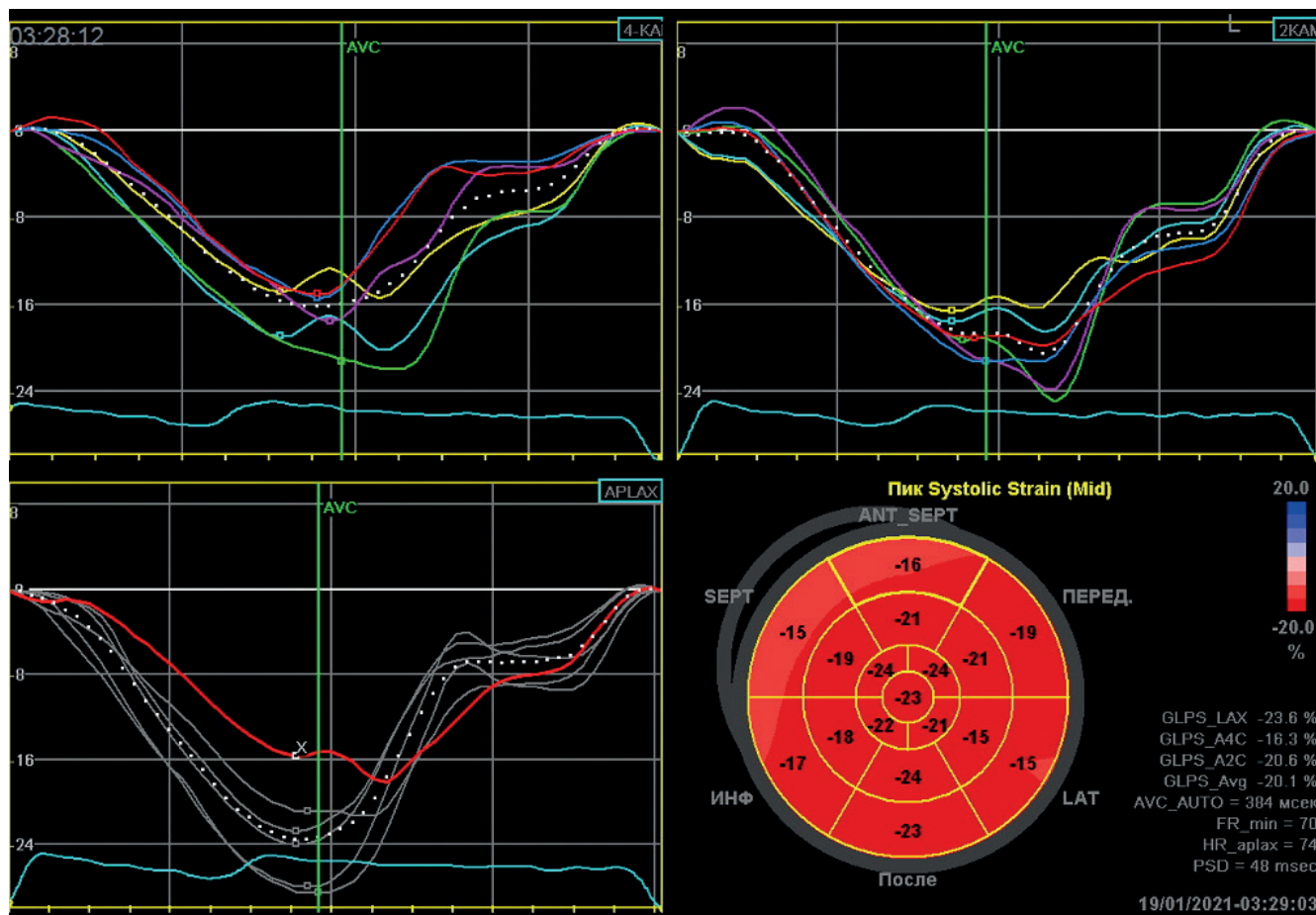


Figure 1. Regional diastolic strain in Bull's Eye mode in a patient of group 1 after COVID-19. A decrease in regional systolic function in the LV basal septal, basal antero-septal and anterior segments is revealed.

diastolic tricuspid annular velocity (A_m) increased in all groups, while the E_m/A_m ratio, on the contrary, decreased depending on disease severity (Table 1) ($P < 0,001$). Right ventricular (RV) IVC period and inferior vena cava diameter were higher in patients in group 3, in contrast to the control group. There was an increase in right heart sizes in patients with a severe COVID-19. The systolic pulmonary artery pressure in patients of groups 2 and 3 was higher than in the control group, while the highest value was in patients with a severe disease course and amounted to 39,7 [28,1; 45,2] mm Hg. The established changes suggest an impaired RV diastolic function in patients after COVID-19, and these violations worsened with an increase in disease severity. Patients with severe COVID-19 also showed an increase in right heart sizes, inferior vena cava and pulmonary artery pressure.

When studying LV diastolic function by tissue Doppler echocardiography in patients of groups 2 and 3, a decrease in E_m/A_m ratio and E_m in comparison with the control group was revealed, while more pronounced abnormalities were found

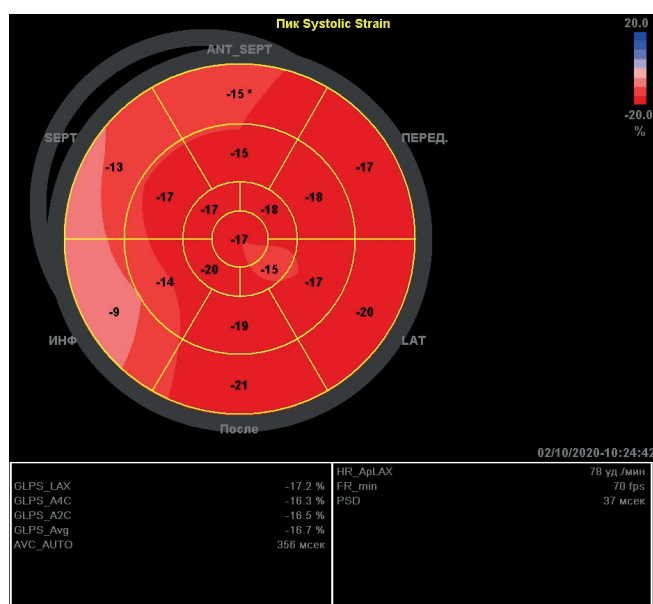


Figure 2. Regional diastolic strain in Bull's Eye mode in a patient of group 3 after COVID-19. A decrease in regional systolic function in the LV basal and middle septal, basal antero-septal and basal anterior segments is revealed.

Table 2

Parameters of LV longitudinal strain in patients after COVID-19 (in %)

Segments	Control group	Group 1	Group 2	Group 3
Septal segments				
Basal	-21 [19;24,5]	-17 [16;20]*	-16,5 [14;19,7]*†	-15,9 [14,5;18,8]*†
Middle	-21 [19;22]	-21 [15;23]	-14,5 [12,7;17,2]*	-16 [14,7;18,5]*
Antero-septal segments				
Basal	-21 [19,5;23]	-17 [16;19]*	-16,5 [16;19,7]*†	-16,3 [15,1;21,7]*†
Middle	-21 [19;22]	-18 [21;21,05]	-14,5 [11,7;18]*	-15,4 [14,1;20,1]*
Anterior segments				
Basal	-22 [19,3;24,6]	-22 [17;23]	-18,5 [14,7;20,2]*	-16,8 [15,3;20]*
Middle	-22 [19,1;25,5]	-24 [18;25,3]	-17,5 [17,2;19,7]*	-17,2 [15,3;19,1]*
Apical	-23 [19,5;24,5]	-21 [20;23]	-17,5 [17,2;19]*	-17,8 [13,5;19,5]*
Lateral segments				
Middle	-21 [19;24]	-17 [20;21]	-13 [10,5;14,7]*	-13 [12;17]*
Apical	-22 [19,4;23]	-18,3 [17,3;22,4]	-16 [15,5;19,7]*	-13,8 [12,3;17,9]*
Posterior segments				
Basal	-18 [17;21]	-17,2 [16;20]*	-15,4 [15;20,7]*†	-15 [14,5;21]*†
Middle	-20 [18,5;21]	-18 [16;19]	-16 [13,2;18,7]*	-15,4 [13,8;19,2]*
Inferior segments				
Basal	-20 [18,4;21]	-18 [16;22,5]	-16 [13,3;18,9]*	-17 [14;19]*
Middle	-21 [19;24]	-21,4 [17;21,8]	-18,3 [10,5;18,9]	-17 [12,5;22]*†
Avg	-21 [19,6;22,5]	-20,8 [18,1;21,9]	-21 [20,8;22,1]	-17,75 [14,6;19,4]*†

Note: * — significance of differences compared with control group ($P < 0,001$), † — significance of differences compared with group 1 ($P < 0,001$).

Abbreviation: Avg — global systolic strain.

in patients with severe COVID-19. In addition, in patients with moderate and severe course, left atrial volume increased, as well as the LV end-diastolic pressure (E/Em); these disorders were more pronounced in patients with a severe disease course (Table 1) ($P < 0,001$). Thus, in patients with a moderate and severe COVID-19, a LV diastolic dysfunction develops, and more pronounced abnormalities regard patients after severe COVID-19.

In 4 (19,9%), 7 (22%), and 5 (26,3%) patients of group 1, 2, and 3, respectively, pericardium was involved in the inflammatory process: according to echocardiography, an insignificant amount of fluid in pericardial cavity was revealed. In addition, in 3 (11%) patients with moderate and 3 (15,7%) patients with severe course, there was a pericardial thickening, mainly behind the LV posterior wall.

Studying the LV longitudinal strain using the Speckle Tracking technology, there was a decrease in regional strain rate in the LV basal segments (septal, antero-septal and posterior) in patients of experimental groups compared with control one. Moreover, in patients with a moderate and severe

disease course, this parameter was lower than in patients with a mild COVID-19 ($P < 0,001$). In comparison with control group, patients of groups 2 and 3 also showed a decrease in regional strain rate in LV basal segment of inferior wall, middle segments (septal, antero-septal, anterior, lateral, and posterior). In addition, in groups 2 and 3, the regional strain rate in LV apical segments of anterior and lateral walls decreased. In patients with severe course, there was a decrease in regional velocity in the middle segment of inferior wall, a decrease in LV global systolic function in comparison with control and first groups (Figure 1, 2, Table 2). Revealed areas with reduced regional strain rate correspond to blood supply system of left anterior descending artery and right coronary artery and, possibly, indicate an impaired regional LV function, which is a marker of myocardial ischemia. In patients with severe course, not only the regional strain rate decreased, but also the global LV systolic function.

According to 24-hour ECG monitoring, in patients of groups 2 and 3, cardiac arrhythmias were most often represented by supraventricular premature beats (in 15 (55%) and 13 (68,4%)

patients, respectively), ventricular premature beats (in 8 (29,6%) and 11 (57,8%) patients, respectively), atrial fibrillation (in 1 (3,7%) and 2 (10%) patients, respectively), nonsustained supraventricular tachycardia (2 (7%) and 6 (31,5%), respectively), QT interval prolongation (in 2 (7%) and 6 (31,5%), respectively). In addition, in these groups there was a decrease in total HRV SDNN, an increase in Lf/Hf ratio, which probably indicates a shift in autonomic balance towards sympathetic nervous system (Table 1). Patients of group 1 were found to have supraventricular (n=6 (19,3%)) and ventricular (n=3 (9,6%)) premature beats, nonsustained supraventricular tachycardia (n=3 (9,6%)).

Analysis of correlation between coronavirus (+) RNA activity and myocardial structure and function revealed that (+) RNA correlated with Em/Am ratio ($r=0,75$, $P<0,001$), pulmonary artery pressure ($r=0,60$, $P<0,001$) and global LV systolic strain ($r=0,54$, $P<0,001$). Given these data, it can be assumed that coronavirus activity contributes to disruption of cardiac structure and function with an increase in pulmonary artery pressure.

Discussion

Thus, 3 months after the diagnosis of COVID-19, cardiovascular disorders were detected in 22 (71%), 25 (93%), and 18 (95%) patients with mild, moderate, and severe disease course, respectively. It is possible that after the penetration of virus into upper respiratory tract in patients with a mild disease course, an early immune system response to the pathogen occurs. A pronounced immune response restrains the infection, but heart is still involved, which is manifested by a decrease in Em/Am and an increase in peak late diastolic tricuspid velocity. In addition, in this group, there is a decrease in myocardial regional strain rates of the basal segments of septal, antero-septal areas, the posterior wall of LV, as well as arrhythmias and signs of pericarditis were revealed. In patients with moderate severity, in addition to above abnormalities, more segments with a decrease in regional strain rate were revealed; in addition to the basal segments, strain rate in the middle LV segments decrease, RV diastole is impaired, and pulmonary artery pressure rises. More pronounced structural and functional cardiac abnormalities were found in patients with severe course: there were more segments with decreased in regional strain rate; in addition to the basal, the middle and apical segments of LV decreased; LV global longitudinal strain was also reduced. Diastolic

dysfunction of not only the RV, but also the LV were revealed. In addition, right heart was enlarged, as well as inferior vena cava diameter and pulmonary artery pressure increased.

Thus, more severe the disease progresses, the more LV segments are involved, and most often — the segments of interventricular septum. It should be noted that in-depth assessment of cardiac function may be a strong predictor of stable myocardial ischemia. Possibly, these disorders occur as a result of endothelial dysfunction and injury of small coronary vessels [1-4, 10], activation of inflammation factors by cytokines and immune complexes, as well as due to effect of viruses on cardiomyocytes with fibrosis formation [5, 11], which can be manifested by increased stiffness and impaired LV diastolic function.

The studied correlations established between the viral (+) RNA and diastolic tricuspid annular velocities, pulmonary artery pressure and global LV systolic strain, can confirm the direct toxic effect of viruses on myocardium with an impairment of its structure and function.

In addition, a decrease in vagal control, impaired myocardial metabolism, its increased rigidity contributes to arrhythmias, in the development of which toxic drugs such as hydroxychloroquine, antiviral agents, and some antibiotics causing QT interval prolongation can play an important role [1, 5, 6].

Conclusion

Cardiovascular injury 3 months after COVID-19 was found in 71%, 93%, and 95% of patients with mild, moderate and severe course. In mild course patients, a decrease in regional myocardial strain in LV basal segments, signs of past pericarditis, and various cardiac arrhythmias were noted. In patients of moderate severity, these changes were more pronounced and were accompanied by an additional decrease in regional strain in LV middle segments, impaired right ventricular diastole and increased pulmonary artery pressure. In severe patients, in addition to the above changes, dilatation of the right heart and inferior vena cava was recorded, as well as LV diastolic and global systolic function decreased. Given these data, for timely diagnosis of long COVID, all patients after disease are recommended to conduct an echocardiography and 24-hour ECG monitoring.

Relationships and Activities: none.

References

1. Wei ZY, Qian HY. Myocardial injury in patients with COVID-19 pneumonia. *Zhonghua XinXue GuanBing ZaZhi*. 2020;48(0):E006. doi:10.3760/cma.j.issn.cn112148-20200220-00106.
2. He XW, Lai JS, Cheng J, et al. Impact of complicated myocardial injury on the clinical outcome of severe or critically ill COVID-19 patients. *Zhonghua XinXue GuanBing ZaZhi*. 2020;48(6):456-60. doi:10.3760/cma.j.cn112148-20200228-00137.
3. Shlyakho EV, Konradi AO, Arutyunov GP, et al. Guidelines for the diagnosis and treatment of circulatory diseases in the context of the COVID-19 pandemic. *Russian Journal of Cardiology*. 2020;25(3):3801. (In Russ.) doi:10.15829/1560-4071-2020-3-3801.
4. Bubnova MG, Shlyakhto EV, Aronov DM, et al. Coronavirus disease 2019: features of comprehensive cardiac and pulmonary rehabilitation. *Russian Journal of Cardiology*. 2021;26(5):4487. (In Russ.) doi:10.15829/1560-4071-2021-4487.
5. Poteshkina NG, Lysenko MA, Kovalevskaya EA, et al. Cardiac damage in patients with COVID-19 coronavirus infection. "Arterial'naya Gipertenziya" ("Arterial Hypertension"). 2020;26(3):277-87. (In Russ.) doi:10.18705/1607-419X-2020-26-3-277-287.
6. Huang C, Wang Y, Li X, et al. Clinical features of patients infected with 2019 novel coronavirus in Wuhan, China. *Lancet*. 2020;395(10223):497-506. doi:10.1016/S01406736(20)30183-5.
7. Arutyunov GP, Tarlovskaya EI, Arutyunov AG, et al. International register "Dynamics analysis of comorbidities in SARS-CoV-2 survivors" (AKTIV SARS-CoV-2): analysis of predictors of short-term adverse outcomes in COVID-19. *Russian Journal of Cardiology*. 2021;26(4):4470. (In Russ.) doi:10.15829/1560-4071-2021-4470.
8. Post-covid syndrome in individuals admitted to hospital with covid-19: retrospective cohort study. *BMJ*. 2021;372:n693. doi:10.1136/bmj.n693. (Published 31 March 2021).
9. Guo T, Fan Y, Chen M, et al. Cardiovascular Implications of Fatal Outcomes of Patients With Coronavirus Disease 2019 (COVID-19). *JAMA Cardiol*. 2020;5(7):811-8. doi:10.1001/jamacardio.2020.1017.
10. Kogan EA, Berezovskiy YuS, Blagova OV, et al. Myocarditis in Patients with COVID-19 Confirmed by Immunohistochemical. *Kardiologia*. 2020;60(7):4-10. (In Russ.) doi:10.18087/cardio.2020.7.n1209.
11. Krishnamoorthy P, Croft LB, Ro R, et al. Biventricular strain by speckle tracking echocardiography in COVID-19: findings and possible prognostic implications. *Future Cardiology*. 2020;17(4). doi:10.2217/fca-2020-0100.
12. Szekeley Y, Lichter Y, Taieb P, et al. Spectrum of Cardiac Manifestations in COVID-19: A Systematic Echocardiographic Study. *Circulation*. 2020;142(4):342-53. doi:10.1161/CIRCULATIONAHA.120.047971.
13. Fend C. The real cause of post-COVID myocarditis is anxiety: MedPage <https://www.medpagetoday.com/> (8 September 2020).
14. Lindner D, Fitzek A, Bräuninger H, et al. Association of Cardiac Infection With SARS-CoV-2 in Confirmed COVID-19 Autopsy Cases. *JAMA Cardiol*. 2020;e203551. doi:10.1001/jamacardio.2020.3551.
15. Puntmann VO, Carerj ML, Wieters I, et al. Outcomes of Cardiovascular Magnetic Resonance Imaging in Patients Recently Recovered From Coronavirus Disease 2019 (COVID-19). *JAMA Cardiol*. 2020;e203557. doi:10.1001/jamacardio.2020.3557.



Algorithm for selecting predictors and prognosis of atrial fibrillation in patients with coronary artery disease after coronary artery bypass grafting

Geltser B. I.¹, Shahgeldyan K. I.^{1,2}, Rublev V. Yu.¹, Shcheglov B. O.¹, Kokarev E. A.³

Aim. To develop an algorithm for selecting predictors and prognosis of atrial fibrillation (AF) in patients with coronary artery disease (CAD) after coronary artery bypass grafting (CABG).

Material and methods. This retrospective study included 886 case histories of patients with CAD aged 35 to 81 years (median age, 63 years; 95% confidence interval [63; 64]), who underwent isolated CABG under cardiopulmonary bypass. Eighty-five patients with prior AF were excluded from the study. Two groups of persons were identified, the first of which consisted of 153 (19,1%) patients with newly recorded AF episodes, the second — 648 (80,9%) patients without cardiac arrhythmias. Preoperative clinical and functional status was assessed using 100 factors. Chi-squared, Fisher, and Mann-Whitney tests, as well as univariate logistic regression (LR) were used for data processing and analysis. Multivariate LR and artificial neural networks (ANN) were used to develop predictive models. The boundaries of significant ranges of potential predictors were determined by stepwise assessment of the odds ratio and p-value. The model accuracy was assessed using 4 metrics: area under the ROC-curve (AUC), sensitivity, specificity, and accuracy.

Results. A comprehensive analysis of preoperative status of patients made it possible to identify 11 factors with the highest predictive potential, linearly and nonlinearly associated with postoperative AF (PAF). These included age (55-74 years for men and 60-78 years for women), anteroposterior and superior-inferior left atrial dimensions, transverse and longitudinal right atrial dimensions, tricuspid valve regurgitation, left ventricular end systolic dimension >49 mm, RR length of 1000-1100 ms, PQ length of 170-210 ms, QRS length of 50-80 ms, QT >420 ms for men and >440 ms for women, and heart failure with ejection fraction of 45-60%. The metrics of the best predictive ANN model were

as follows: AUC — 0,75, specificity — 0,73, sensitivity — 0,74, and accuracy — 0,73. These values in best model based on multivariate LR were lower (0,75; 0,7; 0,68 and 0,7, respectively).

Conclusion. The developed algorithm for selecting predictors made it possible to verify significant predictive ranges and weight coefficients characterizing their influence on PAF development. The predictive model based on ANN has a higher accuracy than multivariate HR.

Keywords: postoperative atrial fibrillation, coronary artery bypass grafting, predictors, predictive models, artificial neural networks.

Relationships and Activities. This work was supported by Russian Foundation for Basic Research grants within the research projects № 18-29-03131 and № 19-29-01077.

¹Far Eastern Federal University, School of Biomedicine, Primorsky Krai, Russky Island, Ajax; ²Vladivostok State University of Economics and Service, Institute of Information Technologies, Vladivostok; ³Primorsky Regional Clinical Hospital № 1, Vladivostok, Russia.

Geltser B. I. ORCID: 0000-0002-9250-557X, Shahgeldyan K. I. ORCID: 0000-0002-4539-685X, Rublev V. Yu.* ORCID: 0000-0001-7620-4454, Shcheglov B. O. ORCID: 0000-0002-2262-1831, Kokarev E. A. ORCID: 0000-0002-8726-0491.

*Corresponding author:
dr.rublev.v@gmail.com

Received: 25.05.2021

Revision Received: 16.06.2021

Accepted: 03.07.2021



For citation: Geltser B. I., Shahgeldyan K. I., Rublev V. Yu., Shcheglov B. O., Kokarev E. A. Algorithm for selecting predictors and prognosis of atrial fibrillation in patients with coronary artery disease after coronary artery bypass grafting. *Russian Journal of Cardiology*. 2021;26(7):4522. (In Russ.) doi:10.15829/1560-4071-2021-4522

Postoperative atrial fibrillation (POAF) is one of the most common complications of cardiac surgery and is recorded in 35-40% of patients [1-3]. Despite numerous preventive strategies developed over the past few decades, the incidence of POAF has not changed significantly [4, 5]. Unfavorable consequences of POAF are primarily associated with a 4-fold increase in the risk of asystole, ischemic stroke, bleeding, acute renal failure, as well as a 2-fold increase in 30-day and 6-month mortality [6]. Despite the absence of universal pathophysiological concept describing POAF development, it is assumed that it is based on a combination of altering factors of local and systemic inflammation. A wide range of potential perioperative predictors has been analyzed in various studies to stratify the risk of POAF [4, 6, 7]. In patients with coronary artery disease (CAD) after coronary artery bypass grafting (CABG), the following factors are most often considered as POAF predictors: age over 65 years, male sex, body mass index (BMI) >30 kg/m², class III-IV angina pectoris, hypertension (HTN), diabetes, chronic kidney disease, chronic obstructive pulmonary disease, heart failure (HF), prior myocardial infarction (MI), and valvular heart disease [8, 9]. In some studies, systemic inflammatory response indicators (pro-inflammatory cytokines, C-reactive protein, neutrophil-to-lymphocyte ratio, platelet-to-lymphocyte ratio, erythrocyte sedimentation rate, etc.) were verified as POAF predictors [10]. Based on mathematical statistics, a number of prognostic scales were developed, in which predictors characterizing the preoperative status of patients were used to assess its risk: post-operative atrial fibrillation (POAF), Kolec and Predictors of AF After CABG (PAFAC) [11-13]. In addition, in a number of studies, POAF was predicted using the CHA₂DS₂-VASc and HAS-BLED scores, parameters of which (female sex, age, HTN, etc.) were linearly associated with its risk [14]. At the same time, despite a significant number of publications where the predictive potential of POAF risk factors is analyzed, unified clinical risk scores have not been developed to date.

In recent years, machine learning methods have been increasingly used to implement predictive studies in clinical and preventive cardiology, including artificial neural networks (ANN) [15]. ANN-based predictive models demonstrate higher accuracy compared to conventional statistical methods [16]. Their application makes it possible not only to automate the processing and analysis of big data, but also to reveal silent or unobvious patterns, as well as to gain new knowledge necessary for risks stratification of adverse events.

The aim of the study to develop an algorithm for selecting predictors and prognosis of POAF in patients with CAD after CABG.

Material and methods

This retrospective study included electronic medical records (EMR) of 886 CAD patients (men, 685; women, 181) aged 35 to 81 years with a median (ME) of 63 years and a 95% confidence interval (CI) of [63; 64], who underwent isolated on-pump CABG in the period from 2008 to 2019 at cardiac surgery department of the Primorsky Regional Clinical Hospital № 1 (Vladivostok). All patients before CABG received standard medical therapy for CAD (long-acting nitrates, beta-blockers, angiotensin-converting enzyme inhibitors or angiotensin II receptor blockers, fixed-dose combinations). Patients with prior atrial fibrillation (AF) of any type were excluded from the study. The total number of such patients was 85, in 25 of whom paroxysmal AF was recorded before CABG, in 21 — persistent, in 39 — chronic. Finally, the study included data on 801 patients with CAD. Verification of POAF was carried out according to continuous electrocardiographic monitoring for at least 96 hours after CABG. Among the surveyed cohort, 2 groups of persons were identified. The first of them included 153 (19,1%) patients who had postoperative AF episodes, while the second — 648 (80,9%) patients without cardiac arrhythmias. The preoperative blood electrolyte levels (K, Na, Ca) did not differ in the comparison groups and were excluded from further analysis. In-hospital mortality in the first group was 9,8% (n=15), and in the second — 4,6% (n=30). The death cause in 12 patients of the first group was intra- and postoperative MI; in other cases, pancreatic necrosis (1), subarachnoid hemorrhage (1), and mediastinitis (1) was detected. In the second group, in 24 patients, the established cause of death was postoperative MI, in 6 — acute renal failure.

The design of our study corresponded to European System for Cardiac Operative Risk Evaluation II (EuroSCOREII), in which the selection of predictors is carried out according to preoperative clinical and functional parameters of patients. The latter was assessed using 100 factors, the main of which are presented in Table 1. For processing and analysis, data from EMR was transformed into a dataset. The values of some parameters that were absent in EMR were supplemented with information from the archival paper-based medical records. Echocardiographic measurements were using GE Vivid-7 ultrasound system according to standard protocol [17]. Left atrial (LA) volume index was determined by prolate ellipse method according to

Table 1

Clinical and functional characteristics of patients

Parameters	Sample size	Group 1, n=153	Group 2, n=648	OR, 95% CI	p-value
Age, years	801	64 [63; 66]	63 [62; 64]		0,00076
Female sex, abs/%	801	39 (25,5%)	134 (20,7%)	1,3 [0,86; 1,97]	0,23
BMI, kg/m ²	708	27,7 [26,8; 29,1]	28,2 [27,7; 28,7]		0,64
Class III-IV HF, abs (%)	790	38 (24,8%)	91 (14%)	2 [1,3; 3]	0,0023
Prior MI, abs (%)	774	30 (19,6%)	122 (18,8%)	1,04 [0,66; 1,6]	0,96
HTN, abs (%)	797	146 (95,4%)	590 (91%)	1,88 [0,89;4,6]	0,15
EF, %	783	59 [57; 60]	60 [60; 60]		0,039
RLVMI, %	641	1,04 [0,99; 1,11]	1,01 [0,98; 1,03]		0,07
RWTI, CU	731	0,42 [0,4; 0,43]	0,42 [0,41; 0,42]		0,91
LV ESD, mm	733	350 [330; 360]	340 [330; 350]		0,037
Pulmonary artery pressure, mm Hg	726	25 [25; 25]	25 [24; 25]		0,72
Aortic stenosis, abs (%)	801	6 (3,9%)	21 (3,2%)	1,2 [0,44; 3]	0,86
TR, abs (%)	801	34 (22,2%)	79 (12,2%)	2 [1,3; 3,2]	0,002
MR, abs (%)	801	61 (40%)	227 (35%)	1,2 [0,85; 1,8]	0,303
AR, abs (%)	801	16 (10,5%)	61 (9,4%)	1,13 [0,6; 2]	0,81
LA1, mm	734	38 [38; 40]	40 [39; 40]		0,2
LA2, mm	734	41 [40; 42]	39 [39; 40]		0,026
LA3, mm	734	38 [37; 39]	37 [36; 37]		0,013
LA2×LA3, mm ²	734	160 [147; 168]	144 [141; 148]		0,011
LA volume index, ml/m ²	734	32,6 [30,6; 34,3]	30,5 [29,3; 31,5]		0,15
RA1, mm	734	39,5 [3,9; 40]	37 [36; 37]		0,00007
RA2, mm	734	43 [41; 43]	39 [38; 40]		0,00003
RA1×RA2, mm ²	734	164 [160; 176]	144 [140; 148]		0,000012
P, ms	801	100 [100; 100]	100 [100; 100]		0,12
PQ, ms	801	160 [150; 160]	150 [140; 150]		0,1
QRS, ms	801	80 [80; 100]	100 [80; 100]		0,0019
RR, ms	761	936,5 [909; 1000]	920 [882,4; 950]		0,22
QT, ms	761	400 [400; 410]	400 [380; 400]		0,00012
Creatinine clearance, μmol/l	633	73,1 [67,2; 78,1]	74 [71,7; 76,6]		0,49
CKD, abs (%)	801	17 (11,1%)	62 (9,6%)	1,2 [0,65; 2,1]	0,67
COPD, abs (%)	801	18 (11,8%)	68 (10,6%)	1,13 [0,63; 1,92]	0,8
Diabetes, abs (%)	801	37 (24,2%)	153 (23,6%)	1 [0,7; 1,6]	0,96
Prior stroke	801	10 (6,5%)	41 (6,3%)	1 [0,48; 2]	1

Note: OR were calculated only for categorical variables.

Abbreviations: HTN — hypertension, CI — confidence interval, MI — myocardial infarction, BMI — body mass index, RWTI — left ventricular relative wall thickness index, ESD — end systolic dimension, LV — left ventricle, LA — left atrium, RLVMI — relative left ventricular mass index, AR — aortic regurgitation, MR — mitral regurgitation, TR — tricuspid regurgitation, OR — odds ratio, RA — right atrium, SBP — systolic blood pressure, EF — ejection fraction, CKD — chronic kidney disease, COPD — chronic obstructive pulmonary disease, HF — heart failure, HR — heart rate, LA1 — medial-lateral left atrial dimension, LA2 — anterior-posterior left atrial dimension, LA3 — superior-inferior left atrial dimensions, RA1 — longitudinal right atrial dimension, RA2 — transverse right atrial dimension.

following equation: $(LA1 \times LA2 \times LA3) \times 0,523$, where LA1 is its medial-lateral dimension; LA2 — anterior-posterior, LA3 — inferior-superior, 0,523 — constant [18], as well as longitudinal (RA1) and transverse (RA2) dimensions of right atrium (RA). During

statistical data processing, BMI was estimated in all patients, as well as echocardiographic parameters of left ventricular (LV) hypertrophy: LV relative wall thickness index and LV mass index (LVMI). To rule out the influence of sex, LVMI was normalized to

Table 2

Threshold values of risk factors for POAF with the best predictive potential

	Group 1, n=153	Group 2, n=648	OR, 95% CI	p-value
Age, years M 55-74 F 60-78	142 (92,8%)	511 (78,9%)	3,4 [1,9; 6,9]	0,0001
EF, % 45-60%	81 (52,9%)	268 (41,4%)	1,68 [1,17; 2,42]	0,0058
ESD >49 mm	7 (4,6%)	11 (1,7%)	2,9 [1,05; 7,7]	0,049
LA2×LA3 >160 mm ²	67 (43,8%)	191 (29,5%)	2,1 [1,4; 3]	0,0002
RA1×RA2 >150 mm ²	92 (60%)	269 (41,5%)	2,5 [1,7; 3,8]	<0,0001
PQ of 170-210 ms	38 (24,8%)	47 (7,3%)	2,2 [2,6; 6,8]	0,0004
QRS of 50-80 ms	88 (57,5%)	303 (46,8%)	1,53 [2,2; 14,4]	0,021
RR of 1000-1100 ms	70 (45,8%)	175 (27%)	2 [1,4; 2,9]	0,00033
QT, ms M >420 ms F >440 ms	45 (30,8%)	100 (16,3%)	2,3 [1,5; 3,5]	0,00013

Abbreviations: CI — confidence interval, F — female, M — male, OR — odds ratio, EF — ejection fraction, LA2 — anterior-posterior left atrial dimension, LA3 — superior-inferior left atrial dimensions, RA1 — longitudinal right atrial dimension, RA2 — transverse right atrial dimension, ESD — end systolic dimension.

upper limit of its sex-associated reference values: 115 g/m² for men and 95 g/m² for women [19]. The study endpoint was presented by POAF as a categorical binary feature (“absence” or “presence”). Input traits were a subgroup of potential predictors, which was expressed as continuous and categorical variables. Statistical analysis and machine learning methods were used to process and analyze the data. Chi-squared, Fisher, and Mann-Whitney tests, as well as univariate logistic regression (LR) were used for data processing and analysis. Multivariate LR and artificial neural networks (ANN) were used to develop predictive models. The ANN architecture was selected by maximizing the area under the ROC-curve (AUC) and consisted of two hidden layers of 90 and 80 neurons each. “Sigmoid” was used as the ANN activation function. The model accuracy was assessed using 4 metrics: area under the ROC-curve (AUC), sensitivity (Sen), specificity (Spec), and accuracy (Acc). The models were developed on a learning sample (9/10) of patients and verified on a test sample (1/10).

The study included 4 stages. At first, statistical analysis was used, which made intergroup comparisons of potential POAF predictors. For continuous variables, the Mann-Whitney test was used. The chi-squared test was used to compare categorical variables, and Fisher’s exact test — to assess the odds ratio (OR) and CI. At the second stage, using these methods, the boundaries of analyzed factors with the best predictive potential were determined. This procedure included testing hypotheses on the equality of trait distributions in comparison groups. The selection of significant

prognostic ranges was carried out with a testing step of 0,05-0,1 CU for various parameters. The selection criteria corresponded to the boundaries of factors, p-value of which had the minimum, and the OR — the maximum value. At the third stage, according to normalized characteristics, using univariate LR, weighting coefficients were determined that corresponded to the significance of influence of individual characteristics on POAF development. At the fourth stage, multivariate models based on LR and ANN were developed, which was step by step supplemented with potential predictors of POAF with an assessment of quality metrics. With an increase of the latter, the indicator included in model was considered as a predictor of POAF. Data processing and analysis were carried out in the R language using R-studio environment and in the Python language using the keras and tensorflow packages.

Results

Comparative analysis of factors characterizing the preoperative clinical and functional status of patients with POAF and without cardiac arrhythmias after CABG showed that significant intergroup differences were recorded only for 11 following parameters: age of patients, class III-IV HF, ejection fraction (EF), LA2, LA3, RA1, RA2, QRS and QT interval duration, tricuspid regurgitation (TR), LV end systolic dimension (ESD) (Table 1). At the same time, the greatest significance of differences in the comparison groups regarded RA1, RA2 and QT interval duration (p-value <0,0001). Compared to persons without arrhythmia, patients with

POAF had significantly higher AFP and LA2, LA3 dimensions, while QRS duration was significantly shorter. Subsequent testing showed that the product of LA2 and LA3, as well as RA1 and RA2, had a higher significance of intergroup differences than isolated atrial sizes, which was taken into account at further study stages. Less noticeable, but significant differences between patients with POAF and those without arrhythmia were associated with older age, an increase in LV ESD, and QRS interval reduction, as well as a significantly higher (1,8 times) prevalence of class III-IV HF and presence of TR. It should be noted that different variants of comorbidities (chronic kidney disease, chronic obstructive pulmonary disease, diabetes, hypertension, stroke, valvular heart disease (excluding TR)) in the comparison groups were recorded with the same frequency, which excluded their use in prognostic models. According to preliminary analysis, the sex, LV hypertrophy parameters (relative wall thickness index and relative LVMI), prior myocardial infarction also did not affect the development of POAF.

At the second study stage, among the parameters with significant differences, the ranges of highest predictive potential were verified (Table 2). The results of analysis made it possible to identify age intervals in men (55-74 years old) and in women (60-78 years old), which significantly increased the risk of POAF (OR=3,4, $p<0,0001$). At the same time, HF with mid-range and preserved EF (45-60%) increased the risk of this complication by 1,7 times ($p=0,0058$). Comparable odds for developing POAF were associated with electrophysiological parameters characterizing a tendency to QRS

shortening (OR=1,5, $p=0,021$) and PQ interval increase (OR=2,2, $p=0,0004$). A more noticeable likelihood of POAF was associated with RR intervals (1000-1100 ms) and QT >420 ms in men and >440 ms in women. Similar OR values were correlated with indicators $RA1 \times RA2 >150 \text{ mm}^2$ and $LA2 \times LA3 >160 \text{ mm}^2$. At the same time, an increase in LV ESD >49 mm increased the risk of POAF by 2,9 times.

Table 3
Weighting coefficients of univariate LR models for assessing the POAF risk

Parameter	Coefficient	p-value
Age, years M 55-74 F 60-78	1,24	0,00015
EF, % 45-60%	0,42	0,03
$LA2 \times LA3 >160 \text{ mm}^2$	0,73	0,00016
$RA1 \times RA2 >150 \text{ mm}^2$	0,94	<0,0001
TR	0,72	0,0016
PQ of 170-210 ms	1,44	<0,0001
QRS of 50-80 ms	1,63	0,0005
RR of 1000-1100 ms	0,87	<0,0001
QT, ms M >420 ms F >440 ms	0,78	0,00016
LV ESD >49 mm	1,07	0,03
Class III-IV HF	0,68	0,0018

Abbreviations: F — female, M — male, OR — odds ratio, TR — tricuspid regurgitation, EF — ejection fraction, HF — heart failure, LA2 — anterior-posterior left atrial dimension, LA3 — superior-inferior left atrial dimensions, RA1 — longitudinal right atrial dimension, RA2 — transverse right atrial dimension, ESD — end systolic dimension.

Table 4
Evaluation of the accuracy of predictive models for POAF on test samples

№	Predictors	Multifactorial LR				ANN			
		Sen	Spec	AUC	ACC	Sen	Spec	AUC	ACC
1	QRS	0,97	0,15	0,56	0,3	0,39	0,61	0,55	0,57
2	QRS + PQ	0,24	0,93	0,63	0,8	0,24	0,93	0,62	0,8
3	QRS + PQ + Age	0,72	0,46	0,66	0,5	0,38	0,8	0,67	0,73
4	QRS + PQ + Age + RR	0,56	0,75	0,7	0,71	0,58	0,74	0,71	0,71
5	QRS + PQ + Age + RR + QT	0,67	0,69	0,72	0,69	0,68	0,68	0,72	0,68
6	QRS + PQ + Age + RR + QT + $RA1 \times RA2$	0,63	0,74	0,75	0,72	0,63	0,75	0,75	0,73
7	QRS + PQ + Age + RR + QT + $RA1 \times RA2$ + $LA2 \times LA3$	0,69	0,71	0,74	0,7	0,65	0,74	0,75	0,72
8	QRS + PQ + Age + RR + QT + $RA1 \times RA2$ + $LA2 \times LA3$ + TR	0,68	0,71	0,74	0,7	0,65	0,74	0,74	0,73
9	QRS + PQ + Age + RR + QT + $RA1 \times RA2$ + $LA2 \times LA3$ + TR + LV ESD	0,68	0,7	0,75	0,7	0,7	0,71	0,74	0,71
10	QRS + PQ + Age + RR + QT + $RA1 \times RA2$ + $LA2 \times LA3$ + TR + LV ESD + EF	0,68	0,7	0,75	0,7	0,74	0,73	0,75	0,73

Abbreviations: ANN — artificial neural network, TR — tricuspid regurgitation, LR — logistic regression, EF — ejection fraction, HF — heart failure, LA2 — anterior-posterior left atrial dimension, LA3 — superior-inferior left atrial dimensions, RA1 — longitudinal right atrial dimension, RA2 — transverse right atrial dimension, ESD — end systolic dimension.

To verify possible interrelationships of risk factors with POAF, we created univariate LR models with estimation of weighting coefficients characterizing the predictive value of analyzed parameters. This approach significantly expands the possibilities for processing and analyzing information due to a more detailed assessment of the influence of potential predictors on resulting variable (Table 3).

Analysis found that a significant level of weighting coefficients took place in 11 following variables: age of patients, class III-IV HF, EF of 45-60%, LV ESD >49 mm, LA2×LA3 >160 mm², RA1×RA2 >150 mm², presence of TR, duration of PQ, QRS, RR and QT intervals. At the same time, the maximum level of weighting coefficient (1,63) was associated with the QRS of 50-80 ms ($p=0,0005$). The weighting coefficients of PQ (1,44), age (1,24), LV ESD (1,1) and RA1×RA2 (0,94) were lower, but comparable in terms of significance. In the developed univariate models, all the weights had a positive value, which indicated an increase in POAF risk in the presence of these traits or an increase in their level. Thus, the assessment of weighting coefficients confirmed the high predictive potential of analyzed factors and indicated rationale for their use to develop predictive models (Table 4). When creating the latter, the QRS was used as a basic predictor, since it had the highest significance (Table 3). The step-by-step inclusion of other factors with a high level of weighting factors in models led to a sequential increase in quality metrics. Their most noticeable rise was recorded when 6 factors (PQ, age, RR, RA1×RA2, and QT) were combined in the model. Subsequent use of LA2×LA3, TR, LV ESD in models 7-9 led to an increase in only individual quality metrics without significant change of their average value. At the same time, model 10 based on ANN, in comparison with multivariate LR, demonstrated a higher level of accuracy after the inclusion of EF.

Discussion

POAF is one of the most common complications developing in patients with coronary artery disease after CABG [2-3]. In our study, the clinical significance of POAF was confirmed by a high in-hospital mortality rate, which in this group of patients was 2 times higher than in those without cardiac arrhythmias. The pathophysiological mechanisms of POAF are complex and not fully understood, which is due to a significant number of factors affecting the onset of arrhythmia [4]. Typical pathological processes initiating POAF include oxidative and nitrosative stress, excessive proteolysis, extracellular matrix degradation, systemic inflammatory response, electrolyte imbalance with impaired volemic status, etc. [5]. At the same

time, complex causal relationships of pathogenetic factors of POAF limit its personalized prognosis. That is why numerous attempts to create prognostic score stratifying its risk after CABG have not led to the creation of unified tools, which can be used in everyday clinical practice. Over the past decade, the informativeness of perioperative predictors of CABG-related POAF has been analyzed in numerous publications. Thus, elderly and senile age as a high-risk factor for POAF is presented in most studies. It has been shown, in particular, that the probability of this complication in patients aged 60 years is 25-30%, and at the age of 80 years — 60% [6]. In our study, the highest risk of POAF was recorded in men aged 55-74 years, and in women — 60-78 years old. These data indicate a shift in risk of POAF in men towards a younger age. Taking into account the fact that elderly and senile age in CAD patients is usually associated with degenerative and inflammatory myocardial changes, in the studies of many authors, in addition to age, electrophysiological, structural, and functional cardiac parameters are used as predictors of POAF. It has been shown, in particular, the relationship between POAF and LA dilatation, LA volume index >36 ml/m², LV diastolic dysfunction. At the same time, P wave did not affect the accuracy of POAF prediction [20]. In our study, predictors with the highest predictive potential were identified based on a multistep selection procedure. Calculation of numerical ranges and weighting coefficients of these factors made it possible to detail the degree of their influence on endpoint. Thus, in addition to the age of patients, the basic predictors of POAF included QRS, PQ, RR durations. QRS of 50-80 ms had the maximum predictive potential, which is associated with the pathophysiological complications of accelerated ventricular depolarization and their transmural activation, contributing to electrical instability of myocardium. In addition, QRS shortening may indicate increased sodium channel activity and a higher risk of ventricular arrhythmias [21]. According to our study, the PQ interval of 170–210 ms in patients with POAF was recorded 3,4 times more often than in patients without arrhythmia, which indicates the relationship between inhibition of atrioventricular conduction and development of this complication [22]. It is important to emphasize that the predictive potential of this factor was more often manifested when it was combined with RR value, which in 45,8% of patients with POAF was recorded at the lower limit of normal range indicating a tendency to bradycardia. The combination of these features in predictive models of POAF was previously presented [9]. The use of PQ >210 ms and RR >100 ms as predictors

did not increase or decrease the accuracy of models. It should also be noted that the inclusion of QT >420 ms in the model did not significantly affect quality metrics (Table 4) (model 5). Its predictive potential was realized only with indicators of RA and LA dilatation (models 6 and 7). Most studies have shown that LA remodeling is the main cause of AF, including after cardiac surgery [6]. It was also found that the extent of LA dilation in patients with CAD is closely related to level of in-hospital mortality and incidence of POAF after CABG [7]. In our study, the LA volume index was not used a predictor, and the latter was products of linear RA and LA dimensions, which indirectly characterize the severity of their structural and functional changes. The increase in RA dimensions in patients with POAF was also associated with TR, which was recorded in 22,2% of patients in this group. Moreover, the influence of this factor on model quality was manifested only when it was combined with EF of 45-60% and LV ESD (models 8-10). It can be assumed that an increase in predictive value of a combination of these factors is due to more accurate characterization of morphological and functional status ischemic myocardium, which serves as a substrate for POAF.

In this work, the identification of AF predictors was carried out by analysis of clinical and functional parameters in patients before CABG, which corresponds to EUROSCORE II system [23]. In

previous studies, where this principle was used to predict POAF, the AUC was 0,60-0,69 [11-13, 24]. In our work, the prediction value was significantly higher, which was provided by a multistep procedure for selecting predictors and using ANN.

Study limitations. Study limitations include the need to increase the sample size, use an adjusted QT interval, validate models in cohorts of patients from other hospitals, and expand the list of potential predictors.

Conclusion

An algorithm using data on preoperative status of patients with CAD was developed to select predictors that were used to predict POAF. The factors with the highest predictive potential included the age of patients (55-74 years for men, 60-78 years for women), RR of 1000-1100 ms, QRS of 50-80 ms, PQ of 170-210 ms, QT (>420 ms for men; >440 ms for women), product of linear dimensions of LA >160 mm² and PP >150 mm², presence of TR, EF of 45-60%, LV ESD >49 mm and class III-IV HF. ANN-based model had a higher predictive accuracy compared to multivariate LR.

Relationships and Activities. This work was supported by Russian Foundation for Basic Research grants within the research projects № 18-29-03131 and № 19-29-01077.

References

- Villareal RP, Hariharan R, Liu BC, et al. Postoperative atrial fibrillation and mortality after coronary artery bypass surgery. *J Am Coll Cardiol*. 2004;43:742-8. doi:10.1016/j.jacc.2003.11.023.
- Maisel WH, Rawn JD, Stevenson WG. Atrial fibrillation after cardiac surgery. *Ann Intern Med*. 2001;135:1061-73. doi:10.7326/0003-4819-135-12-200112180-00010.
- Mathew JP, Fontes ML, Tudor IC, et al. A multicenter risk index for atrial fibrillation after cardiac surgery. *JAMA*. 2004;291:1720-9. doi:10.1001/jama.291.14.1720.
- Revishvili AS, Popov VA, Korostelev AN, et al. Predictors of new onset of atrial fibrillation after coronary artery bypass grafting surgery. *Journal of Arrhythmology*. 2018;(94):11-6. (In Russ). doi:10.25760/VA-2018-94-11-16.
- Lomivorotov VV, Efremov SM, Pokushalov EA, et al. Atrial fibrillation after cardiac surgery: pathophysiology and prevention techniques. *Messenger of anesthesiology and resuscitation*. 2017;14(1):58-66. (In Russ.) doi:10.21292/2078-5658-2017-14-1-58-66.
- Greenberg JW, Lancaster TS, Schuessler RB, et al. Postoperative atrial fibrillation following cardiac surgery: a persistent complication. *Eur J Cardiothorac Surg*. 2017;52(4):665-72. doi:10.1093/ejcts/ezx039.
- Bockeria LA, Sokolskaya NO, Kopylova NS, et al. Echocardiographic predictors of the severity of the early postoperative period in patients after surgical myocardial revascularization. *Anesteziologiya i reanimatologiya*. 2015;60(5):8-11. (In Russ.)
- Dogan A, Gunesdogdu F, Sever K, et al. Atrial fibrillation prediction by surgical risk scores following isolated coronary artery bypass grafting surgery. *J Coll Physicians Surg Pak*. 2019;29(11):1038-42. doi:10.29271/jcsp.2019.11.1038.
- Thorén E, Wernroth M, Christersson C, et al. Compared with matched controls, patients with postoperative atrial fibrillation (POAF) have increased long-term AF after CABG, and POAF is further associated with increased ischemic stroke, heart failure and mortality even after adjustment for AF. *Clin Res Cardiol* (2020). doi:10.1007/s00392-020-01614-z.
- Shao Q, Chen K, Rha SW, et al. Usefulness of Neutrophil/Lymphocyte Ratio as a Predictor of Atrial Fibrillation: A Meta-analysis. *Arch Med Res*. 2015;46(3):199-206. doi:10.1016/j.arcmed.2015.03.011.
- Kolek MJ, Muehlschlegel JD, Bush WS, et al. Genetic and clinical risk prediction model for postoperative atrial fibrillation. *Circ Arrhythm Electrophysiol*. 2015;8(1):25-31. doi:10.1161/CIRCEP.114.002300.
- Lin SZ, Crawford TC, Suarez-Pierre A, et al. A Novel Risk Score to Predict New Onset Atrial Fibrillation in Patients Undergoing Isolated Coronary Artery Bypass Grafting. *Heart Surg Forum*. 2018;21(6):E489-E496. doi:10.1532/hcf.2151.
- Mariscalco G, Biancari F, Zanobini M, et al. Bedside tool for predicting the risk of postoperative atrial fibrillation after cardiac surgery: the POAF score. *J Am Heart Assoc*. 2014;3(2):e000752. doi:10.1161/JAHA.113.000752.
- Burgos LM, Seoane L, Parodi JB, et al. Postoperative atrial fibrillation is associated with higher scores on predictive indices. *J Thorac Cardiovasc Surg*. 2019;157(6):2279-86. doi:10.1016/j.jtcvs.2018.10.091.
- Geltser BI, Tsivanyuk MM, Shakhgelyan KI, et al. Machine learning as a tool for diagnostic and prognostic research in coronary artery disease. *Russian Journal of Cardiology*. 2020;25(12):3999. (In Russ.) doi:10.15829/1560-4071-2020-3999.
- Steele AJ, Denaxas SC, Shah AD, et al. Machine learning models in electronic health records can outperform conventional survival models for predicting patient mortality in coronary artery disease. *PLOS ONE*. 2018;13(8):e0202344. doi:10.1371/journal.pone.0202344.
- Galderisi M, Cosyns B, Edvardsen T, et al. Standardization of adult transthoracic echocardiography reporting in agreement with recent chamber quantification, diastolic function, and heart valve disease recommendations: An expert consensus document of the European Association of Cardiovascular Imaging. *European Heart Journal — Cardiovascular Imaging*. 2017;18(12):1301-10. doi:10.1093/ehjci/jex244.
- Jiamsripong P, Honda T, Reuss CS, et al. Three methods for evaluation of left atrial volume. *Eur J Echocardiogr*. 2008;9(3):351-5. doi:10.1016/j.euje.2007.05.004.
- Geltser BI, Shahgelyan KJ, Rublev VY, et al. Machine Learning Methods for Prediction of Hospital Mortality in Patients with Coronary Heart Disease after Coronary Artery Bypass Grafting. *Kardiologiya*. 2020;60(10):38-46. (In Russ.) doi:10.18087/cardio.2020.10.n1170.
- Ozben B, Akaslan D, Sunbul M, et al. Postoperative Atrial Fibrillation after Coronary Artery Bypass Grafting Surgery: A Two-dimensional Speckle Tracking Echocardiography Study. *Heart Lung Circ*. 2016;25(10):993-9. doi:10.1016/j.hlc.2016.02.003.
- Xiong F, Yin Y, Dubé B, et al. Electrophysiological changes preceding the onset of atrial fibrillation after coronary bypass grafting surgery. *PLoS One*. 2014;9(9):e107919. doi:10.1371/journal.pone.0107919.
- Sigurdsson MI, Muehlschlegel JD, Fox AA, et al. Genetic Variants Associated with Atrial Fibrillation and PR Interval Following Cardiac Surgery. *J Cardiothorac Vasc Anesth*. 2015;29(3):605-10. doi:10.1053/j.jvca.2014.10.028.
- Ad N, Holmes SD, Patel J, et al. Comparison of EuroSCORE II, Original EuroSCORE, and The Society of Thoracic Surgeons Risk Score in Cardiac Surgery Patients. *Ann Thorac Surg*. 2016;102(2):573-9. doi:10.1016/j.athoracsur.2016.01.105.
- Shakhgelyan KI, Rublev VYu, Geltser BI, et al. Predictive potential assessment of preoperative risk factors for atrial fibrillation in patients with coronary artery disease after coronary artery bypass grafting. *The Siberian Journal of Clinical and Experimental Medicine*. 2020;35(4):128-36. (In Russ.) doi:10.29001/2073-8552-2020-35-4-128-136.



Evaluation of the long-term effectiveness of cardiac resynchronization therapy

Chumarnaya T. V.^{1,2}, Lyubimtseva T. A.³, Solodushkin S. I.⁴, Lebedeva V. K.³, Lebedev D. S.³, Solovieva O. E.^{1,4}

Aim. To determine quantitative criteria for assessing the therapeutic benefits and the most informative time frames after cardiac resynchronization therapy (CRT) to assess its long-term effectiveness (1, 2, 3 years of follow-up) based on retrospective analysis. To assess the CRT effectiveness, parameters of left ventricular (LV) reverse remodeling and signs characterizing the clinical CRT response were considered.

Material and methods. This single-center, retrospective, non-randomized study included data from 278 patients with implanted CRT devices. Quantitative criteria for assessing CRT effectiveness were determined using a two-step cluster analysis of patients 1, 2, and 3 years after CRT by LV reverse remodeling parameters.

Results. In the dataset with satisfactory division accuracy, after the first year, two clusters were identified, which are conventionally named as “non-responders” and “responders”. Two and three years after therapy, patients were classified into three clusters: “non-responders”, “responders” and “super-responders”. For the obtained clusters, we found cutoff values for LV reverse remodeling parameters, which can be used as criteria for response to therapy.

The study identified the most informative time frames for assessing the postoperative CRT effectiveness 1, 2, 3 years after the surgery. At the same time, the clinical response to therapy is manifested earlier in comparison with the reverse LV remodeling.

Despite the high divisibility of patients into responders and non-responders, predictive models of CRT effectiveness created using the available data from standard diagnostic protocols for heart failure patients have insufficient accuracy to be used for making decisions on therapy appropriateness. This circumstance indicates the need to receive additional data to improve the forecasting quality.

Conclusion. The study revealed a period for assessing the clinical response and changes in LV reverse remodeling after CRT surgery, which is important for the optimal choice of postoperative therapy. It has been shown that in most

cases, one year after surgery is sufficient to assess the clinical response, and the process of LV reverse remodeling can last up to two years on average.

When assessing the CRT effectiveness by reverse remodeling, along with a change in LV end-systolic volume (ESV), it is necessary to take into account LV end-diastolic volume (EDV) changes. The change in LV ejection fraction showed a significantly lower value among the analyzed parameters in assessing the CRT effectiveness. Based on the cluster classification of patients, a dividing rule was established for responders and non-responders in the first and second years after surgery with an accuracy of 97%: a decrease in LV ESV and EDV by 9% or more compared to preoperative values.

Keywords: cardiac resynchronization therapy, cardiac resynchronization therapy effectiveness, forecasting models, long-term postoperative period.

Relationships and Activities. This work was supported by a Russian Science Foundation grant № 19-14-00134.

¹Institute of Immunology and Physiology, Yekaterinburg;

²Ural State Medical University, Yekaterinburg; ³Almazov National Medical Research Center, St. Petersburg; ⁴Ural Federal University, Yekaterinburg, Russia.

Chumarnaya T. V.* ORCID: 0000-0002-7965-2364, Lyubimtseva T. A. ORCID: 0000-0002-8651-7777, Solodushkin S. I. ORCID: 0000-0002-1959-5222, Lebedeva V. K. ORCID: none, Lebedev D. S. ORCID: 0000-0002-2334-1663, Solovieva O. E. ORCID: 0000-0003-1702-2065.

*Corresponding author:
chumarnaya@gmail.com

Received: 31.05.2021

Revision Received: 16.06.2021

Accepted: 03.07.2021



For citation: Chumarnaya T. V., Lyubimtseva T. A., Solodushkin S. I., Lebedeva V. K., Lebedev D. S., Solovieva O. E. Evaluation of the long-term effectiveness of cardiac resynchronization therapy. *Russian Journal of Cardiology*. 2021;26(7):4531. (In Russ.) doi:10.15829/1560-4071-2021-4531

Heart failure (HF) is the most severe cardiovascular disease with a high risk of adverse events, including sudden cardiac death. The prevalence of HF in Russia reaches 7% and continues to grow every year, twice exceeding this value in other developed countries [1]. Based on numerous clinical studies, cardiac resynchronization therapy (CRT) is recognized as a non-medication method that improves functional status, improves the quality of life, and the survival rate of patients with HF [2]. CRT is aimed at reducing atrioventricular, inter- and intraventricular myocardial dyssynchrony, at increasing the left ventricular (LV) contractility. This treatment leads to reverse LV remodeling, as evidenced by an increase in LV filling time and ejection fraction (EF), as well as a decrease in LV end-diastolic (EDV) and end-systolic volumes (ESV) and a decrease in mitral regurgitation and interventricular septal dyskinesia [3].

The possibility of achieving the CRT effect is individual in each case, since it is associated with the functional and structural cardiac features, as well as with their changes over time. On the other hand, unsafe for patients and expensive implantation of such devices is often redundant due to inappropriate patient selection [4].

The development of patient selection algorithms, the choice of optimal conditions for surgical intervention and postoperative treatment based on modern research technologies remain urgent tasks of cardiology.

Numerous studies have made it possible to expand indications for CRT for patients with lower HF class, but more significant systolic dysfunction or a wide QRS complex with a failure of optimal medication therapy and disease progression [5, 6]. To date, there remains a number of potential opportunities for clarifying the stratification of patient selection for CRT and increasing the efficiency of these devices.

The question remains, in what time frame after CRT and by what indicators to evaluate the its effectiveness. Thus, the parameters used to assess the success of CRT in randomized clinical trials are not consistent with clinical practice [7, 8]. In most studies, efficacy is assessed by the characteristics of LV reverse remodeling, such as ESV and EF, while in clinical practice, an important criterion of efficacy is a relief of HF symptoms and improvement of the quality of life [9].

This study was aimed at finding the most informative period for assessing the effectiveness of CRT and quantitative criteria for it, as well as identifying predictors of response to CRT.

Material and methods

Study design. This single-center retrospective non-randomized study included 278 patients with

implanted CRT devices according to national clinical guidelines [6]. The data collection period was 36 months. Patients were examined before CRT and after CRT in multiples of 12 months. The study was approved by the ethics committee of the Almazov National Medical Research Center.

Population. The mean age of patients was 63 ± 12 years. At the time of CRT, 76% had sinus rhythm, 21% — permanent AF, 3% — complete atrioventricular block and atrial fibrillation. We analyzed LV remodeling parameters and heart valve status by transthoracic echocardiography. In addition, six-minute walk test and EQ- 5D-5L (Kansas) questionnaire results were analyzed to assess HF functional class.

There were following inclusion criteria:

- age >18;
- NYHA class II-IV HF at the outpatient stage of treatment;
- LVEF $\leq 35\%$ (Simpson method);
- QRS complex >20 ms;
- sinus rhythm, complete left bundle branch block;
- optimal medication therapy for HF;
- signed informed consent.

There were following exclusion criteria:

- prior myocardial infarction, transient ischemic attack, stroke <3 months before the start of the study;
- patients who were scheduled for myocardial revascularization or heart transplantation during the follow-up period;
- congenital and acquired defects, as well as heart tumors, LV aneurysm, when their surgical treatment was planned during the follow-up period;
- active inflammatory and autoimmune myocardial diseases;
- thyrotoxicosis at the time of enrollment;
- anemia with a hemoglobin ≤ 90 g/l;
- diseases limiting life expectancy (<1 year).

Parameters for assessing the CRT effectiveness.

Parameters of LV reverse remodeling: relative decrease in LV EDV (Δ EDV), relative decrease in LV ESV (Δ ESV). A negative Δ EDV and Δ ESV means a decrease in LV volumes in comparison with preoperative indicators. The relative increase in LVEF (Δ EF). A positive Δ EF means an increase in LVEF in comparison with the preoperative indicator. The clinical response was assessed by a decrease in HF functional class compared with the preoperative one.

Methods for determining the criterion for assessing the CRT effectiveness. The classification of these patients to determine quantitative criteria for assessing the effectiveness of CRT at various postoperative periods was carried out using a two-step cluster ana-

lysis. To assess the quality of connectivity and separability of clusters, a silhouette value was used, which is measured from -1 to 1. The value from -1 to 0,2 is considered unsatisfactory for separation into clusters, from 0,2 to 0,49 — moderate separability, from 0,5 to 1 — good separability. ROC analysis was used to assess the diagnostic value and find cut-off thresholds for clustering parameters. The area under the ROC curve (AUC) was used as a measure of diagnostic value. Cut-off thresholds were determined with a balance of sensitivity and specificity.

Models for predicting changes in reverse remodeling parameters at different postoperative periods. The following blocks of standard preoperative diagnostic protocols were used to construct models for predicting the values of Δ EDV, Δ ESV, Δ EF at different postoperative periods:

- Demographic: sex, height, weight;
- Cardiovascular disease and prior surgery: myocardial infarction, stenting, CABG, radiofrequency ablation, valve replacement;
- Heart failure (HF): etiology of dilated cardiomyopathy (ischemic and non-ischemic), HF class (six-minute walk test, EQ-5D-5L questionnaire (Kansas));
- Electrocardiography: QRS, P, PQ, QT, the presence of blocks and delayed conduction;
- Echocardiography: LV EDV and ESV, LVEF, end-diastolic and end-systolic dimensions of the LV and right ventricle, left and right atrial dimensions. Presence/absence of interventricular and intraventricular dyssynchrony, according to tissue Doppler echocardiography;
- Medication therapy.

To improve the predictive models, the following characteristics obtained during the implantation of an implantable electronic device (IED) were used: location of pacing poles in right and left ventricular leads; electrocardiographic characteristics during pacing. For the forecast in 2nd and 3rd years after the operation, to improve the quality of models, we also used the characteristics Δ EDV, Δ ESV, Δ EF in the first year after CRT.

Predictive models were created using stepwise logistic regression (criterion for stepwise selection of parameters: inclusion of a parameter in model with a significance $\leq 0,05$; excluding a parameter from the model with a significance $< 0,10$). The determination coefficient R^2 was used to assess the linear relationship between predicted parameters and predictors: the closer the value is to 1, the stronger the relationship. The R^2 coefficient provides an estimate of model quality: what percentage of cases this model is able to describe.

Statistical analysis and creation of information models were carried out using the IBM SPSS 23

program. For quantitative variables, the arithmetic mean and standard deviations ($m \pm sd$) were calculated in case of normal distribution. For nonnormally distributed variables, median and [25%; 75%] percentile were used. The critical level of significance was 0,05. The normal distribution of variables was assessed using the Shapiro-Wilk test. For pairwise comparisons, the nonparametric Wilcoxon signed-rank test was used. Comparison of two independent groups was carried out using the Mann-Whitney Test. Comparison with hypothetical median was performed using the one-sample Wilcoxon signed rank test.

Results

Analysis of CRT effectiveness in long-term postoperative period

The analysis of CRT performance within three years after surgery was carried out in order to determine the optimal postoperative period for assessing the CRT effectiveness.

LVEF

The analysis of changes in LVEF was carried out according to echocardiography before CRT and 1, 2 and 3 years after surgery (Figure 1).

It was shown that the mean LVEF increased significantly after implantation of CRT devices for all considered stages in comparison with the preoperative data (Figure 1).

For pairwise comparisons, in the first year after CRT initiation, there was a subgroup of 173 patients, of which in 77% of cases, LVEF increased, in 17% — decreased, and in 6% — remained unchanged. The percentage of LVEF increase in the first year after CRT was 28% [4; 57]. There was a significant difference in percentage of increase from zero ($p=0,000$).

The mean LVEF value 2 years after CRT did not significantly differ from the value of 1 year after CRT (35 ± 9 and 33 ± 8 , $p=0,070$). However, the additional increase at the stage from 1 to 2 years was significantly different from zero ($p=0,033$) and amounted to 3% [-10; 24] (Figure 1). For pairwise comparisons, in the interval from one to two years, there was a subgroup of 119 patients, in 54% of which LVEF became higher, in 43% — lower, and in 3% — remained unchanged.

When comparing LVEF at the stage from 2 to 3 years after surgery, the difference was insignificant (35 ± 9 and 36 ± 9 , $p=0,459$) and the additional increase in LVEF did not significantly differ from zero ($p=0,326$) (Table 1). For pairwise comparisons in the interval from 2 to 3 years after CRT, the subgroup included 88 patients: in 48% of cases, LVEF became higher, in 42% — lower, in 10% — remained unchanged.

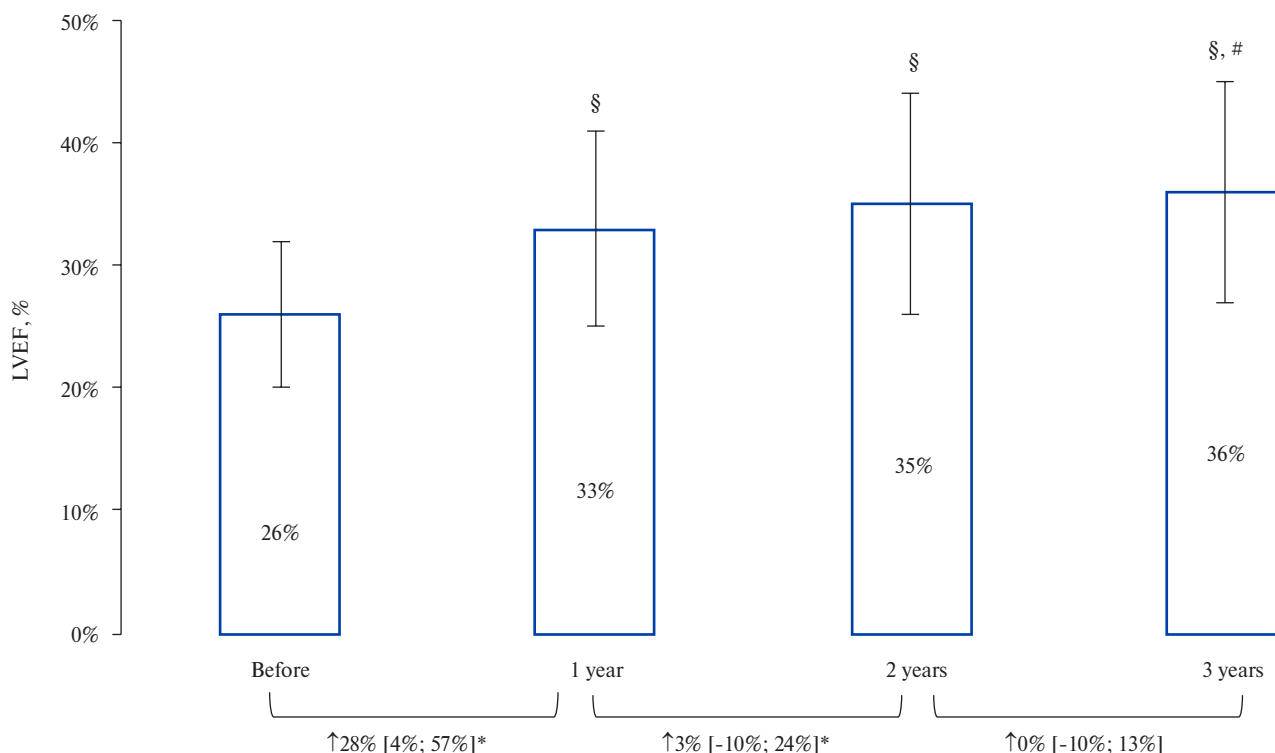


Figure 1. LVEF 1, 2, 3 years after CRT.

Note: ↑ — Δ EF (%) Me [25%;75%], * — $p < 0,05$ Δ EF is significantly different from zero, § — $p < 0,05$ comparison with LVEF before CRT, # — $p < 0,05$ comparison with LVEF 1 year after CRT.

Abbreviations: LVEF — left ventricular ejection fraction, CRT — cardiac resynchronization therapy.

LV EDV

The analysis of changes in LV EDV was carried out according to echocardiography before CRT and 1, 2 and 3 years after surgery (Figure 2).

It was shown that the mean value of LV EDV significantly decreased after CRT device implantation at all considered stages in comparison with the preoperative data (Table 2).

For pairwise comparisons, in the first year after device implantation, there was a subgroup of 173 patients, of whom in 71% of cases, LV EDV decreased, in 29% — increased. The percentage of LV EDV reduction in the first year after CRT was 17% [-6%; 35%] with a significant difference from zero ($p < 0,001$).

LV EDV value at 2 years after CRT did not significantly differ from the value at 1 year after CRT (240 ± 101 and 231 ± 91 , $p = 0,286$). The decrease at the stage from 1 to 2 years also did not differ significantly from zero ($p = 0,968$) (Figure 2). For pairwise comparisons, in the interval from 1 to 2 years, there was a subgroup of 119 patients, of whom in 70% of cases, LV EDV decreased, in 29% — increased, in 1% — remained unchanged.

When comparing LV EDV at the stage from 2 to 3 years after surgery, the difference was insignificant

(231 ± 91 and 220 ± 90 , $p = 0,171$) and the decrease did not significantly differ from zero ($p = 0,342$) (Figure 2). For pairwise comparisons, in the interval from 2 to 3 years after CRT, the subgroup included 88 patients, of whom in 72% of cases, LV EDV decreased, in 28% — increased.

LV ESV

The analysis of changes in LV ESV was carried out according to echocardiography before CRT and 1, 2 and 3 years after surgery (Figure 3).

It was shown that the mean value of LV ESV significantly decreased after CRT device implantation at all considered stages in comparison with the preoperative data (Figure 3).

For pairwise comparisons, in the first year after device implantation, there was a subgroup of 173 patients, of whom in 73% of cases, LV ESV decreased, in 27% — increased. The percentage of LV ESV reduction in the first year after CRT was 21% [-4%; 39%] with a significant difference from zero ($p < 0,001$).

LV ESV value at 2 years after CRT did not significantly differ from the value at 1 year after CRT (165 ± 83 and 155 ± 78 , $p = 0,180$). The decrease at the stage from 1 to 2 years also did not differ significantly from zero ($p = 0,577$) (Figure 2). For

Table 1

Correlation analysis between HF class and LV reverse remodeling parameters

HF class		LV EDV				LV ESV				LVEF			
		До	1	2	3	До	1	2	3	До	1	2	3
Before	r	-0,01	-0,01	0,05	0,02	0,01	0,04	0,06	0,04	-0,06	-0,19	-0,11	-0,13
	p	0,97	0,97	0,62	0,83	0,86	0,56	0,49	0,71	0,35	0,01	0,24	0,23
1 year	r	0,08	0,20	0,17	0,32	0,08	0,23	0,22	0,34	-0,11	-0,24	-0,29	-0,31
	p	0,33	0,01	0,14	0,01	0,32	0,01	0,05	0,01	0,18	0,00	0,01	0,01
2 year	r	-0,188	0,27	0,21	0,24	-0,13	0,25	0,25	0,26	0,02	-0,16	-0,35	-0,26
	p	0,07	0,01	0,03	0,08	0,16	0,02	0,01	0,04	0,85	0,14	0,00	0,05
3 year	r	-0,14	0,32	0,33	0,27	-0,12	0,35	0,41	0,32	0,07	-0,33	-0,48	-0,41
	p	0,24	0,01	0,02	0,02	0,31	0,01	0,03	0,01	0,54	0,01	0,00	0,00

Abbreviations: EDV — end-diastolic volume, ESV — end-systolic volume, LVEF — left ventricular ejection fraction, HF — heart failure, r — Spearman's rank correlation coefficient, p — significance of difference r from zero.

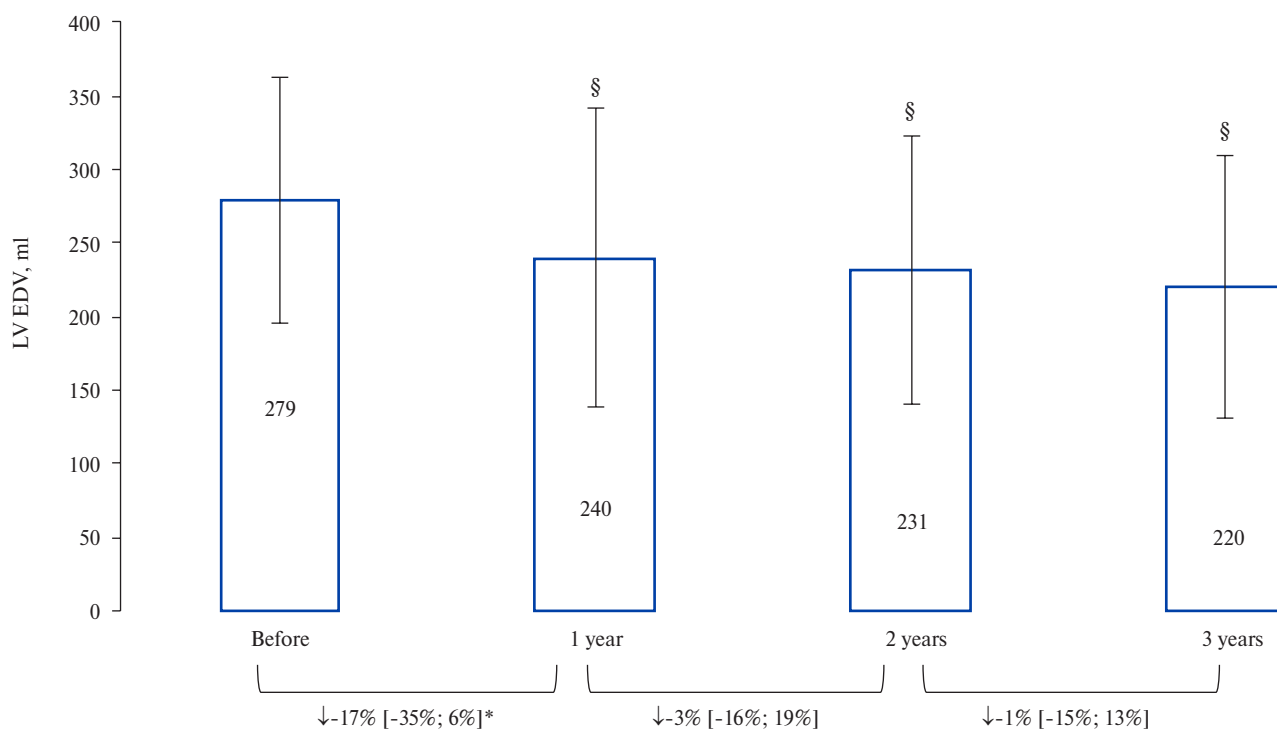


Figure 2. LV EDV 1, 2, 3 years after CRT.

Note: ↓ — Δ EDV (%) Me [25%;75%], * — $p < 0,05$ Δ EDV is significantly different from zero, § — $p < 0,05$ comparison with LV EDV before CRT.

Abbreviations: LV — left ventricle, CRT — cardiac resynchronization therapy, EDV — end-diastolic volume.

pairwise comparisons, in the interval from 1 to 2 years, there was a subgroup of 119 patients, of whom in 72% of cases, LV ESV decreased, in 27% — increased, in 1% — remained unchanged.

When comparing LV ESV at the stage from 2 to 3 years after surgery, the difference was insignificant (155 ± 78 and 145 ± 75 , $p = 0,377$) and the decrease did not significantly differ from zero ($p = 0,435$) (Figure 2). For pairwise comparisons, in the interval

from 2 to 3 years after CRT, the subgroup included 88 patients, of whom in 73% of cases, LV ESV decreased, in 27% — increased.

HF class

We analyzed changes in HF functional class in patients within 3 years after CRT (Figure 4).

In the subgroup of patients ($n = 80$), for whom there was information on HF class at all stages, the following changes were observed — Table 3.

In 70,1% of patients, HF class improved over the entire period. After 1 year, a positive trend was observed in 48,8%. Taking into account the patients who did not show a favorable change (26%), it is

possible to recommend evaluating the effectiveness of CRT 1 year after surgery.

Relationship of HF class and LV reverse remodeling parameters

The relationship between LV reverse remodeling parameters and HF was investigated. Correlation analysis showed a weak but significant relationship

Table 2
Descriptive statistics data for subgroups with/without decrease in HF class in the first year after CRT

Parameter		Decrease in HF class after 1 year		Significance of differences
		Yes	No	
LVEF (%)	Before	26±0,6	25±0,8	0,071
	1 year	34±0,8	32±1,1	0,052
	2 year	38±1,3	31±1,4	0,002
	3 year	39±1,5	32±2,2	0,007
LV ESV (ml)	Before	200±8	221±10	0,09
	1 year	142±7	190±12	0,003
	2 year	137±11	189±13	0,004
	3 year	129±11	191±16	0,006
LV EDV (ml)	Before	277±9	300±11	0,189
	1 year	213±9	275±15	0,002
	2 year	216±14	265±15	0,018
	3 year	204±14	272±19	0,011

Table 3
Combinations of changes in HF class

Improvement (decrease in HF class), n=56	
Decreased by 1 year and remained unchanged	32,5%
Decreased by 2 year and remained unchanged	10%
Decreased by 3 year	11,3%
Decreased by 1 and 2 years, and remained unchanged	11,3%
Decreased by 1 year, unchanged by 2 year, decreased by 3 year	5%
Unfavorable changes (increase in HF class or no changes), n=24	
Remained unchanged, increased by 2 year	1,3%
Decreased by 1 and 2 years and increase by 3 year	1,3%
Decreased by 1 year, increased by 2 year, unchanged by 3 year	1,3%
Did not change	26%

Abbreviations: EDV — end-diastolic volume, ESV — end-systolic volume, LVEF — left ventricular ejection fraction, HF — heart failure.

Abbreviation: HF — heart failure.

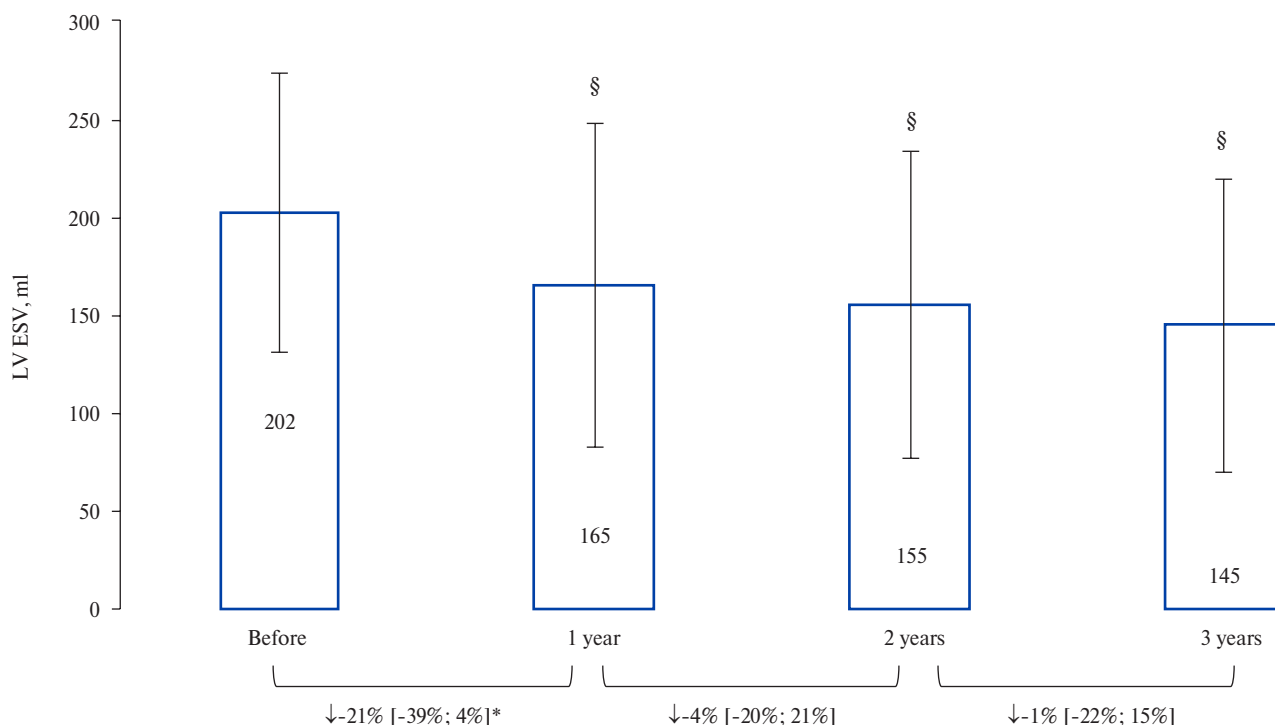


Figure 3. LV ESV 1, 2, 3 years after CRT.

Note: ↓ — ΔESV (%) Me [25%;75%], * — p<0,05 ΔESV is significantly different from zero, § — p<0,05 comparison with LV ESV before CRT.

Abbreviations: LV — left ventricle, CRT — cardiac resynchronization therapy, ESV — end-systolic volume.

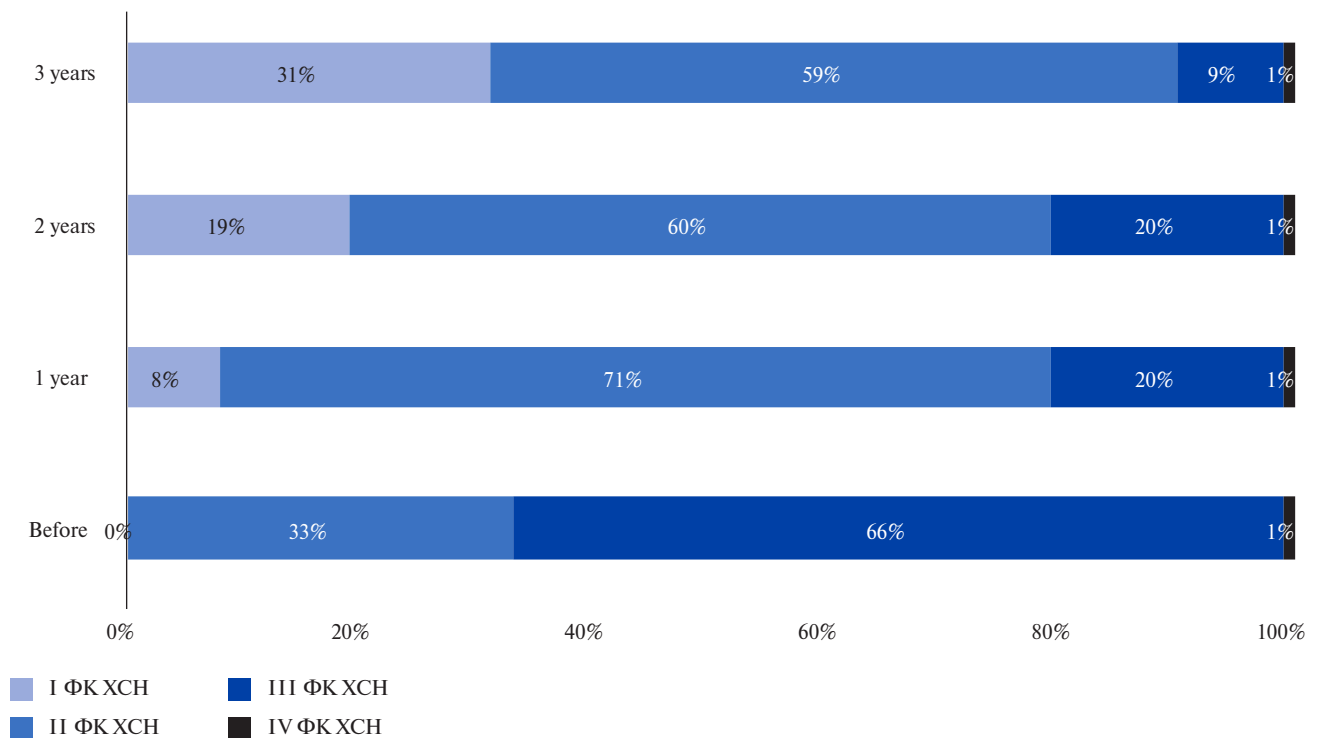


Figure 4. HF class 1, 2, 3 years after CRT.
Abbreviations: HF — heart failure.

between LV reverse remodeling parameters and HF at all postoperative stages considered (Table 1).

To compare the timing of a decrease in HF class and LV reverse remodeling after CRT, the group of patients was divided into two subgroups: group 1 — HF class decreased during the first year after CRT, group 2 — HF class did not decrease (remained the same or increased). The subgroups did not significantly differ in LVEF, ESV, and EDV before CRT initiation (Table 1). In the first year after CRT implantation, in patients whose HF class decreased, there was a tendency for a greater increase in LVEF compared with patients whose HF class did not decrease (from 26% to 34% and from 25% to 32%, respectively (Table 1)), but this trend was insignificant. Only after two years was there a significant difference between LVEF for the considered subgroups. In the group of patients whose HF class decreased in the first year after CRT, LV ESV and EDV became significantly lower compared to group of patients whose HF class did not decrease in the first postoperative year. The same findings were observed at 2 and 3 years after CRT.

Criterion for assessing the CRT effectiveness in terms of LV reverse remodeling. A two-step cluster analysis was used to classify patients at 1, 2, and 3 years after CRT. The classification was carried out depending on LV Δ EF, Δ ESV and Δ EDV at the indicated time. The change in HF class was assessed

during clustering, but did not participate in the classification, because for all periods, the change in HF class had practically zero importance during separation and sharply reduced the silhouette value of clustering.

In the first year, with the best silhouette value of cluster connectivity of 0,54, 2 clusters were identified (Figure 5). The most important parameter for cluster separation was LV Δ ESV, then, in decreasing order of importance, LV Δ EDV and Δ EF (Figure 6). We conditionally named the first cluster “non-responders”, the second cluster “responders”, and found the separation criteria for them (Table 4, Figure 5). In “non-responders” cluster in a larger number of patients, the HF class did not change (increase — 2%; no changes — 51%; decrease — 47%), while in the cluster of “responders”, there were more patients who had a decrease HF class (increase — 1%; no changes — 38%; decrease — 61%).

At the stage of two years after CRT, with the best cluster connectivity of 0,57, 3 clusters were identified. The most important parameter in dividing the clusters, as in the first year, was LV Δ ESV with a highest value of 1,00. Δ EDV was also of high importance in separation, while Δ EF had the least effect on clustering (Figure 6). Thus, the first cluster included patients with unfavorable changes in ESV, EDV and LVEF, and 90% of it consisted of patients from the “non-responder” cluster obtained from

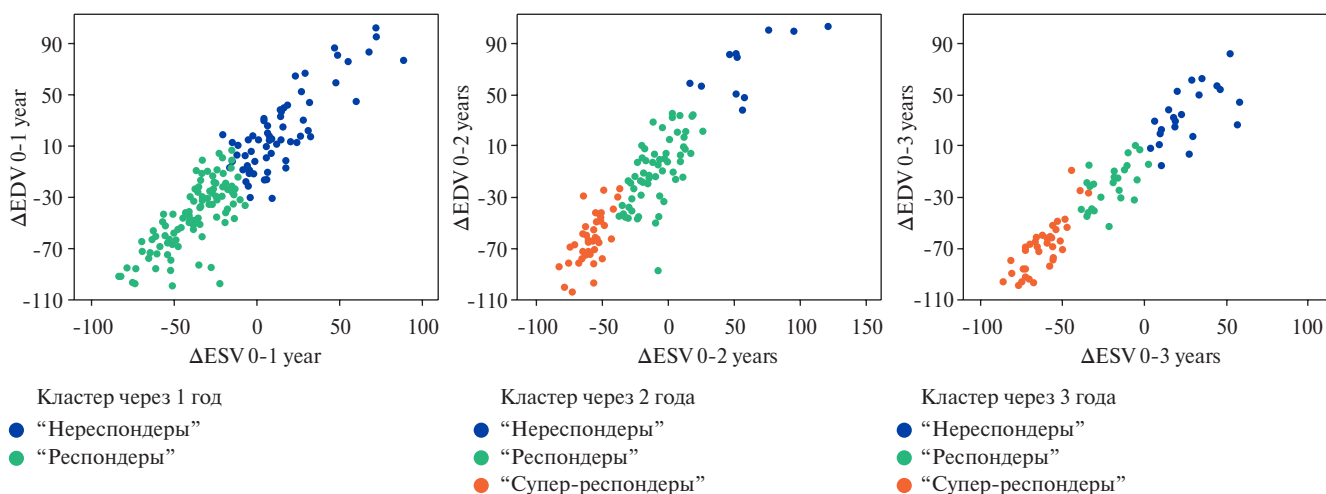


Figure 5. Clustering at different postoperative periods.
Abbreviations: ESV — end-systolic volume, EDV — end-diastolic volume.

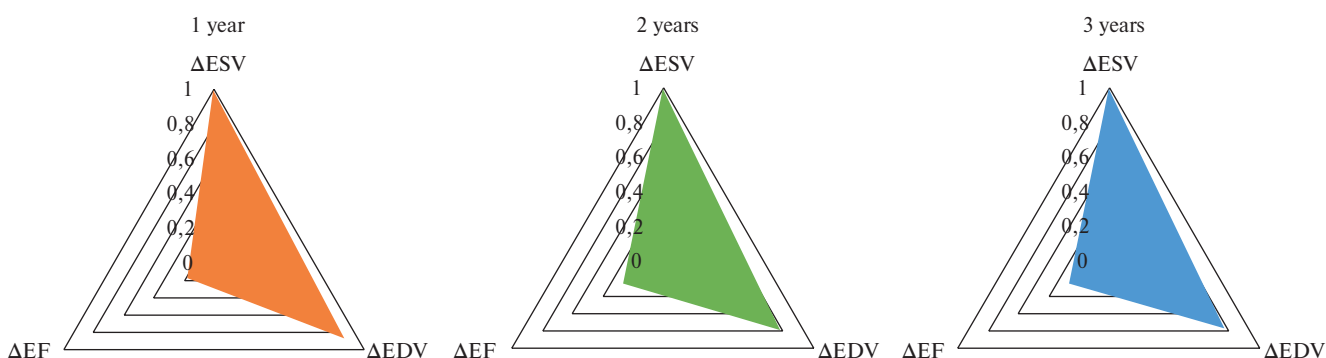


Figure 6. Importance of parameters for clustering in the considered postoperative periods.
Abbreviations: ESV — end-systolic volume, EDV — end-diastolic volume, EF — ejection fraction.

data for 1 year. The second and third clusters were patients with favorable dynamics. In the second cluster, 54% of patients in the first year were “non-responder” cluster and 46% — “responders” cluster. The third cluster consisted entirely of patients who were included in the “responders” cluster in the first year. According to data for the second year, we conditionally named the resulting clusters: the first cluster — “non-responders”, the second cluster — “responders” and the third — “super-responders”. In the group of “non-responders”, there was an increase in HF class in 8%, no change — in 75%, and a decrease — in 17%; among “responders” and “super-responders”, an increase in HF class was observed in 2%, no change — in 31%, and a decrease — in 67%.

Three years after CRT, 3 clusters were also identified with the best cluster connectivity of 0,56. The most important parameter for cluster separation was LV Δ EDV, slightly less important — Δ ESV, and Δ EF had the least effect on clustering (Figure 6). As in the previous stage, the first cluster included

patients with negative changes in ESV, EDV and LVEF and 100% of it consisted of patients from the “non-responder” cluster obtained from the second year. The second and third clusters are patients with favorable dynamics, consisting of patients of the “responder” and “super-responder” clusters obtained from the second year. Among “non-responders”, an increase in HF class was observed in 8%, no change — in 81% and a decrease — in 11%; among the “responders” and “super-responders”, HF class remained unchanged in 12% of patients, and in 88% there was a decrease in HF class.

For the obtained clusters, we found the separation criteria (Table 4, Figure 5). Based on the assessment of importance of clustering parameters, diagnostic value and obtained cut-off thresholds for these parameters, in the first year after CRT, “responders” should be considered as with a relative decrease in LV $ESV \geq 10\%$, in LV $EDV \geq 9\%$ compared to preoperative data. Two years after CRT, there were criteria for separability of clusters as follows: “non-responders” are the same as according to first year —

Table 4

Cluster analysis of LV reverse remodeling parameters

Year	Parameter	Cluster	Median (%) [25%; 75%]	Cut-off threshold (%), (Se, Sp)	AUC [95% CI]	P
1	ΔESV	“non-responders” (n=67, 39%)	8 [-4; 25]	>-9 (0,96,0,91)	0,995 [0,989; 1,00]	0,000
		“responders” (n=106, 61%)	-36 [-52; -25]	≤-9 (0,96,0,91)		
	ΔEDV	“non-responders”	11 [-3; 24]	>-9 (0,9, 0,89)	0,962 [0,939; 0,985]	0,000
		“responders”	-30 [-43; -18]	≤-9 (0,9, 0,89)		
	ΔLVEF	“non-responders”	5 [-12; 26]	<15 (0,75, 0,72)	0,754 [0,678; 0,830]	0,000
		“responders”	40 [15; 71]	≥15 (0,75, 0,72)		
2	ΔESV	“non-responders” (n=24, 20%)	52 [50; 62]	>-9 (1, 0,92)	0,998 [0,990; 1]	0,000
		“responders” (n=59, 50%)	-10 [-20; 3]	≤-9 и >-37 (1, 0,98)		
		“super-responders” (n=36, 30%)	-56 [-64; -51]	≤-37 (1, 1)		
	ΔEDV	“non-responders”	78 [5; 86]	>-9 (1, 0,80)	0,959 [0,929; 0,992]	0,000
		“responders”	-13 [-26; -4]	≤-9 и >-40 (0,95, 0,85)		
		“super-responders”	-65 [-77; -52]	≤-40 (0,9, 0,9)		
	ΔLVEF	“non-responders”	6 [-27; 25]	<0 (0,59, 0,80)	0,677 [0,491; 0,860]	0,045
		“responders”	18 [0; 40]	≥0 и <43 (0,71, 0,80)		
		“super-responders”	72 [47; 115]	≥43 (0,8, 0,8)		
3	ΔESV	“non-responders” (n=23, 26%)	18 [11; 33]	>0 (1, 0,99)	0,998 [0,991; 1]	0,000
		“responders” (n=26, 30%)	-19 [-33; -12]	≤0 и >-37 (0,98, 0,98)		
		“super-responders” (n=39, 44%)	-63 [-73; -56]	≤-37 (0,97, 0,97)		
	ΔEDV	“non-responders”	28 [20; 49]	>0 (0,95, 0,95)	0,978 [0,952; 1]	0,000
		“responders”	-20 [-37; -9]	≤0 и >-40 (0,93, 0,93)		
		“super-responders”	-70 [-87; -61]	≤-40 (0,92, 0,92)		
	ΔLVEF	“non-responders”	13 [0; 30]	<15 (0,69, 0,67)	0,769 [0,661; 0,877]	0,000
		“responders”	27 [13; 39]	≥15 и <42 (0,75, 0,73)		
		“super-responders”	77 [56; 119]	≥42 (0,82, 0,82)		

Abbreviations: CI — confidence interval, EDV — end-diastolic volume, ESV — end-systolic volume, LVEF — left ventricular ejection fraction, HF — heart failure, Se — sensitivity, Sp — specificity, P — significance of AUC.

those patients with LV ESV and EDV not exceeding 9% in 2 years. With a decrease in LV ESV and EDV by more than 37% and 40%, respectively, the patient falls into the cluster of “super-responders”. In 3 years after CRT, the border between the clusters of “non-responders” and “responders” changes. So, with any decrease in LV ESV and EDV that is different from zero, within 3 years after CRT, the patient falls into the cluster of “responders”. The borderline between “responders” and “super-responders” remains the same as for a period of 2 years (Table 4).

Information models for predicting CRT effectiveness

Using logistic regression, we created prognostic models for entering a cluster with unfavorable changes (“non-responders”) in reverse remodeling parameters and to clusters with favorable changes (“responders” and “super-responders”) (Table 5). To create the models, we used the blocks of preoperative dia-

gnostic protocols described in the section “Material and Methods”.

The created models based on preoperative diagnostic protocols turned out to be significant, but the predictive power of these models was low and the classification accuracy did not exceed 62% (Table 5). When using the parameters obtained during IED implantation, the prediction quality in the first year improved and the classification accuracy increased to 70%. Using information on changes in LVEF, ESV, and EDV in the first year after CRT initiation, it was possible to improve the accuracy of prognostic models for the second and third postoperative years, but their accuracy also did not exceed 72%.

Discussion

Three-year analysis was carried out in order to determine the most informative postoperative period for assessing the CRT effectiveness, the search for a reliable quantitative rule for assessing the CRT

Table 5

Information models for CRT prognosis depending on postoperative period

Parameter	Unstandardized coefficients		R ²	P	Accuracy of classification
	Value	P			
1 year					
Parameters before CRT					
Sex (0-M; 1-F)	0,72	0,033	0,22	0,031	62%
Constant	0,28	0,191			
Improvement of the model (+ parameters during IED implantation)					
Sex (0-M; 1-F)	0,92	0,032	0,48	0,000	70%
Left atrial area	-0,59	0,046			
QRS on pacing	-0,02	0,019			
Constant	6,34	0,002			
2 year					
Parameters before CRT					
LV ESV before	-0,01	0,024	0,31	0,042	58%
Constant	1,58	0,026			
Improvement of the model (+ change in EF, ESV, EDV in the first year)					
ΔESV by 1 year	-0,04	0,000	0,64	0,000	69%
LV ESV before	-0,01	0,179			
Constant	1,67	0,033			
3 year					
Parameters before CRT					
LVEF before	0,07	0,059	0,19	0,010	53%
Constant	-1,68	0,80			
Improvement of the model (+ change in EF, ESV, EDV in the first year)					
LVEF	0,03	0,590	0,47	0,001	72%
ΔESV by 1 year	-0,08	0,000			
Constant	1,18	0,452			

Abbreviations: IED — implantable electronic device, EDV — end-diastolic volume, ESV — end-systolic volume, LVEF — left ventricular ejection fraction, CRT — cardiac resynchronization therapy.

effectiveness in indicated periods and the search for predictors of changes in reverse remodeling parameters at 1, 2, 3 years after surgery.

First, we assessed the response to CRT using parameters characterizing LV reverse remodeling. In the majority of patients, LV ESV and EDV decreases compared to preoperative ones during all three years after CRT. The rate of decline in these indicators slows down 2 and 3 years after CRT initiation and does not significantly differ from zero. Based on this, it is reasonable to evaluate the change in these parameters 1 year after CRT implantation. At the same time, in most patients, LVEF continues to increase in comparison with the preoperative value for a longer period at three years after CRT placement, although the growth rate of LVEF 2 and 3 years after surgery also slows down compared to the first year after implantation. Considering that

in the interval from a year to two years, an increase in LVEF is observed that is significantly different from zero, and at the stage from two to three years, the increase does not significantly differ from zero, to assess the change in LVEF 2 years after CRT should be considered. Similar results were obtained in studies reviewed by Cleland JG, et al. [10].

The assessment of clinical response to CRT was carried out by assessing the change in HF class within three years after CRT initiation. A decrease in HF class is observed throughout the study as compared to the preoperative data, while improvement in HF class over the entire follow-up period is demonstrated by 70,1% of patients. After 1 year, improvement is observed in 48,8%, and in 26% of patients there is no improvement either in the first year or in further periods under consideration. So, 74,5% of patients after the first year have a clinical

response to therapy. In this regard, evaluating the effectiveness of CRT in changing the HF class 1 year after implantation should be considered.

Based on results obtained, a hypothesis has been developed that the decrease in HF class occurs earlier than the reverse LV remodeling. We showed that in patients with decrease in HF class a year after CRT, both EDV and ESV is significantly less compared to LV volume in patients without a decrease in HF class, but the difference between the LVEF in the considered groups remains insignificant up to 2 years of CRT. Reverse remodeling lasts up to 2 years after the CRT initiation, while we observe a decrease in HF class already a year after implantation, and then it does not decrease in most cases. These findings support the hypothesis of an earlier decrease in HF class compared with reverse remodeling. The time interval for assessing the success of CRT remains an open question [7, 10]; in most studies, the success of CRT is considered 6 months after therapy. As our studies show, this period is insufficient to assess the effectiveness of therapy. Similar conclusions were made in the study by V. Kuznetsov, et al. [11], which showed that the most “responders” and all “super-responders” appear in the late postoperative period. Moreover, patients with a rapid response to CRT in 3-month postoperative period had lower 5-year survival rates after starting CRT [11].

Quantitative criteria for assessing CRT success are also under discussion. A review [4, 10] provides about ten criteria for CRT effectiveness used in different studies using the parameters of LV reverse remodeling. To objectify quantitative parameters to assess the effectiveness of CRT, we applied a two-step cluster analysis and performed an automated classification of patients at 1, 2, and 3 years after CRT according to reverse remodeling parameters. For all postoperative periods, the relative decrease in LV ESV and EDV are of high importance when dividing into clusters, while the change in LVEF had lower significance during clustering. In a period of 1 year after CRT, there are 2 clusters with good separability. We conditionally named one cluster with unfavorable changes of reverse remodeling parameters “non-responders”, and a cluster with improvement in reverse remodeling parameters — “responders”. There were following criterion for evaluating the effectiveness in the first year after CRT based on cluster analysis: a decrease in LV ESV and EDV by 9% or more compared to preoperative data [4]. In further periods after the start of CRT, 3 clusters with good separability are distinguished. One cluster, as in the first year, is “non-responders”. But patients with improvement are divided into 2 clusters, which we called “responders” and “super-responders”. Stratification of patients into a cluster of “super-responders” is consistent

with studies that indicate super-responders precisely in the long-term postoperative periods [11-13], and according to our data, this occurs 2 years after CRT. There were following cluster separability criteria: “non-responders”, as in the first year, are patients with change in LV ESV and EDV did not exceed 9% for 2 years. With a decrease in LV ESV and EDV by more than 37% and 40%, respectively, the patient falls into the cluster of “super-responders”. Three years after CRT, the border between the clusters of “non-responders” and “responders” slightly changes, so with any decrease in LV ESV and EDV within 3 years after CRT, the patient falls into the cluster of “responders”. This result may be associated with the smallest, compared to the past, cohort of 88 patients whose data were used for clustering. The criteria for falling into the “super-responders” cluster are the same as in the previous period.

Using the criteria for evaluating the success of CRT, obtained based on our cluster analysis, using logistic regression, prognostic models of CRT effectiveness were constructed according to preoperative parameters obtained in the clinic with standard diagnostic protocols for patients with HF. Although the created models show significance, the predictive power of these models is low. Thus, the model created based on preoperative data for predicting the response to therapy after 1 year includes only patient sex, has a $R^2 < 0,22$. So, the model correctly describes only 22% of cases, while the classification accuracy in the considered sample of 62% is also low. With an increase in postoperative period, the predictive power of models decreases even more. When using the additional characteristics obtained during IED implantation, as well as LV Δ EDV, Δ ESV, Δ EF one year after CRT implantation, to predict the response in 2- and 3-year period, the predictive power of the models increases, but R^2 does not exceed 0,64, and the classification accuracy is 72%. The results obtained indicate that the considered blocks of preoperative diagnostic parameters and patient stratification for CRT do not allow significantly predicting the effectiveness of CRT in the long-term postoperative period, which is consistent with studies [14, 15].

Study limitations. The study considered intervals that are multiples of 1 year after therapy; retrospective data did not allow for an additional study at 3, 6, 18, 30 months after therapy, which would make it possible to more accurately assess the timing of response to CRT.

A decrease in the number of patients in a cohort after 2 and especially 3 years after CRT compared to the number of patients after 1 year could affect the accuracy of assessing changes in EDV, ESV, EF, HF class and the accuracy of clustering.

Conclusion

The study revealed a period for assessing the clinical response and changes in LV reverse remodeling after CRT surgery, which is important for the optimal choice of postoperative therapy. It has been shown that in most cases, one year after surgery is sufficient to assess the clinical response, and the process of LV reverse remodeling can last up to two years on average.

When assessing the CRT effectiveness by reverse remodeling, along with a change in LV ESV, it is necessary to take into account LV EDV changes. The change in LVEF showed a significantly lower value among the analyzed parameters in assessing the CRT effectiveness. Based on the cluster classification

of patients, a dividing rule was established for responders and non-responders in the first and second years after surgery with an accuracy of 97%: a decrease in LV ESV and EDV by 9% or more compared to preoperative values.

Predictive models of CRT effectiveness, based on standard preoperative diagnostic protocols for HF patients, are not sufficiently accurate to be used for making decisions about the appropriateness of therapy. This indicates the need to receive additional data to improve the quality of prediction.

Relationships and Activities. This work was supported by a Russian Science Foundation grant № 19-14-00134.

References

- Fomin IV. Chronic heart failure in Russian Federation: what do we know and what to do. *Russ J Cardiol.* 2016;(8):7-13. (In Russ.) doi:10.15829/1560-4071-2016-8-7-13.
- Bleeker GB, Schalij MJ, Van Der Wall EE, Bax JJ. Postero-lateral scar tissue resulting in non-response to cardiac resynchronization therapy. *Journal of cardiovascular electrophysiology.* 2006;17(8):899-901. doi:10.1111/j.1540-8167.2006.00499.x.
- Cleland JG, Daubert J-C, Erdmann E, et al. The effect of cardiac resynchronization on morbidity and mortality in heart failure. *New England Journal of Medicine.* 2005;352(15):1539-49. doi:10.1056/NEJMoa050496.
- Zhang Q, Zhou Y, Yu C-M. Incidence, definition, diagnosis, and management of the cardiac resynchronization therapy non-responder. *Current opinion in cardiology.* 2015;30(1):40-9. doi:10.1097/HCO.0000000000000140.
- Dickstein K, Normand C, Auricchio A, et al. CRT Survey II: a European Society of Cardiology survey of cardiac resynchronization therapy in 11 088 patients who is doing what to whom and how? *European journal of heart failure.* 2018;20(6):1039-51. doi:10.1002/ejhf.1142.
- Bokeria L, Neminushchiy N, Postol A. Cardiac resynchronization therapy. Indications and novel approaches to the improvement of its efficiency. *Complex Issues of Cardiovascular Diseases.* 2018;7(3):102-16. (In Russ.) doi:10.17802/2306-1278-2018-7-3-102-116.
- Daubert C, Behar N, Martins RP, et al. Avoiding non-responders to cardiac resynchronization therapy: a practical guide. *European heart journal.* 2017;38(19):1463-72. doi:10.1093/eurheartj/ehw270.
- Tomassoni G. How to define cardiac resynchronization therapy response. *J Innov Card Rhythm Manag.* 2016;7:S1-7. doi:10.19102/icrm.2016.070003.
- van't Sant J, Mast T, Bos M, et al. Echo response and clinical outcome in CRT patients. *Netherlands Heart Journal.* 2016;24(1):47-55. doi:10.1007/s12471-015-0767-5.
- Cleland JG, Ghio S. The determinants of clinical outcome and clinical response to CRT are not the same. *Heart failure reviews.* 2012;17(6):755-66. doi:10.1007/s10741-011-9268-9.
- Kuznetsov VA, Soldatova AM, Krinochkin DV, Enina TN. Cardiac resynchronisation therapy in patients with congestive heart failure: whether we should expect for an "early" response? *Russian Heart Failure Journal.* 2017;18(3):172-7. (In Russ.) doi:10.18087/rhfj.2017.3.2341.
- Ghani A, Delnoy PPH, Adiyaman A, et al. Predictors and long-term outcome of super-responders to cardiac resynchronization therapy. *Clinical cardiology.* 2017;40(5):292-9.
- Liu X, Hu Y, Hua W, et al. A Predictive Model for Super-Response to Cardiac Resynchronization Therapy: The QQ-LAE Score. *Cardiol Res Pract.* 2020;2020:3856294. doi:10.1155/2020/3856294.
- Poulidakis E, Aggeli C, Sideris S, et al. Echocardiography for prediction of 6-month and late response to cardiac resynchronization therapy: implementation of stress echocardiography and comparative assessment along with widely used dyssynchrony indices. *The international journal of cardiovascular imaging.* 2019;35(2):285-94. doi:10.1007/s10554-018-01520-6.
- Feeny AK, Rickard J, Patel D, et al. Machine learning prediction of response to cardiac resynchronization therapy: Improvement versus current guidelines. *Circulation: Arrhythmia and Electrophysiology.* 2019;12(7):e007316. doi:10.1161/CIRCEP.119.007316.



Electroanatomic substrate of atrial fibrillation in patients after COVID-19

Osadchy An. M.¹, Semenyuta V. V.², Kamenev A. V.³, Shcherbak S. G.^{1,4}, Lebedev D. S.³

Aim. To determine the features of left atrial electroanatomic structure and the arrhythmia substrate in patients with atrial fibrillation (AF) after coronavirus disease 2019 (COVID-19).

Material and methods. The pilot study included 20 patients with AF who underwent catheter radiofrequency ablation. Ten patients had COVID-19 and 10 patients were included as a control group. AF substrate was identified using anatomic and bipolar mapping. Zones with following amplitudes were analyzed: <0,25 mV, <0,5 mV, from 0,5 to 0,75 mV inclusive, and >0,75 mV. Left atrial volume was determined based on anatomic map.

Results. The groups were homogeneous in AF type, number of patients after prior pulmonary vein isolation, and heart rate during mapping. In the COVID-19 group, there was a higher area of fibrous zones with an amplitude of <0,25 mV (51,5±16,6% vs 29,1±16,1% in the control group, p=0,007), <0,5 mV (76,7±11,5% vs 45,6±22,7% in the control group, p=0,001) and a lower area of intact myocardium with an amplitude >0,75 mV (11,6±8,0% vs 45,0±25,0% in the control group, p=0,001). In 7 COVID-19 patients, the posterior wall was isolated due to low-amplitude zones. Of these, three patients underwent surgery for the first time. According to ROC analysis, in patients after COVID-19, fibrous tissue (<0,5 mV) occupies more than half of the area, while normal tissue (>0,75 mV) — ~30% or less.

Conclusion. This study shows that SARS-CoV-2 infection may cause left atrial remodeling in the form of diffuse fibrosis. The arrhythmia substrate in patients after COVID-19 can be localized not only in pulmonary vein mouths, but

also in other left atrial areas. This must be taken into account before ablation, even if the procedure is being performed for the first time. It is recommended to perform amplitude mapping for all patients who have had SARS-CoV-2 infection in order to identify fibrous zones and plan the operation extent.

Keywords: atrial fibrillation, radiofrequency ablation, coronavirus infection, fibrosis, amplitude mapping.

Relationships and Activities: none.

¹City Hospital № 40 of Kurortny District, St. Petersburg;

²I. I. Mechnikov North-Western State Medical University, St. Petersburg;

³Almazov National Medical Research Center, St. Petersburg;

⁴Saint Petersburg State University, Saint Petersburg, Russia.

Osadchy An. M.* ORCID: 0000-0002-2406-942X, Semenyuta V. V. ORCID: 0000-0002-9402-3179, Kamenev A. V. ORCID: none, Shcherbak S. G. ORCID: none, Lebedev D. S. ORCID: 0000-0002-2334-1663.

*Corresponding author:

an_osadchy@mail.ru

Received: 27.05.2021

Revision Received: 15.06.2021

Accepted: 03.07.2021



For citation: Osadchy An. M., Semenyuta V. V., Kamenev A. V., Shcherbak S. G., Lebedev D. S. Electroanatomic substrate of atrial fibrillation in patients after COVID-19. *Russian Journal of Cardiology*. 2021;26(7):4526. (In Russ.) doi:10.15829/1560-4071-2021-4526

Coronavirus disease 2019 (COVID-19) has been studied by researchers around the world since its inception. To date, the proportion of patients who have suffered a disease caused by the severe acute respiratory syndrome-related coronavirus 2 (SARS-CoV-2) is consistently increasing. A large number of observations show that a more severe course and high mortality are associated with cardiovascular comorbidities. However, the pathogenesis of infection and the effect of virus on cardiac structure are not fully understood.

The central mechanism of SARS-CoV-2 penetration into cells is its binding with angiotensin-converting enzyme 2. This enzyme is also actively expressed in cardiac tissue and, to a greater extent, in cardiomyocytes themselves [1]. It is assumed that it is through this receptor that the virus can have a direct pathogenic effect on myocardium.

To a certain extent, cardiac tissue affinity is not unique to SARS-CoV-2. Other, more studied viruses, including other human coronaviruses — SARS-CoV and MERS-CoV, as well as the influenza A virus subtype H1N1, has similar properties [2]. A number of clinical observations of patients with COVID-19 have been published, which show that myocardial damage is observed in 12-23% of patients [3]. Morphologically, such damage has no specifics and manifests as moderate mononuclear cell infiltration [4].

The manifestations of myocardial involvement in COVID-19 are diverse and non-specific. There are abnormalities according to electrocardiography and transthoracic echocardiography, including ischemic. In some patients, there is an increased level of troponins I and T, creatine phosphokinase MB, as well as a heart failure marker N-terminal pro-brain natriuretic peptide [5]. Moreover, a high level of troponin I is also associated with a more severe course of infection [6]. However, an increase in this particular marker as a criterion of myocardial involvement in COVID-19 remains not entirely convincing. There is evidence that troponin I is elevated in all COVID-19 patients. An increase >99 percentile is observed in 8-12% of cases [7]. Also, an increase in troponin I concentration is observed in patients with renal failure due to slow metabolism and elimination of the enzyme from blood [3].

Elevated troponin levels may reflect both myocardial ischemic damage and myocardial inflammation. Previously, using magnetic resonance imaging (MRI), it has already been proven that some types of coronaviruses can cause acute myocarditis [8].

In patients with COVID-19-related fulminant myocarditis, blood interleukin-6 level is significantly increased, which, in turn, is associated with a more

severe disease course [5]. Also, in the serum of patients, there is an increase in other pro-inflammatory cytokines, for example, CXCL10, interleukin-8, tumor necrosis factor-alpha, etc. [9]. Inflammatory mediators, in particular transforming growth factor beta, contribute to atrial fibrosis and electrophysiological abnormalities in myocardium, increasing the risk of cardiac arrhythmias, including atrial fibrillation (AF) [10]. This is confirmed by recent clinical studies where arrhythmias in patients with COVID-19 were detected in 12,9% of cases, of which AF was observed in 61,5% of patients [11].

Left atrial (LA) myocardial fibrosis plays a significant role in the initiation and maintenance of AF, as well as recurrence after lapse after pulmonary vein isolation [12]. One of the methods for determining electroanatomic substrate of AF is contact mapping using 3D endocardial navigation systems. The combined use of amplitude mapping and contrast-enhanced MRI made it possible to establish that LA areas with an amplitude of <0,5 mV are associated with fibrosis zones [13, 14].

Large low-amplitude areas associated with LA myocardial fibrosis are an unfavorable predictor of AF recurrence after pulmonary vein isolation. Given this, it is especially important to perform amplitude mapping before radiofrequency ablation (RFA) in patients after COVID-19, since this can change surgery strategy.

The aim was to determine the features of left atrial electroanatomic structure and arrhythmia substrate in patients with AF after COVID-19.

Material and methods

The pilot study included 20 patients with AF who underwent RFA between May 2020 and May 2021. Of these, 10 patients had COVID-19 and 10 patients were included as a control group. The inclusion criterion in the COVID-19 group was a prior mild or moderate viral respiratory infection verified by real-time polymerase chain reaction (PCR) test. Three participants with moderate COVID-19 received in-hospital treatment, while the rest of patients were treated on an outpatient basis. Patients underwent a full course of treatment followed by determination of anti-SARS-CoV-2 immunoglobulin G level by quantitative enzyme-linked immunosorbent assay (ELISA) at least 1 month later. Hospitalization for RFA was performed at least 1,5 months after an infection. The average time from virus verification to surgery was 124±98 days (minimum — 45; maximum — 313). The inclusion criterion for control group was the absence of documented COVID-19 and recorded contacts with COVID-19 patients, as well as the absence of anti-SARS-CoV-2 IgG antibodies by ELISA for

Table 1

Clinical characteristics of patients

Parameter	Control group (n=10)	COVID-19 (n=10)	p	ES
Age, years	61±7 [56; 67]	66±6 [61; 70]	0,180	0,62
Sex Male/female	8 (80%)/2 (20%)	4 (40%)/6 (60%)	0,085	0,41
AF/AFL	4 (40%)	7 (70%)	0,301	0,35
Type Paroxysmal/persistent	4 (40%)/6 (60%)	3 (30%)/7 (70%)	0,639	0,10
Prior surgery Primary/repeated	5 (50%)/5 (50%)	6 (60%)/4 (40%)	0,653	0,10
Baseline rhythm Sinus/AF-AFL	5 (50%)/5 (50%)	1 (10%)/9 (90%)	0,070	0,44

Abbreviations: ES — effect size, AF — atrial fibrillation, AFL — atrial flutter.

at least 1 month before procedure. After negative ELISA results for IgG antibodies, two patients in the control group underwent a course of vaccination within 1,5 months before surgery. There were following exclusion criteria: two or more prior RFA procedures; a negative ELISA for IgG antibodies with a positive PCR for SARS-CoV-2; a negative PCR test with a positive ELISA for IgG antibodies.

All patients underwent real-time PCR test of oropharyngeal swabs for SARS-CoV-2 RNA before hospitalization. Prior to study inclusion, all patients signed written informed consent. The operation was performed under local anesthesia using right common femoral vein access. Interatrial septum puncture with a BRK-1 needle was performed using fluoroscopy guidance. Determination of AF electroanatomic substrate was performed by automatic anatomical and bipolar mapping using the CARTO 3 system (Biosense Webster) and the Confidence module with a SmartTouch ThermoCool ablation catheter or a LassoNav catheter. Points was included evenly along the LA anterior and posterior walls, roof, as well as in the area of venous pools. Points at pulmonary vein orifices and mitral annulus were excluded from the analysis. The area of substrate was determined using a standard Area Measurement tool. Amplitude areas were analyzed in the range <0,25 mV, <0,5 mV, from 0,5 to 0,75 mV inclusive, as well as >0,75 mV. The LA volume was determined based on anatomical map.

Statistical analysis was performed using SPSS v.26 and STATISTICA 12 software. Distribution normality was assessed by the Shapiro-Wilk method. Quantitative variables are presented as mean and standard deviation (SD) with 95% confidence interval (CI) (Mean±SD [CI -95%; CI +95%]), as well as median and quartiles (Me [Q25; Q75]). The significance of differences in quantitative variables was assessed using the Student's t-test and Welch's

t-test, as well as the Mann-Whitney U-test. The effect size is represented by Cohen's d coefficient, while d value >0,8 was regarded as a high level of effect. To exclude the influence of independent factors, multivariate analysis of variance with Tukey's test was performed. The optimal threshold values of quantitative variables were determined by receiver operating characteristic (ROC) analysis. The cut-off point was chosen by the Youden method. Testing the hypothesis on differences in the contingency tables was assessed using Fisher's exact and χ^2 -Pearson tests, and the effect size (ES) — using phi coefficient and Cramer's V. Correlation analysis was carried out using the Pearson correlation coefficient, while assessment of statistical significance — using the t-test. Differences were considered significant at $p < 0,05$ and test power $1 - \beta > 0,8$.

Results

The clinical characteristics of patients are presented in Table 1. The groups are homogeneous in AF type, number of patients after prior pulmonary vein isolation, and heart rate during mapping. These factors, both individually and in combination, did not significantly affected on the area of analyzed amplitude zones ($p > 0,05$).

Mapping was performed immediately before ablation and, in the presence of sinus rhythm, was performed on atrial pacing at a cycle length of 600 ms. The number of points in the groups did not differ significantly (625 [491; 864] in the control group versus 938 [680; 1035] in the COVID-19 group, $p = 0,1$). The analysis of anatomical and amplitude maps is presented in Table 2. Patients with prior COVID-19, significant and with a high effect level, had a higher fibrosis area with an amplitude of <0,25 mV, <0,5 mV and a lower area of normal atrial tissue with an amplitude >0,75 mV (Figure 1, 2). In the COVID-19 group, there is a tendency to an increase

Table 2

Analysis of anatomic and amplitude maps

Parameter	Control group (n=10)	COVID-19 (n=10)	p	Cohen's d
Left atrial volume, ml	101,2±40,5 [72,2; 130,1]	128,6±50,3 [92,5; 164,6]	0,197	0,599
Zone <0,25 mV, %	29,1±16,1 [17,5; 40,6]	51,5±16,6 [39,6; 63,4]	0,007	1,370
Zone <0,5 mV, %	45,6±22,7 [29,4; 61,8]	76,7±11,5 [68,4; 84,9]	0,001	1,728
Zone of 0,5-0,75 mV, %	9,4±3,7 [6,7; 12,0]	11,7±6,2 [7,3; 16,2]	0,312	0,465
Zone >0,75 mV, %	45,0±25,0 [27,1; 62,9]	11,6±8,0 [5,9; 17,3]	0,001	1,799

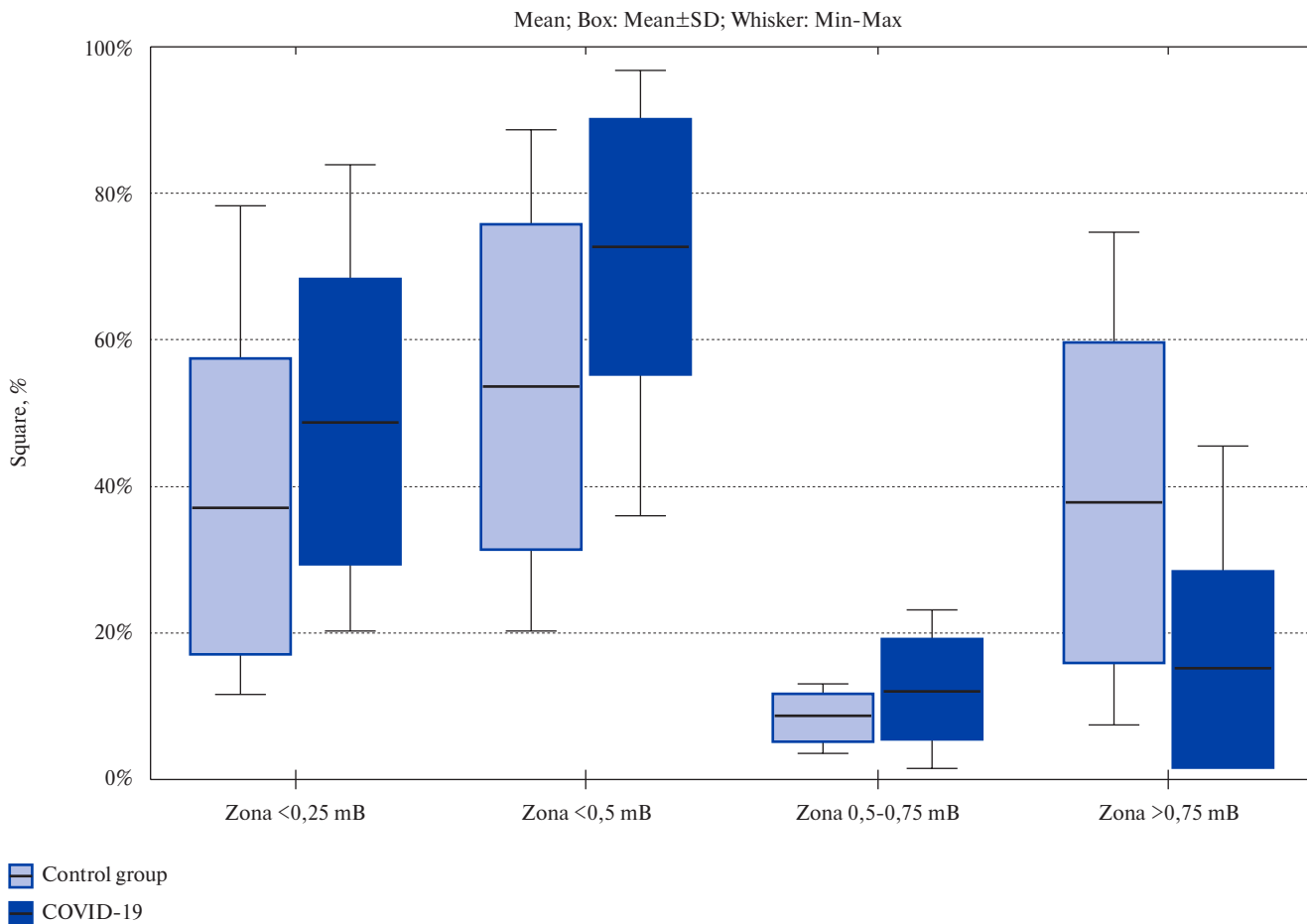


Figure 1. Area of amplitude zone. Abbreviation: SD — standard deviation.

in LA volume and area with delayed conduction with an amplitude of 0,5-0,75 mV; the effect level was moderate, but differences were insignificant. These changes did not show any correlation taking into account the time from virus verification to operation (Table 3).

The volume of operations performed is presented in Table 4. Isolation of LA posterior wall was performed in 1 patient in the control group due to absence of electrical activity in pulmonary vein orifices after previous ablation. In the COVID-19 group, posterior wall isolation was required in 7

cases, and in 3 patients the operation was performed for the first time (Figure 3). In one case, there was also no electrical activity in pulmonary vein orifices after previous isolation. In other cases, the reason was the presence of diffuse low-amplitude zones in LA.

The ROC analysis (Figure 4) showed that in patients after COVID-19, fibrous tissue (<0,5 mV) occupies more than half of the area (Table 5), while normal tissue (>0,75 mV) ~30% or less. LA volume after infection tends to increase and reaches >120 ml (maximum, 206,9 ml).

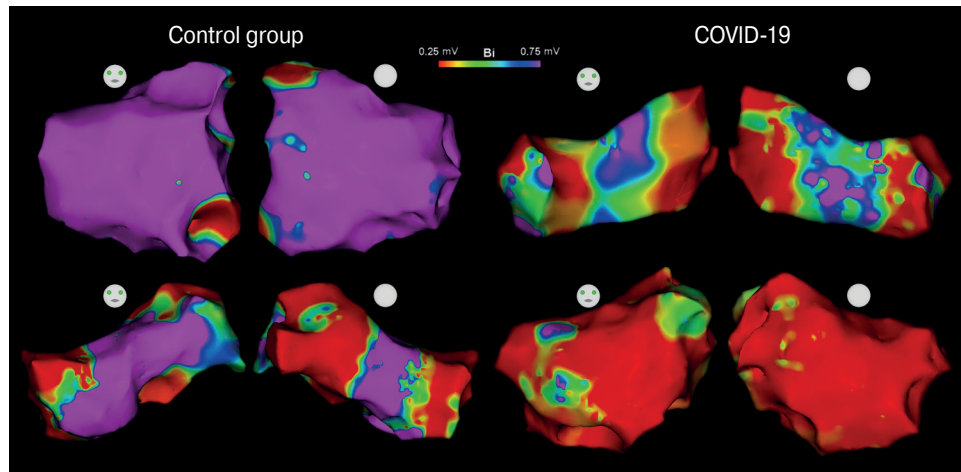


Figure 2. Amplitude maps of patients.

Abbreviation: the figure shows LA bipolar amplitude maps. Fibrous areas with an amplitude $<0,25$ mV are shown in red, and normal tissue with an amplitude $>0,75$ mV — purple. Both patients in the control group completed the full course of vaccination 1,5 months before surgery. Above shows the amplitude maps of patients who underwent surgery for the first time, below — patients with prior pulmonary vein isolation.

Abbreviation: LA — left atrial.

Table 3

**Correlation analysis taking into account
the time from SARS-CoV-2 verification to the operation**

Parameter	Pearson coefficient (R)	Determination coefficient (R^2)	p
Left atrial volume, ml	0,44	0,189	0,209
Zone $<0,25$ mV, %	-0,05	0,003	0,883
Zone $<0,5$ mV, %	-0,39	0,150	0,269
Zone of 0,5-0,75 mV, %	-0,09	0,008	0,803
Zone $>0,75$ mV, %	0,63	0,394	0,051

Table 4

RFA volume

Parameter	Control group (n=10)	COVID-19 (n=10)	p	ES
Pulmonary vein isolation	9 (90%)	9 (90%)	0,763	0
Posterior wall isolation	1 (10%)	7 (70%)	0,010	0,61
CTI ablation	2 (20%)	3 (30%)	0,500	0,12

Abbreviation: ES — effect size, CTI — cavotricuspid isthmus.

Conclusion

Amplitude map points in presented work was included either at sinus rhythm or at AF. In both groups, there are patients with paroxysmal and persistent AF. Some studies have described the effect of heart rate and AF type on the signal amplitude during endocardial mapping, but this effect was not found in our study.

One study compared amplitude maps for AF and sinus rhythm after electrical cardioversion in the same patients [15]. According to study results,

the baseline rhythm significantly correlates with the average amplitude of bipolar signal and also depends on arrhythmia type. In paroxysmal AF, the average amplitude is higher than in persistent AF, both in sinus rhythm and in AF. So, it follows that the total amplitude $<0,5$ mV obtained during AF corresponds to an amplitude $<1,5$ mV at sinus rhythm, and this error must be taken into account when comparing these groups of patients. At the same time, other researchers have not confirmed these results [16].

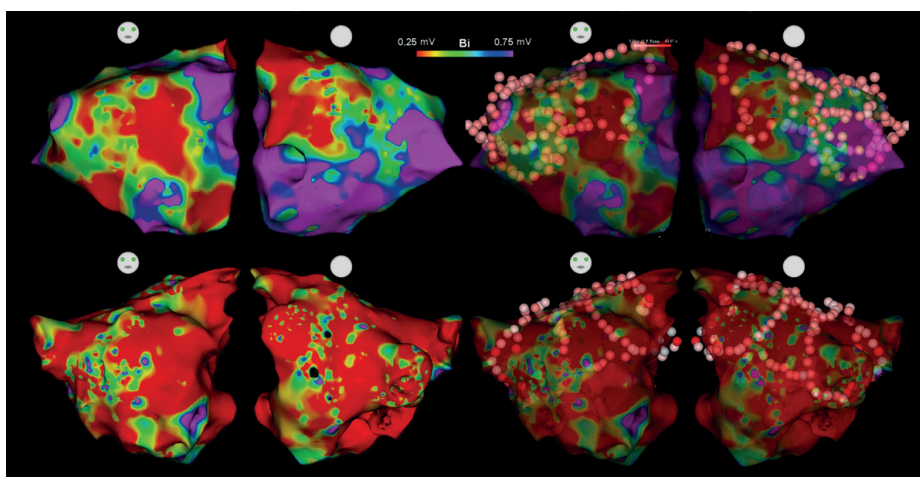


Figure 3. Amplitude maps of COVID-19 patients.

Note: the figure shows LA bipolar amplitude maps in two patients after COVID-19, who underwent RFA for the first time in combination with LA posterior wall isolation. Fibrous areas with an amplitude $<0,25$ mV are shown in red, and normal tissue with an amplitude $>0,75$ mV — purple. Ablation points are projected on the right maps.

Abbreviations: LA — left atrial, RFA — radiofrequency ablation.

Table 5

ROC-analysis

Parameter	Cut-off point	Sensitivity	Specificity	AUC±SD [CI +95%; CI -95%]	p
Left atrial volume, ml	121,9	80%	80%	0,710±0,128 [0,460; 0,960]	$>0,05$
Zone $<0,25$ mV, %	40,5%	80%	80%	0,850±0,085 [0,682; 1,018]	$<0,001$
Zone $<0,5$ mV, %	58,6%	100%	70%	0,920±0,060 [0,803; 1,037]	$<0,001$
Zone of 0,5-0,75 mV, %	10,7%	70%	70%	0,650±0,129 [0,396; 0,904]	$>0,05$
Zone $>0,75$ mV, %	29,8%	100%	70%	0,930±0,055 [0,822; 1,038]	$<0,001$

Abbreviations: AUC — area under the ROC curve, CI — confidence interval, SD — standard deviation.

Also, this conclusion does not correlate with other studies that compared amplitude maps and fibrosis images on delayed contrast-enhanced MRI. These studies did not take into account the rhythm during mapping and AF type. The results of both studies show that the fibrous areas according to contrast-enhanced MRI have an amplitude $<0,5$ mV [13, 14].

In another study, also when comparing amplitude maps with fibrosis images on delayed contrast-enhanced MRI, but in patients after previous ablation, the cutoff point for scarring identification was chosen $<0,2$ mV for pulmonary veins and posterior wall and $<0,45$ mV for the rest areas of LA [17]. The authors suggest that inconsistency of cut-off points is due to the fact that all patients had previously undergone pulmonary vein ablation.

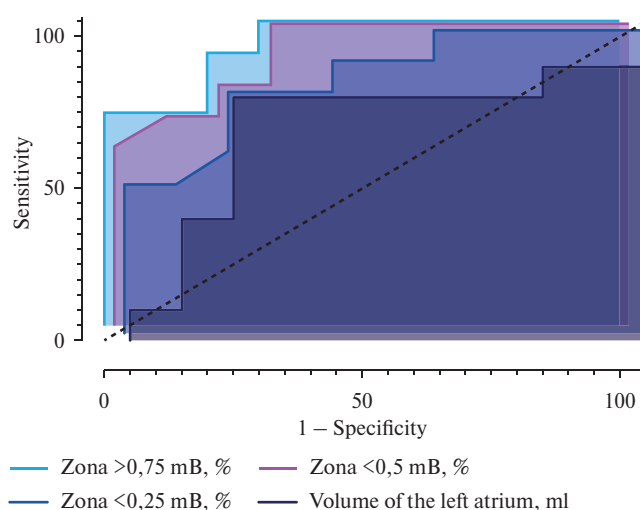


Figure 4. ROC curves for analyzed parameters.

The authors also assume that the cut-off point for fibrosis, not related with RFA, may differ. However, when compared with delayed contrast-enhanced MRI images, the authors chose a cut-off point of 0,27 mV to define the scar area.

It is also assumed that the region with an amplitude $\leq 0,75$ mV possesses the properties of arrhythmogenic substrate, since it is associated with a conduction slowing [18]. However, there is no conclusive evidence that an area with an amplitude of 0,5-0,75 mV is fibrous tissue.

Based on this, it follows that the fibrous tissue of LA has an amplitude of $<0,45$ - $<0,5$ mV and does not depend on either the heart rate during mapping or arrhythmia type. Therefore, there is no need to take into account the error in mean signal amplitude from LA when assessing the fibrotic area.

Considering that the extensive fibrous LA areas are an unfavorable prognostic factor for AF recurrence after pulmonary vein isolation, some researchers have proposed a modified individual approach for AF substrate ablation [19]. It consists in performing isolation of LA posterior wall in the presence of fibrous areas, identified during amplitude mapping. A further large-scale study by these authors found an improved prognosis for recurrent arrhythmias in patients with a modified approach [20].

Study limitations. This is a pilot study and is currently ongoing. Due to the small number of patients meeting the inclusion and exclusion criteria, it was decided to combine patients referred for primary surgery with patients after prior pulmonary vein isolation, patients with different AF types and different heart rhythms during mapping. However, these indicators, both in univariate and multivariate analysis, did not have a significant effect on the area of analyzed amplitude zones.

Conclusion

This study shows that SARS-CoV-2 infection may cause left atrial remodeling in the form of diffuse fibrosis. These abnormalities can be detected using bipolar endocardial mapping. The arrhythmia substrate in patients after COVID-19 can be localized not only in pulmonary vein orifices, but also in other left atrial areas. Moreover, the arrhythmia substrate is mainly represented by fibrotic areas with an amplitude of $<0,25$ mV and $<0,5$ mV. This must be taken into account before ablation, even if the procedure is being performed for the first time. It is recommended to perform amplitude mapping for all patients who have had SARS-CoV-2 infection in order to identify fibrous zones and plan the operation extent.

Relationships and Activities: none.

References

- Nicin L, Abplanalp WT, Mellentin H, et al. Cell type-specific expression of the putative SARS-CoV-2 receptor ACE2 in human hearts. *Eur Heart J*. 2020;41(19):1804-6. doi:10.1093/eurheartj/ehaa311.
- Kochi AN, Tagliari AP, Forleo GB, et al. Cardiac and arrhythmic complications in patients with COVID-19. *J Cardiovasc Electrophysiol*. 2020;31(5):1003-8. doi:10.1111/jce.14479.
- Yang X, Yu Y, Xu J, et al. Clinical course and outcomes of critically ill patients with SARS-CoV-2 pneumonia in Wuhan, China: a single-centered, retrospective, observational study. *Lancet Respir Med*. 2020;8(5):475-81. doi:10.1016/S2213-2600(20)30079-5.
- Xu Z, Shi L, Wang Y, et al. Pathological findings of COVID-19 associated with acute respiratory distress syndrome. *Lancet Respir Med*. 2020;8(4):420-2. doi:10.1016/S2213-2600(20)30076-X.
- Chen C, Zhou Y, Wang DW. SARS-CoV-2: a potential novel etiology of fulminant myocarditis. *Herz*. 2020;45(3):230-2. doi:10.1007/s00059-020-04909-z.
- Lippi G, Lavie CJ, Sanchis-Gomar F. Cardiac troponin I in patients with coronavirus disease 2019 (COVID-19): Evidence from a meta-analysis. *Prog Cardiovasc Dis*. 2020;63(3):390-1. doi:10.1016/j.pcad.2020.03.001.
- Lippi G, Plebani M. Laboratory abnormalities in patients with COVID-2019 infection. *Clin Chem Lab Med*. 2020;58(7):1131-4. doi:10.1515/cclm-2020-0198.
- Alhogbani T. Acute myocarditis associated with novel Middle east respiratory syndrome coronavirus. *Ann Saudi Med*. 2016;36(1):78-80. doi:10.5144/0256-4947.2016.78.
- Del Valle DM, Kim-Schulze S, Huang H-H, et al. An inflammatory cytokine signature predicts COVID-19 severity and survival. *Nat Med*. 2020;26(10):1636-43. doi:10.1038/s41591-020-1051-9.
- Hu Y-F, Chen Y-J, Lin Y-J, et al. Inflammation and the pathogenesis of atrial fibrillation. *Nat Rev Cardiol*. 2015;12(4):230-43. doi:10.1038/nrcardio.2015.2.
- Coromilas EJ, Kochav S, Goldenthal I, et al. Worldwide Survey of COVID-19-Associated Arrhythmias. *Circ Arrhythmia Electrophysiol*. 2021;14(3):285-95. doi:10.1161/CIRCEP.120.009458.
- Marrouche NF, Wilber D, Hindricks G, et al. Association of Atrial Tissue Fibrosis Identified by Delayed Enhancement MRI and Atrial Fibrillation Catheter Ablation: The DECAAF Study. *JAMA*. 2014;311(5):498-506. doi:10.1001/jama.2014.3.
- Spragg DD, Khurram I, Zimmerman SL, et al. Initial experience with magnetic resonance imaging of atrial scar and co-registration with electroanatomic voltage mapping during atrial fibrillation: Success and limitations. *Hear Rhythm*. 2012;9(12):2003-9. doi:10.1016/j.hrthm.2012.08.039.
- Badger TJ, Daccarett M, Akoum NW, et al. Evaluation of left atrial lesions after initial and repeat atrial fibrillation ablation: lessons learned from delayed-enhancement MRI in repeat ablation procedures. *Circ Arrhythm Electrophysiol*. 2010;3(3):249-59. doi:10.1161/CIRCEP.109.868356.
- Yagishita A, De Oliveira S, Cakulev I, et al. Correlation of Left Atrial Voltage Distribution Between Sinus Rhythm and Atrial Fibrillation: Identifying Structural Remodeling by 3-D Electroanatomic Mapping Irrespective of the Rhythm. *J Cardiovasc Electrophysiol*. 2016;27(8):905-12. doi:10.1111/jce.13002.
- Saghy L, Callans DJ, Garcia F, et al. Is there a relationship between complex fractionated atrial electrograms recorded during atrial fibrillation and sinus rhythm fractionation? *Hear Rhythm*. 2012;9(2):181-8. doi:10.1016/j.hrthm.2011.09.062.
- Kapa S, Desjardins B, Callans DJ, et al. Contact Electroanatomic Mapping Derived Voltage Criteria for Characterizing Left Atrial Scar in Patients Undergoing Ablation for Atrial Fibrillation. *J Cardiovasc Electrophysiol*. 2014;25(10):1044-52. doi:10.1111/jce.12452.
- Orshanskaya VS, Kamenev AV, Belyakova LA, et al. Left atrial electroanatomic substrate as a predictor of atrial fibrillation recurrence after circular radiofrequency pulmonary veins isolation. Observational prospective study results. *Russ J Cardiol*. 2017;148(8):82-9. (In Russ.) doi:10.15829/1560-4071-2017-8-82-89.
- Kottkamp H, Berg JAN, Bender R, et al. Box Isolation of Fibrotic Areas (BIFA): A Patient-Tailored Substrate Modification Approach for Ablation of Atrial Fibrillation. *J Cardiovasc Electrophysiol*. 2016;27(1):22-30. doi:10.1111/jce.128709.
- Schreiber D, Rieger A, Moser F, et al. Catheter ablation of atrial fibrillation with box isolation of fibrotic areas: Lessons on fibrosis distribution and extent, clinical characteristics, and their impact on long-term outcome. *J Cardiovasc Electrophysiol*. 2017;28(9):971-83. doi:10.1111/jce.13278.



Molecular mechanisms of left atrial fibrosis development in patients with atrial fibrillation and metabolic syndrome: what biomarkers should be used in clinical practice?

Ionin V. A.¹, Zaslavskaya E. L.¹, Barashkova E. I.¹, Pavlova V. A.¹, Borisov G. I.¹, Averchenko K. A.¹, Morozov A. N.¹, Baranova E. I.^{1,2}, Shlyakhto E. V.^{1,2}

Aim. To determine the blood concentration of fibrosis biomarkers in patients with atrial fibrillation (AF) in combination with metabolic syndrome (MS) and to analyze the relationship with myocardial fibrosis.

Material and methods. This cross-sectional case-control study included 547 patients aged 35 to 65 years: experimental group — patients with MS (n=373), of which 202 patients had AF; comparison group — AF patients without MS (n=110); healthy subjects without cardiovascular diseases and metabolic disorders (n=64). Patients with AF and MS who underwent electroanatomic mapping before pulmonary vein isolation (n=79) were assessed for left atrial (LA) fibrosis severity.

Results. It was found that the blood concentration of circulating profibrogenic biomarkers in patients with AF and MS is higher than in patients with AF without MS: aldosterone (135,1 (80,7-224,1) and 90,1 (68,3-120,3) pg/ml, p<0,0001), galectin-3 (10,6 (4,8-15,4) and 5,8 (4,8-8,3) pg/ml, p=0,0001), GDF15 (938,3 (678,3-1352,1) and 671,0 (515,7-879,5) pg/ml, p=0,001), TGF-beta-1 (4421,1 (2513,5-7634,5) and 2630,5 (2020,7-3785,4) pg/ml, p=0,001), CTGF (167,8 (78,9-194,3) and 124,3 (74,4-181,9) pg/ml, p<0,0001), PIIINP (88,5 (58,6-120,4) and 58,958,9 (40,7-86,1) ng/ml, p<0,0001), PINP (3421,4 (1808,1-4321,7) and 2996,1 (2283,8-3894,3) pg/ml, p<0,0001). Patients with paroxysmal AF have higher concentrations of TGF-beta1, CTGF and PINP than patients with persistent and permanent AF. In patients with persistent AF and MS, the concentrations of galectin-3, aldosterone, and PIIINP were higher than in patients with paroxysmal AF, while in patients with permanent AF, they were significantly lower. The plasma concentration of galectin-3 positively correlated with levels of PINP ($\rho=0,465$, p<0,0001), PIIINP ($\rho=0,409$, p<0,0001), GDF-15 ($\rho=0,369$, p<0,0001), CTGF ($\rho=0,405$, p<0,0001). According to multivariate regression, of all studied biomarkers, GDF-15 had a greater effect on PIIINP concentration ($\beta=0,234$, p=0,038), and galectin-3 — on PINP

($\beta=0,248$, p<0,021). Positive correlations of the severity of left atrial fibrosis with the concentration of galectin-3 ($\rho=0,563$, p<0,0001), PINP ($\rho=0,620$, p<0,0001), TGF-beta-1 ($\rho=0,390$, p<0,0001) and CTGF ($\rho=0,551$, p<0,0001). According to linear multivariate regression, the most significant effect on LA fibrosis severity among the studied biomarkers is exerted by galectin-3 ($\beta=0,432$, p<0,0001), PINP ($\beta=0,343$, p=0,001) and PIIINP ($\beta=0,286$, p=0,008).

Conclusion. An increase in the blood concentration of profibrogenic biomarkers galectin-3, TGF-beta-1, CTGF, PIIINP, and PINP is associated with an increase in LA fibrosis severity and probably has a pathogenetic role in increasing the AF risk in patients with MS.

Keywords: aldosterone, galectin-3, GDF-15, TGF-beta-1, CTGF, PINP, PIIINP, atrial fibrillation, metabolic syndrome.

Relationships and Activities: none.

¹First Pavlov State Medical University, St. Petersburg; ²Almazov National Medical Research Center, St. Petersburg, Russia.

Ionin V. A. * ORCID: 0000-0001-7293-1144, Zaslavskaya E. L. ORCID: 0000-0002-1209-7765, Barashkova E. I. ORCID: 0000-0002-7888-4374, Pavlova V. A. ORCID: 0000-0002-8479-0331, Borisov G. I. ORCID: 0000-0002-3116-5671, Averchenko K. A. ORCID: 0000-0001-6973-7519, Morozov A. N. ORCID: 0000-0002-7047-432X, Baranova E. I. ORCID: 0000-0002-8788-0076, Shlyakhto E. V. ORCID: 0000-0003-2929-0980.

*Corresponding author: ionin.v.a@gmail.com

Received: 03.07.2021

Revision Received: 15.07.2021

Accepted: 16.07.2021



For citation: Ionin V. A., Zaslavskaya E. L., Barashkova E. I., Pavlova V. A., Borisov G. I., Averchenko K. A., Morozov A. N., Baranova E. I., Shlyakhto E. V. Molecular mechanisms of left atrial fibrosis development in patients with atrial fibrillation and metabolic syndrome: what biomarkers should be used in clinical practice? *Russian Journal of Cardiology*. 2021;26(7):4579. (In Russ.) doi:10.15829/1560-4071-2021-4579

Prevalence of atrial fibrillation (AF) in developed countries is 1,5% [1]. Metabolic syndrome (MS) increases the risk of AF by 67%, as previously shown in the prospective Atherosclerosis Risk in Communities Study (ARIC). Among all the MS components, cardiac remodeling is primarily affected by hypertension (HTN) and abdominal obesity [2, 3]. HTN promotes AF due to increased afterload and developing cardiac remodeling, as well as due to hyperactivation of renin-angiotensin-aldosterone system (RAAS), which leads to myocardial structural changes with the formation of arrhythmia substrate — left atrial (LA) fibrosis [3]. Evidence for the role of HTN and RAAS in AF development is the fact that primary aldosteronism, characterized by HTN and high blood aldosterone levels, increases the risk of AF by 12 times [4]. Recently, special attention has been paid to obesity, primarily visceral obesity, as a possible cause of AF [5]. Obesity causes hemodynamic impairment — an increase in circulating plasma volume, contributing to dilatation of cardiac cavities, including LA. In addition, adipose tissue has a powerful fibrogenic and pro-inflammatory effect on cardiovascular system, promotes apoptosis and fibrosis. It is known that the development of AF is based on electrical instability of myocardium, its remodeling and structural remodeling. That is why such profibrotic conditions as HTN, heart failure, myocardial infarction, inflammation, obesity, and diabetes play a key role in the predisposition to arrhythmias. At the same time, the molecular mechanisms underlying the remodeling of atrial extracellular matrix are still not fully defined. Currently, a number of humoral factors have been established that have a fibrogenic effect: angiotensin II, aldosterone, galectin-3, transforming growth factor-beta1 (TGF-beta1), platelet-derived growth factor (PDGF) and connective tissue growth factor (CTGF), the role of which in AF development is currently being actively studied [6-9]. Studies on the problem of fibrogenesis previously showed that aldosterone regulates the production of TGF-beta1 and CTGF, which, in turn, are pleiotropic triggers for fibroblast activation, production of types I and III procollagen, and development of fibrosis [10, 11]. Understanding the mechanisms of AF development, including in MS, is essential for creation of approaches to its prevention and treatment. The search for myocardial fibrosis markers and predictors of AF development and progression in patients with MS is extremely important, because this will make it possible to identify groups at risk of developing AF and to provide primary and secondary prevention.

The aim of study was to determine the association of blood plasma levels of fibrosis markers

(aldosterone, galectin-3, growth differentiation factor-15 (GDF-15), TGF-beta1, CTGF, N-terminal propeptide of procollagen type I and III) with the severity of left atrial fibrillation fibrosis in patients with AF and MS, as well as to identify AF predictors in patients with MS.

Material and methods

In the period from 2014 to 2018, 1307 patients with AF admitted to therapy department of the University Clinic were examined, of which 721/1307 (55,2%) patients were diagnosed with coronary artery disease (CAD), 46/1307 (3,5%) — valvular heart disease, 80/1307 (6,1%) — inflammatory heart diseases. Further prospective follow-up included 547 subjects of both sexes aged 35-65 years: those with AF and MS (n=202); with AF and without MS (n=110); with MS without AF (n=171); healthy subjects (n=64). First and second groups included patients with paroxysmal (n=193), persistent (n=70) and permanent (n=49) AF types.

The study was carried out in accordance with the Good Clinical Practice (GCP) and the Declaration of Helsinki standards. The study protocol was approved by the Ethics Committee of the First Pavlov State Medical University of St. Petersburg. All patients signed written informed consent.

All MS patients had 3 or more components diagnosed according to the IDF criteria (2005). The study excluded patients with acute diseases and exacerbations of chronic inflammatory diseases, valvular heart disease, systemic diseases and cancer, as well as patients with impaired renal and liver function, thyroid diseases and primary hyperaldosteronism, strokes, cardiac surgery or other interventions in history. In all participants, anthropometric and diagnostic investigations were assessed, including electrocardiography and echocardiography. Echocardiography was performed using a Vivid 7 ultrasound system (GE, USA).

All samples of plasma and serum were centrifuged, followed by freezing at -40°C and determination of concentration of studied biomarkers using standard kits of enzyme-linked immunosorbent assay (ELISA). Aldosterone level was determined in blood plasma using an ELISA kit from DBC Inc (Canada). The level of galectin-3 in blood serum was determined by ELISA kit from eBioscience (Austria) with a detection range of 0,47-30,0 ng/ml. GDF-15 was determined in plasma by ELISA kit using BioVendor Human GDF-15/MIC-1 reagent kit (Czech Republic); the minimum detection value was 16,0 pg/ml. The concentration of TGF-beta1 was determined in blood serum by ELISA kit using the ProcartaPlex Human TGF-beta1 Simplex reagent kit from Affymetrix (eBioscience)

Table 1

Clinical, laboratory and echocardiographic characteristics of patients

Parameters	MS- AF- n=64 (1)	MS+ AF- n=171 (2)	MS- AF+ n=110 (3)	MS+ AF+ n=202 (4)	Statistical significance, p
Age, years	54,3±7,6	57,7±8,2	56,2±6,8	58,1±5,2	p>0,05
Sex, male/female	30/33	68/51	33/50	80/69	p>0,05
BMI, kg/m ²	21,5±3,8	32,3±7,3	24,2±5,1	31,1±7,1	p _{1,2} <0,001 p _{1,4} <0,001
Waist circumference, cm	76,5±5,1	112,3±10,5	79,1±10,7	113,9±13,5	p _{1,2} <0,001 p _{1,4} <0,001
Total cholesterol, mmol/l	4,9±0,9	5,4±1,1	4,8±1,2	5,2±1,2	p _{1,2} <0,001 p _{1,4} <0,001
LDL-C, mmol/l	2,8±0,3	3,4±0,3	3,1±0,3	3,1±0,4	p _{1,2} <0,001 p _{1,3} <0,001 p _{1,4} <0,001
HDL-C, mmol/l	1,6±0,3	1,2±0,3	1,4±0,3	1,3±0,4	p _{1,2} <0,001 p _{1,4} <0,001
TG, mmol/l	1,0±0,3	2,1±0,8	1,3±0,4	1,7±1,2	p _{1,2} <0,001 p _{1,4} <0,001
Glucose, mmol/l	4,7±0,6	6,1±1,2	5,1±0,4	6,0±1,4	p _{1,2} <0,001 p _{1,4} <0,001
Echocardiography					
LA diameter, mm	34,9±2,7	44,6±4,2	43,2±2,0	44,5±4,0	p _{1,2} <0,001 p _{1,3} <0,001 p _{1,4} <0,001
LA volume, ml	43,2±9,4	81,9±16,6	60,4±19,8	79,9±19,4	p _{1,2} <0,001 p _{1,3} <0,001 p _{1,4} <0,001 p _{2,3} =0,01 p _{3,4} =0,01
LA volume index, ml/m ²	24,3±4,9	39,2±9,7	30,4±9,0	40,1±11,2	p _{1,2} <0,001 p _{1,3} <0,001 p _{1,4} <0,001 p _{2,3} =0,01 p _{3,4} =0,01
LA volume, ml	41,3±8,9	68,5±14,4	57,5±20,6	65,9±14,7	p _{1,2} <0,001 p _{1,3} <0,001 p _{1,4} <0,001 p _{2,3} =0,01 p _{3,4} =0,01
RA volume index, ml/m ²	23,4±4,3	31,9±7,3	29,2±8,8	32,8±7,8	p _{1,2} <0,001 p _{1,3} <0,001 p _{1,4} <0,001
LVEF, %	65,3±7,0	63,2±6,0	62,4±4,2	61,4±6,0	p>0,05
AF duration, years	-	-	4,4±1,2	4,6±2,2	p>0,05
AF type	Paroxysmal	-	83/110 (75,4%)	110/202 (54,4%)	
	Persistent	-	20/110 (18,2%)	50/202 (24,8%)	
	Permanent	-	7/110 (6,4%)	42/202 (20,8%)	

Abbreviations: BMI — body mass index, LDL-C — low density lipoprotein cholesterol, HDL-C — high density lipoprotein cholesterol, MS — metabolic syndrome, TG — triglycerides, LA — left atrium, RA — right atrium, LVEF — left ventricular ejection fraction, AF — atrial fibrillation.

(Austria); the minimum detection value was 8,6 pg/ml. The concentration of CTGF was determined in blood plasma by ELISA kit using Human CTGF (High Sensitive) Aviscera Bioscience Inc.

reagent kit; the minimum detection value was 30,0 pg/ml. Concentrations procollagen type I N-terminal propeptide (PINP) and procollagen type III N-terminal propeptide (PIIINP) were

Table 2

Plasma and serum concentrations of aldosterone, galectin-3, GDF-15, TGF-beta1, CTGF, PIIINP and PINP in patients with AF and MS

Biomarkers	MS- AF- n=64 (1)	MS+ AF- n=171 (2)	MS- AF+ n=110 (3)	MS+ AF+ n=202 (4)	Statistical significance, p
Aldosterone, pg/ml	97,0 (55,8-125,5)	122,5 (87,0-173,5)	90,1 (68,3-120,3)	135,1 (80,7-224,1)	$p_{1,2}<0,0001$ $p_{1,3}=0,625$ $p_{1,4}<0,0001$ $p_{2,3}=0,01$ $p_{2,4}=0,01$ $p_{3,4}<0,0001$
Galectin-3, ng/ml	3,2 (2,4-4,2)	4,9 (4,2-8,8)	5,8 (4,8-8,3)	10,6 (4,8-15,4)	$p_{1,2}=0,001$ $p_{1,3}<0,0001$ $p_{1,4}<0,0001$ $p_{2,3}=0,467$ $p_{2,4}<0,0001$ $p_{3,4}=0,0001$
GDF-15, pg/ml	439,1 (410,2-474,6)	739,7 (541,9-996,7)	671,0 (515,7-879,5)	938,3 (678,3-1352,1)	$p_{1,2}<0,0001$ $p_{1,3}<0,0001$ $p_{1,4}<0,0001$ $p_{2,3}=0,446$ $p_{2,4}=0,001$ $p_{3,4}=0,001$
TGF-beta1, pg/ml	1840,5 (1414,3-3720,4)	2560,4 (2145,3-4515,8)	2630,5 (2020,7-3785,4)	4421,1 (2513,5-7634,5)	$p_{1,2}=0,01$ $p_{1,3}=0,002$ $p_{1,4}<0,0001$ $p_{2,3}=0,929$ $p_{2,4}=0,002$ $p_{3,4}=0,001$
CTGF, pg/ml	74,5 (45,5-103,8)	133,0 (91,3-172,5)	124,3 (74,4-181,9)	167,8 (78,9-194,3)	$p_{1,2}<0,0001$ $p_{1,3}=0,001$ $p_{1,4}<0,0001$ $p_{2,3}=0,347$ $p_{2,4}<0,0001$ $p_{3,4}<0,0001$
PIIINP, ng/ml	33,3 (23,5-42,6)	55,1 (37,7-86,9)	58,9 (40,7-86,1)	88,5 (58,6-120,4)	$p_{1,2}<0,0001$ $p_{1,3}<0,0001$ $p_{1,4}<0,0001$ $p_{2,3}=0,178$ $p_{2,4}<0,0001$ $p_{3,4}<0,0001$
PINP, pg/ml	1278,8 (775,1-2266,6)	2130,3 (1392,0-2820,1)	2996,1 (2283,8-3894,3)	3421,4 (1808,1-4321,7)	$p_{1,2}=0,008$ $p_{1,3}<0,0001$ $p_{1,4}<0,0001$ $p_{2,3}=0,067$ $p_{2,4}<0,0001$ $p_{3,4}=0,01$

Abbreviations: MS — metabolic syndrome, AF — atrial fibrillation, GDF-15 — growth differentiation factor 15, TGF-beta1 — transforming growth factor-beta1, CTGF — connective tissue growth factor, PINP — N-terminal propeptide of type I procollagen, PIIINP — N-terminal propeptide of type III procollagen.

determined in blood plasma by ELISA kit from Cloud-Clone Corp. (USA) with a detection range of 33-5000 pg/ml and 2,14-400 ng/ml, respectively.

In patients with ineffective antiarrhythmic therapy, indications for interventional treatment of AF have been determined. In an X-ray operation room using a CARTO3 non-fluoroscopic electroanatomical mapping system (Biosense Webster, USA) and a con-

tact force sensing catheter (Smart Touch Thermo-cool, Biosense Webster, USA), with a sinus rhythm, bipolar amplitude maps of LA and local activation time maps was created. Evaluation of low-voltage areas of 0,2-1,0 mV using the Area Measurement tool was carried out in the off line mode. The prevalence of fibrosis was estimated as a percentage of total LA area.

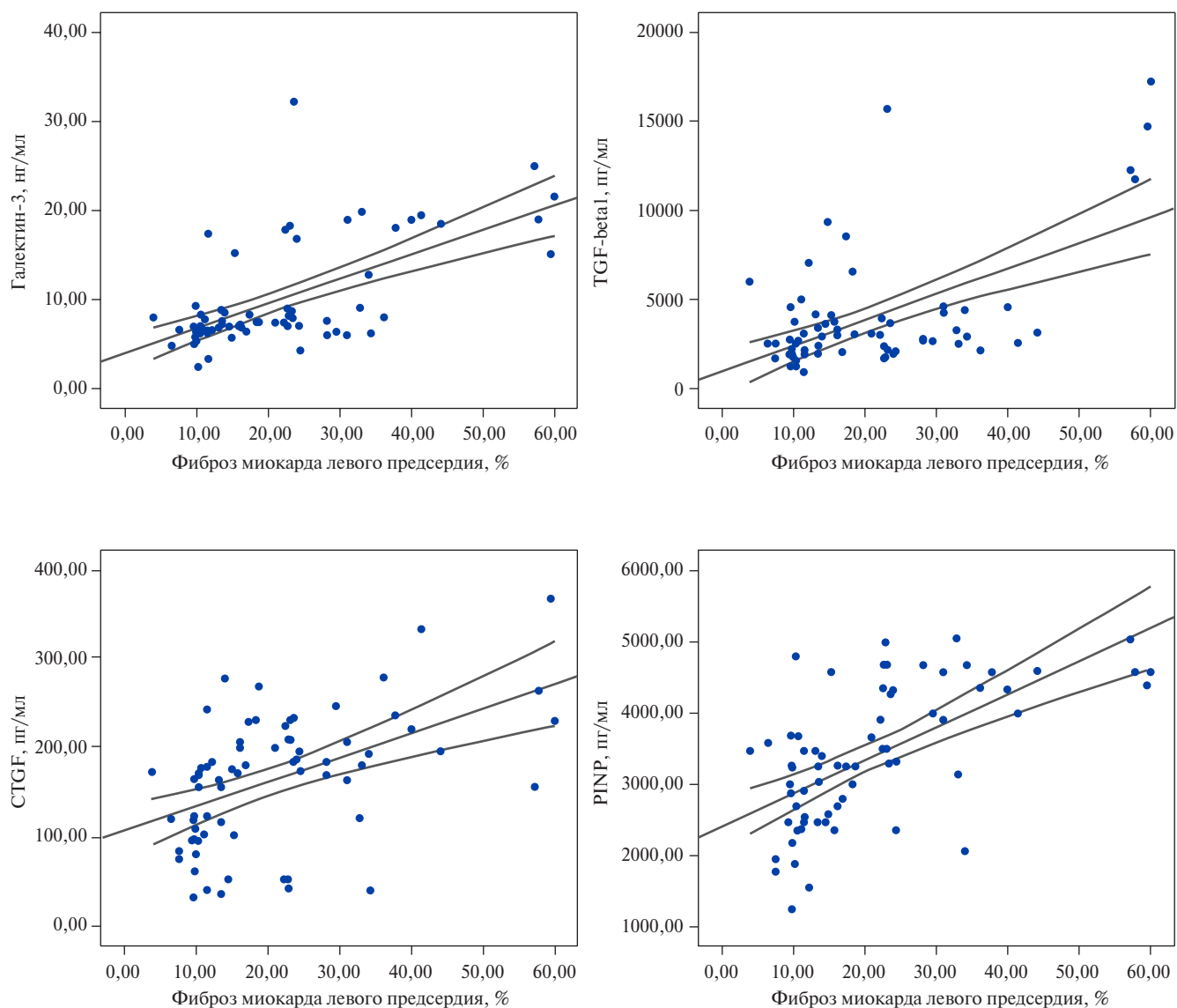


Figure 1. Correlations of galectin-3, TGF-beta1, CTGF and PINP with the severity of myocardial fibrosis in patients with AF and MS.
Abbreviations: TGF-beta1 — transforming growth factor-beta1, CTGF — connective tissue growth factor, PINP — N-terminal propeptide of type I procollagen.

The results were entered into the original database. Distribution normality of the numerical variables was assessed using the Kolmogorov-Smirnov test. Depending on distribution type, normally distributed quantitative variables are presented by the mean (M) \pm standard deviation (σ). Parametric unpaired Student's t-test was used for comparison in independent groups of normally distributed variables. For nonnormally distributed quantitative variables, the data are presented as a median (Me) and interquartile intervals (25-75%). For comparison in independent groups, the nonparametric Mann-Whitney U-test was used. Multiple comparisons in groups (more than two) in parametric statistics were carried out using one-way variance analysis (ANOVA), and for nonparametric

statistics — the Kruskal-Wallis test. In this case, the Bonferroni correction was used. When assessing the significance of correlation coefficient, we used the Pearson (r) tests with a normal distribution and Spearman (ρ) with a nonnormal distribution. We also used linear univariate and multivariate regression analyzes to assess the influence of factors on quantitative variables and binomial regression analysis to predict the probability of event. Statistical analysis was performed using licensed IBM SPSS software, version 22.0.

Results

The study groups were comparable in sex distribution and did not differ significantly by age. The main

Table 3

Plasma and serum concentrations of aldosterone, galectin-3, GDF-15, TGF-beta1, CTGF, PIIINP and PINP in patients with MS and various AF types

Biomarkers	Paroxysmal AF n=110 (1)	Persistent AF n=50 (2)	Permanent AF n=42 (3)	Statistical significance, p
Aldosterone, pg/ml	140,5 (90,4-182,2)	221,5 (107,4-272,9)	85,1 (72,5-111,5)	$p_{1,2}=0,001$ $p_{1,3}<0,0001$ $p_{2,3}<0,0001$
Galectin-3, ng/ml	8,9 (5,0-14,4)	12,5 (5,2-18,3)	6,3 (3,3-12,9)	$p_{1,2}=0,001$ $p_{1,3}=0,001$ $p_{2,3}<0,0001$
GDF-15, pg/ml	792,1 (619,9-1101,1)	982,4 (787,1-1252,0)	1345,0 (1102,7-1729,2)	$p_{1,2}<0,0001$ $p_{1,3}<0,0001$ $p_{2,3}<0,0001$
TGF-beta1, pg/ml	3678,5 (2279,8-6700,6)	2829,9 (1588,8-4349,4)	2228,3 (1839,9-2459,1)	$p_{1,2}=0,015$ $p_{1,3}=0,001$ $p_{2,3}=0,651$
CTGF, pg/ml	172,5 (106,7-208,5)	118,8 (79,2-200,4)	78,6 (61,6-97,5)	$p_{1,2}<0,0001$ $p_{1,3}<0,0001$ $p_{2,3}=0,001$
PIIINP, ng/ml	76,4 (55,6-120,5)	101,3 (84,9-147,1)	78,5 (62,3-89,7)	$p_{1,2}<0,0001$ $p_{1,3}=0,417$ $p_{2,3}\leq 0,0001$
PINP, pg/ml	4567,2 (2456,9-5567,4)	2806,3 (1600,0-4234,1)	1893,6 (1470,3-2521,1)	$p_{1,2}=0,018$ $p_{1,3}=0,001$ $p_{2,3}=0,003$

Abbreviations: AF — atrial fibrillation, GDF-15 — growth differentiation factor 15, TGF-beta1 — transforming growth factor-beta1, CTGF — connective tissue growth factor, PINP — N-terminal propeptide of type I procollagen, PIIINP — N-terminal propeptide of type III procollagen.

clinical, laboratory and echocardiographic characteristics are presented in Table 1.

Table 2 presents data on serum and plasma concentrations of studied biomarkers in subjects. It was found that the blood concentrations of aldosterone and galectin-3 in patients with AF and MS are higher than in patients with MS without AF and higher than in healthy subjects. The highest concentration of TGF-beta1 was found in patients with AF and MS, and there were no significant differences in its concentration in the groups of patients with MS without AF and AF without MS. Serum TGF-beta1 levels in patients with MS and without AF and those with AF and without MS did not differ, but were higher than in healthy subjects. The serum concentration of CTGF in patients with AF and MS was higher than in patients with MS and without AF and higher than in healthy subjects.

As for fibrosis biomarkers, it was found that patients with persistent AF and MS had higher levels of aldosterone, galectin-3, and PIIINP than patients with paroxysmal and permanent AF. Plasma concentration of GDF-15 was higher in patients with permanent AF than in patients with paroxysmal and persistent AF. In patients with paroxysmal AF and MS, plasma levels of CTGF and PINP were higher

than in patients with persistent and permanent AF. TGF-beta1 was higher in paroxysmal AF than in patients with persistent and permanent AF. The data are presented in Table 3.

It was found that the concentration of galectin-3 in blood plasma positively correlated with PINP levels ($\rho=0,465$, $p<0,0001$), PIIINP ($\rho=0,409$, $p<0,0001$), GDF-15 ($\rho=0,369$, $p<0,0001$), CTGF ($\rho=0,405$, $p<0,0001$). The concentration of GDF-15 correlated to a greater extent with PIIINP ($\rho=0,403$, $p<0,0001$) than with PINP ($\rho=0,232$, $p=0,03$). In turn, TGF-beta1 correlated more significantly with PIIINP ($\rho=0,329$, $p<0,0001$), and CTGF — with PINP ($\rho=0,386$, $p<0,0001$). According to multivariate regression analysis, of all studied biomarkers, GDF-15 had a greater effect on PIIINP concentration ($\beta=0,234$, $p=0,038$), and galectin-3, on PINP ($\beta=0,248$, $p<0,021$).

Analysis of voltage maps and assessing the severity of LA myocardial fibrosis in AF patients who underwent pulmonary vein isolation revealed that LA fibrosis is more common in patients with AF and MS than in AF patients without MS (26,1 (14,5-41,5)% and 10,5 (7,3-16,2)%, $p=0,028$). Assessment of the relationship of circulating biomarkers in patients with AF and MS, who underwent electroanatomic

Table 4

**Blood concentrations of fibrosis biomarkers in patients
with AF and MS with varying severity of LA fibrosis**

% of LA fibrosis, quartiles (Q)	≤12,3% (Q1)	12,4-22,4% (Q2)	22,5-33,4% (Q3)	≥33,5% (Q4)	Statistical significance, p
Aldosterone, pg/ml	8,6 (5,9-13,4)	7,4 (6,7-16,0)	8,8 (6,4-18,3)	12,34 (9,3-18,8)	$p_{1,2}=0,06$ $p_{1,3}=0,647$ $p_{1,4}=0,001$ $p_{2,3}=0,08$ $p_{2,4}=0,001$ $p_{3,4}=0,001$
Galectin-3, ng/ml	68,7 (66,1-86,3)	110,0 (75,6-117,1)	89,0 (80,0-120,0)	123,4 (92,6-198,8)	$p_{1,2}=0,001$ $p_{1,3}=0,01$ $p_{1,4}<0,0001$ $p_{2,3}=0,07$ $p_{2,4}<0,0001$ $p_{3,4}=0,0001$
GDF-15, pg/ml	725,9 (613,5-854,1)	641,5 (534,6-829,1)	687,5 (554,8-1501,4)	1020,1 (669,1-1243,9)	$p_{1,2}=0,05$ $p_{1,3}=0,124$ $p_{1,4}<0,0001$ $p_{2,3}=0,236$ $p_{2,4}<0,0001$ $p_{3,4}<0,0001$
TGF-beta1, pg/ml	1961,6 (1434,9-1327,4)	3934,6 (3203,9-5355,4)	2643,1 (2165,9-4259,4)	3678,2 (2348,9-4751,4)	$p_{1,2}=0,01$ $p_{1,3}=0,04$ $p_{1,4}<0,0001$ $p_{2,3}=0,929$ $p_{2,4}=0,245$ $p_{3,4}=0,147$
CTGF, pg/ml	179,8 (164,5-224,6)	175,4 (128,4-203,4)	120,9 (42,8-210,3)	220,9 (178,9-306,4)	$p_{1,2}=0,359$ $p_{1,3}=0,01$ $p_{1,4}<0,0001$ $p_{2,3}=0,04$ $p_{2,4}<0,0001$ $p_{3,4}<0,0001$
PIIINP, ng/ml	58,3 (49,8-90,9)	59,4 (47,7-63,4)	61,6 (57,4-105,5)	92,2 (66,4-125,1)	$p_{1,2}=0,959$ $p_{1,3}=0,781$ $p_{1,4}<0,0001$ $p_{2,3}=0,854$ $p_{2,4}<0,0001$ $p_{3,4}<0,0001$
PINP, pg/ml	2839,1 (1412,1-3458,1)	2986,1 (2623,1-3571,1)	3567,1 (2498,1-4986,1)	4344,1 (4122,1-4567,1)	$p_{1,2}=0,899$ $p_{1,3}=0,01$ $p_{1,4}<0,0001$ $p_{2,3}=0,04$ $p_{2,4}<0,0001$ $p_{3,4}<0,0001$

Abbreviations: LA — left atrium, GDF-15 — growth differentiation factor 15, TGF-beta1 — transforming growth factor-beta1, CTGF — connective tissue growth factor, PINP — N-terminal propeptide of type I procollagen, PIIINP — N-terminal propeptide of type III procollagen.

mapping before pulmonary vein isolation (n=79), revealed positive correlations of LA myocardial fibrosis severity with the concentration of galectin-3 ($\rho=0,563$, $p<0,0001$), PINP ($\rho=0,620$, $p<0,0001$), TGF-beta1 ($\rho=0,390$, $p<0,0001$) and CTGF ($\rho=0,551$, $p<0,0001$), which shown in Figure 1. For detailed analysis, these AF and MS patients were divided into groups depending on the proportion of LA fibrosis, divided into quartiles (25%, 50%,

75%). It was found that patients with the highest severity of LA fibrosis ($\geq 33\%$ — Q4) had higher concentrations of galectin-3, aldosterone, GDF-15, PINP, and PIIINP (Table 4). Linear multivariate regression established that the most significant effect on LA fibrosis severity (% of fibrosis) was exerted by the following biomarkers: galectin-3 ($\beta=0,432$, $p<0,0001$), PINP ($\beta=0,343$, $p=0,001$), and PIIINP ($\beta=0,286$, $p=0,008$).

Discussion

AF pathogenesis is a comprehensive process, which is based on hemodynamic, structural, electrophysiological and molecular mechanisms. There are many clinical risk factors for AF, including advanced age, CAD, thyroid diseases, heart failure, chronic pulmonary diseases, etc. [1]. Our study did not include patients with organic heart diseases, acute and chronic significant comorbidities. In patients with MS, in contrast to the comparison groups, 3 or more MS components were diagnosed, the most frequent among which were HTN, abdominal obesity, and dyslipidemia. HTN contributes to left ventricular hypertrophy and diastolic dysfunction, as well as LA dilatation. The mechanisms of myocardial structural remodeling, including atria, aldosterone plays an important role. The profibrotic role of aldosterone is known and is currently not in doubt. Through the development of fibrosis, which is a possible substrate of nonvalvular AF, aldosterone, in turn, can act as a predictor of this arrhythmia. In 2015, the first data on the role of galectin-3 and aldosterone in AF development were published and it was found that the concentrations of these biomarkers are higher in patients with AF in combination with MS, compared with patients with MS but without AF [12]. This study found that the concentration of aldosterone and galectin-3 in patients with AF combined with MS is higher than in patients with isolated AF without MS, which, in turn, emphasizes the relationship of these biomarkers with MS and its contribution to AF. It is known from experimental studies that aldosterone acts as one of the main initial inducers of cascade of profibrotic factors. It was found that aldosterone induces the secretion of galectin-3 through hyperactivation of macrophages, which, in turn, induces the production of TGF-beta1, while CTGF — effector molecules involved in the activation of fibroblasts and excessive production of PINP and PIIINP into the extracellular matrix [6, 13]. An experimental work by Schreier B. et al. found that aldosterone is able to induce fibrosis in the myocardium and kidneys through the activation of TGF-beta1 synthesis and, as a consequence, an increase in procollagen production, followed by developing heart failure [14]. Aldosterone induces TGF-beta1 synthesis, but at the same time, TGF-beta1 mutually enhances the production of aldosterone and other profibrogenic factors through a positive feedback [15]. TGF-beta1 is a member of a protein family that play a critical role in epithelial-to-mesenchymal transition during embryogenesis of valvular and septal cardiac structures and is secreted by various cells, such as cardiomyocytes, fibroblasts, endothelial cells and inflammatory effectors. Various causes underlying

the onset of AF increase TGF-beta1 expression level, which, in turn, induces interstitial fibrosis [16]. In addition, TGF-beta1 is able to regulate transcription and function of cardiomyocyte sodium channels [17].

We found that plasma concentration of TGF-beta1 in patients with AF and MS is higher than in patients with isolated AF and is significantly higher than in healthy subjects. While TGF-beta1 is a key inducer of fibrosis, another known growth factor (CTGF) promotes it [18]. CTGF is a member of CCN protein family (Cyr61, CTGF, nov), which is one of the main downstream effectors in the development of TGF-beta1-induced fibrosis. In myocardial with active remodeling, combined expression of CTGF and TGF-beta1 was revealed [19]. Ko WC, et al. found that gene expression and secretion of CTGF in atrial tissue of patients with CAD and AF is higher than in patients with sinus rhythm. The authors also found that in an experimental animal model, the administration of angiotensin II caused an increase in CTGF concentration and fibroblast proliferation with the formation of type I collagen, which undoubtedly contributed to AF onset [9]. Lavall D, et al., during the cultivation of atrial tissue obtained from atrial biopsy in patients with mitral valve disease and AF, revealed that aldosterone increased CTGF secretion with activation of fibroblasts and an increase in extracellular matrix mass [20]. CTGF activity is regulated by angiotensin II and TGF-beta1, which enhances the development of fibrosis [21]. In a cohort of patients with AF and MS, we found that the plasma concentration of CTGF is significantly higher than in patients with isolated AF and isolated MS. A positive correlation was found with galectin-3 and circulating procollagens. In the pathogenesis of fibrosis development, galectin-3 is a key factor that triggers complex myocardial remodeling processes. On the one hand, it is able to influence matrix metalloproteinases, limiting extracellular matrix degradation. On the other hand, it activates fibroblasts and increases the synthesis of collagen types I and III, which has been well studied in experimental animal models [22]. PINP and PIIINP are deposited directly in the myocardium in various heart diseases. In particular, a study by Lopez B, et al. established an association between circulating PINP and development of LV myocardial remodeling in patients with HTN [23]. The relationship of these biomarkers with the risk of AF has been established in numerous studies earlier; moreover, it has been proven that in patients with AF, the deposition of type I procollagen, rather than type III procollagen, predominates in LA tissue [24, 25].

According to our study, it was found that plasma concentration of PINP and PIIINP is higher in patients with AF and MS in comparison with patients with isolated AF MS and higher than in patients with isolated MS. A positive correlation of galectin-3, TGF-beta1, and CTGF with plasma concentrations of circulating PINP and PIIINP was established, which emphasizes the relationship between these biomarkers in the development of fibrosis.

Additional analysis of data from patients with AF in combination with MS on various AF types revealed that patients with the paroxysmal AF have higher concentrations of TGF-beta1, CTGF, and PINP than patients with persistent and permanent AF. Probably, these biomarkers play a more significant role in the development of AF in patients with MS in early stages of arrhythmia. On the other hand, in patients with persistent AF and MS, the blood concentrations of galectin-3, aldosterone, and PIIINP were higher than in patients with paroxysmal AF, and in patients with permanent AF, they were significantly lower, which suggests that that these biomarkers to a greater extent specifies the progression of arrhythmia. Attention is also drawn to the fact that the concentration of GDF-15 is highest in patients with permanent AF. This biomarker is also important in pathogenesis of arrhythmia and is a predictor of unfavorable prognosis regarding the risk of cardiovascular events in patients with AF [26]. The study found that in patients with AF in combination with MS, the concentration of GDF-15 is higher than in patients with isolated AF, which is probably due to MS components, since the production of this biomarker is enhanced by inflammation, hypoxemia, and metabolic disorders [27].

Analysis of the data on severity of LA myocardial fibrosis in AF patients who underwent radiofrequency pulmonary vein isolation established that the prevalence of LA fibrosis in patients with AF in combination with MS is higher than in isolated AF. Previously, we published data that the severity of LA myocardial fibrosis in patients with AF and MS is greater than in patients with AF without MS, and is associated with galectin-3 [28]. Currently, more data have been obtained on the relationship of biomarkers with LA myocardial fibrosis. Positive correlations of the severity of LA myocardial fibrosis were revealed not only with galectin-3 and TGF-beta1, but also with PINP and CTGF, which was confirmed by linear univariate regression. Linear

multivariate regression revealed that the prevalence of LA myocardial fibrosis was more significantly influenced by the following biomarkers: galectin-3, PIIINP and PINP. The analysis of concentrations of fibrosis biomarkers in patients with AF in combination with MS in subgroups of patients with different severity of LA fibrosis made it possible to establish that the studied biomarkers are significantly increased in patients with the most severe fibrosis (>33,5%).

Thus, this study investigated the role of molecular fibrosis markers in the pathogenesis of AF in patients with MS. Determination of markers of myocardial fibrosis and predictors of development and progression of AF in patients with MS is of great importance, because will allow identifying patients at high risk of developing AF and carrying out its primary and secondary prevention. Fibrogenic factors may act as a potential target for therapy in patients with AF in combination with MS.

Study limitations. Patients with AF and MS received medications (antiarrhythmic, antihypertensive, antithrombotic, statins), which could to some extent affect the study results. The number of patients assessed for severity of LA fibrosis was relatively small. Therefore, it is necessary to collect more data and conduct further monitoring of patients with MS. To study the prognostic role of studied biomarkers, prospective follow-up of patients should be continued to obtain data on potential of their use in clinical practice.

Conclusion

1. The blood concentration of aldosterone, galectin-3, TGF-beta1, GDF-15, CTGF, PIIINP and PINP in patients with AF in combination with MS is higher than in patients with isolated AF and isolated MS.

2. In patients with paroxysmal AF and MS, the levels of TGF-beta1, CTGF and PINP are higher than in patients with persistent and permanent AF. In patients with persistent AF and MS, the concentrations of galectin-3, aldosterone and PIIINP is higher than in patients with paroxysmal AF.

3. The concentration of galectin-3, TGF-beta1, CTGF, PIIINP and PINP are associated with a severe LA myocardial fibrosis in patients with AF in combination with MS.

Relationships and Activities: none.

References

- Hindricks G, Potpara T, Dagres N, et al. 2020 ESC Guidelines for the diagnosis and management of atrial fibrillation developed in collaboration with the European Association for Cardio-Thoracic Surgery (EACTS). *European Heart Journal*. 2021;42(5):373-498. doi:10.1093/eurheartj/ehaa612.
- Chamberlain AM, Agarwal SK, Ambrose M, et al. Metabolic syndrome and incidence of atrial fibrillation among blacks and whites in the Atherosclerosis Risk in Communities (ARIC) Study. *American Heart Journal*. 2010;159(5):850-6. doi:10.1016/j.ahj.2010.02.005.
- Cuspidi C, Negri F, Sala C, et al. Association of left atrial enlargement with left ventricular hypertrophy and diastolic dysfunction: A tissue Doppler study in echocardiographic practice. *Blood Pressure*. 2012;21(1):24-30. doi:10.3109/08037051.2011.618262.
- Milliez P, Girerd X, Plouin PF, et al. Evidence for an increased rate of cardiovascular events in patients with primary aldosteronism. *Journal of the American College of Cardiology*. 2005;45(8):1243-8. doi:10.1016/j.jacc.2005.01.015.
- Lavie CJ, Pandey A, Lau DH, et al. Obesity and Atrial Fibrillation Prevalence, Pathogenesis, and Prognosis: Effects of Weight Loss and Exercise. *Journal of the American College of Cardiology*. 2017;70(16):2022-35. doi:10.1016/j.jacc.2017.09.002.
- Ionin VA, Baranova EI, Zaslavskaya EL, et al. Galectin-3, N-terminal Propeptides of Type I and III Procollagen in Patients with Atrial Fibrillation and Metabolic Syndrome. *International Journal of Molecular Sciences*. 2020;21(16):5689. doi:10.3390/ijms21165689.
- Li J, Yang Y, Ng CY, et al. Association of plasma transforming growth factor- β 1 levels and the risk of atrial fibrillation: A meta-analysis. *PLoS ONE*. 2016;11(5). doi:10.1371/journal.pone.0155275.
- Musa H, Kaur K, O'Connell R, et al. Inhibition of platelet-derived growth factor-AB signaling prevents electromechanical remodeling of adult atrial myocytes that contact myofibroblasts. *Heart Rhythm*. 2013;10(7):1044-51. doi:10.1016/j.hrthm.2013.03.014.
- Ko WC, Hong CY, Hou SM, et al. Elevated expression of connective tissue growth factor in human atrial fibrillation and angiotensin II-treated cardiomyocytes. *Circulation Journal*. 2011;75(7):1592-600. doi:10.1253/circj.CJ-10-0892.
- Han JS, Choi BS, Yang CW, Kim YS. Aldosterone-induced TGF- β 1 expression is regulated by mitogen-activated protein kinases and activator protein-1 in mesangial cells. *Journal of Korean Medical Science*. 2009;24(suppl.1):S195. doi:10.3346/jkms.2009.24.S1.S195.
- Terada Y, Ueda S, Hamada K, et al. Aldosterone stimulates nuclear factor-kappa B activity and transcription of intercellular adhesion molecule-1 and connective tissue growth factor in rat mesangial cells via serum- and glucocorticoid-inducible protein kinase-1. *Clinical and Experimental Nephrology*. 2012;16(1):81-8. doi:10.1007/s10157-011-0498-x.
- Ionin VA, Soboleva AV, Listopad OV, et al. Galectin 3 and aldosterone in patients with atrial fibrillation and metabolic syndrome. *Russian Journal of Cardiology*. 2015;(4):79-83. (In Russ.) doi:10.15829/1560-4071-2015-04-79-83.
- Calvier L, Martinez-Martinez E, Miana M, et al. The impact of galectin-3 inhibition on aldosterone-induced cardiac and renal injuries. *JACC: Heart Failure*. 2015;3(1):59-67. doi:10.1016/j.jchf.2014.08.002.
- Schreier B, Rabe S, Schneider B, et al. Aldosterone/NaCl-induced renal and cardiac fibrosis is modulated by TGF- β responsiveness of T cells. *Hypertension Research*. 2011;34(5):623-9. doi:10.1038/hr.2011.16.
- Huang W, Xu C, Kahng KW, et al. Aldosterone and TGF- β 1 synergistically increase PAI-1 and decrease matrix degradation in rat renal mesangial and fibroblast cells. *American Journal of Physiology — Renal Physiology*. 2008;294(6). doi:10.1152/ajprenal.00017.2008.
- Cao F, Li Z, Ding WM, et al. LncRNA PVT1 regulates atrial fibrosis via miR-128-3p-SP1-TGF- β 1-Smad axis in atrial fibrillation. *Molecular Medicine*. 2019;25(1). doi:10.1186/s10020-019-0074-5.
- Kaur K, Zarzoso M, Ponce-Balbuena D, et al. TGF- β 1, Released by Myofibroblasts, Differentially Regulates Transcription and Function of Sodium and Potassium Channels in Adult Rat Ventricular Myocytes. *PLoS ONE*. 2013;8(2). doi:10.1371/journal.pone.0055391.
- Miyazono K, Kusanagi K, Inoue H. Divergence and convergence of TGF- β /BMP signaling. *Journal of Cellular Physiology*. 2001;187(3):265-76. doi:10.1002/jcp.1080.
- Chuva De Sousa Lopes SM, Feijen A, Korving J, et al. Connective tissue growth factor expression and Smad signaling during mouse heart development and myocardial infarction. *Developmental Dynamics*. 2004;231(3):542-50. doi:10.1002/dvdy.20162.
- Lavall D, Selzer C, Schuster P, et al. The mineralocorticoid receptor promotes fibrotic remodeling in atrial fibrillation. *Journal of Biological Chemistry*. 2014;289(10):6656-68. doi:10.1074/jbc.M113.519256.
- Ahmed MS, Øie E, Vinge LE, et al. Connective tissue growth factor — A novel mediator of angiotensin II-stimulated cardiac fibroblast activation in heart failure in rats. *Journal of Molecular and Cellular Cardiology*. 2004;36(3):393-404. doi:10.1016/j.yjmcc.2003.12.004.
- de Boer RA, Voors AA, Muntendam P, et al. Galectin-3: A novel mediator of heart failure development and progression. *European Journal of Heart Failure*. 2009;11(9):811-7. doi:10.1093/eurjhf/hfp097.
- López B, González A, Querejeta R, Díez J. The use of collagen-derived serum peptides for the clinical assessment of hypertensive heart disease. *Journal of Hypertension*. 2005;23(8):1445-51. doi:10.1097/01.hjh.0000173780.67308.f1.
- Duprez DA, Heckbert SR, Alonso A, et al. Collagen Biomarkers and Incidence of New Onset of Atrial Fibrillation in Subjects With No Overt Cardiovascular Disease at Baseline. *Circulation Arrhythmia and electrophysiology*. 2018;11(10):e006557. doi:10.1161/CIRCEP.118.006557.
- Swartz MF, Fink GW, Sarwar M, et al. Serum Peptides for Collagen I and III Synthesis Predict Atrial Fibrillation Following Cardiac Surgery. *Heart Rhythm*. 2011;8(11):1827. doi:10.1016/j.hrthm.2011.09.051.
- Shoemaker MB, Stevenson WG. The ABC death risk score: is it time to start measuring GDF-15? Published online 2017. doi:10.1093/eurheartj/ehx584.
- Ost M, Igual Gil C, Coleman V, et al. Muscle-derived GDF15 drives diurnal anorexia and systemic metabolic remodeling during mitochondrial stress. *EMBO reports*. 2020;21(3). doi:10.15252/embr.201948804.
- Zaslavskaya L, Morozov N, Ionin V, et al. The role of transforming growth factor beta-1 and galectin-3 in formation of the left atrium fibrosis in patients with paroxysmal atrial fibrillation and metabolic syndrome. *Russian Journal of Cardiology*. 2018;(2):60-6. (In Russ.) doi:10.15829/1560-4071-2018-2-60-66.

